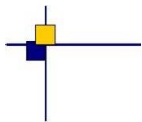


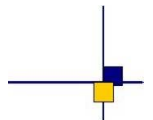


CalVal Saral/ Altika



Saral/ Altika validation and cross calibration activities (Annual report 2014)

Contract No 104685/00 - lot 1.2A



Reference : CLS.DOS/NT/14-234

Nomenclature : SALP-RP-MA-EA-22418-CLS

Issue : 1rev 1

Date : February 24, 2015

Chronology Issues:

| Issue: | Date: | Reason for change: |
|--------|--------------|-----------------------------------|
| 1rev0 | Dec 1, 2014 | Creation |
| 1rev1 | Feb 24, 2015 | Revision after comments from CNES |

People involved in this issue :

| | AUTHORS | COMPANY | DATE | INITIALS |
|-----------------------------------|---------------------------------------|-------------------|-------------|-----------------|
| Written by: | P. Prandi V. Pignot S. Philipps | CLS CLS CLS | | |
| Checked by: | | CLS | | |
| Approved by: | | CLS CLS | | |
| Application authorised by: | | | | |

Index Sheet :

| | |
|------------|--|
| Context: | |
| Keywords: | |
| Hyperlink: | |

Distribution:

| Company | Means of distribution | Names |
|---------|-----------------------|--|
| CLS/DOS | electronic copy | G.DIBARBOURE |
| CNES | electronic copy | thierry.guinle@cnes.fr emilie.bronner@cnes.fr nicolas.picot@cnes.fr amandine.guillot@cnes.fr jean-damien.desjonquieres@cnes.fr aqgp_rs@cnes.fr dominique.chermain@cnes.fr delphine.vergnoux@cnes.fr |

List of tables and figures

List of Tables

| | | |
|---|---|----|
| 1 | <i>Product versions</i> | 3 |
| 2 | <i>Events</i> | 4 |
| 3 | <i>Events (red lines indicates safe hold mode event)</i> | 8 |
| 4 | <i>Missing pass status</i> | 11 |
| 5 | <i>Edited measurement status</i> | 14 |
| 6 | <i>Models and standards adopted for the Saral/AltiKa version "T" products (using Patch 2). Adapted from [4]</i> | 18 |
| 7 | <i>Editing criteria, statistics obtained for cycles 1 to 18</i> | 23 |
| 8 | <i>Standards used for Saral and Jason-2</i> | 61 |
| 9 | <i>Differences between the auxiliary data for the O/I/Gdr products (from [4])</i> | 68 |

List of Figures

| | | |
|---|---|----|
| 1 | <i>Percentage of available measurements over all types of surfaces for SRL and JA2. Gray bands indicate when Saral/AltiKa uses EDP tracking, wheat color band indicates when Saral/AltiKa used Diode/DEM tracking, turquoise color band indicates when Jason-2 used Diode/DEM tracking, gold color band indicates when Saral/AltiKa is on safe-hold mode. Vertical dotted lines in lilac indicate days with special calibrations.</i> | 20 |
| 2 | <i>Map of percentage of available measurements over land for Saral/AltiKa on cycle 14 and for Jason-2 on cycle 220 (right).</i> | 20 |
| 3 | <i>Cycle per cycle percentage of available measurements over ocean (left) and without anomalies (right) for Saral/AltiKa and Jason-2. Gray bands indicate when Saral/AltiKa uses EDP tracking, wheat color band indicates when Saral/AltiKa used Diode/DEM tracking, turquoise color band indicates when Jason-2 used Diode/DEM tracking, gold color band indicates when Saral/AltiKa is on safe-hold mode. Lilac vertical lines, indicate days with special calibrations, which can be over ocean.</i> | 21 |
| 4 | <i>Day per day percentage of eliminated measurements during selection of ocean/lake measurements. Gray bands indicate when Saral/AltiKa uses EDP tracking, wheat color band indicates when Saral/AltiKa used Diode/DEM tracking, elsewhere Median tracking is used. Gold color band indicates when Saral/AltiKa is on safe-hold mode. Vertical dotted lines in lilac indicate days with special calibrations.</i> | 24 |
| 5 | <i>Percentage of edited measurements by ice flag criterion. Left: Daily statistics for GDR Saral/AltiKa (all latitudes: black, limited to 66° latitude: red) and Jason-2 (blue). Gold color band indicates when Saral/AltiKa is on safe-hold mode. Right: Map since beginning of mission (cycles 1 to 18).</i> | 25 |
| 6 | <i>Daily statistics of percentage of edited measurements by threshold criteria for GDR Saral/AltiKa (all latitudes: black, limited to 66° latitude: red) and Jason-2 (blue). Gold color band indicates when Saral/AltiKa is on safe-hold mode.</i> | 26 |
| 7 | <i>Percentage of edited measurements by 40-Hz measurements number criterion (20-Hz for Jason-2). Left: Daily statistics for Saral/AltiKa (all latitudes: black, limited to 66° latitude: red) and Jason-2 (blue). Gold color band indicates when Saral/AltiKa is on safe-hold mode. Right: Map since beginning of mission (cycles 1 to 18).</i> | 27 |

.....

| | | |
|----|---|----|
| 8 | <i>Percentage of edited measurements by 40-Hz measurements standard deviation criterion (20-Hz for Jason-2). Left: Daily statistics for Saral/AltiKa (all latitudes: black, limited to 66° latitude: red) and Jason-2 (blue). Green vertical lines indicate days with maneuvers on Saral/AltiKa and gold band indicates the safe-hold mode on Saral/AltiKa. Right: Map since beginning of mission (cycles 1 to 18).</i> | 28 |
| 9 | <i>Percentage of edited measurements by SWH criterion. Left: Daily statistics for GDR Saral/AltiKa and Jason-2 (blue). Green vertical lines indicate days with maneuvers on Saral/AltiKa and gold band indicates the safe-hold mode on Saral/AltiKa. Right: Map since beginning of mission (cycles 1 to 18).</i> | 28 |
| 10 | <i>Percentage of edited measurements by Sigma0 criterion. Left: Daily statistics for Saral/AltiKa (all latitudes: black, limited to 66° latitude: red) and Jason-2 (blue). Green vertical lines indicate days with maneuvers on Saral/AltiKa and gold band indicates the safe-hold mode on Saral/AltiKa. Right: Map since beginning of mission (cycles 1 to 18).</i> | 29 |
| 11 | <i>Percentage of edited measurements by 40 Hz Sigma0 standard deviation criterion. Left: Daily statistics for Saral/AltiKa (all latitudes: black, limited to 66° latitude: red) and Jason-2 (blue). Green vertical lines indicate days with maneuvers on Saral/AltiKa and gold band indicates the safe-hold mode on Saral/AltiKa. Right: Map since beginning of mission (cycles 1 to 18).</i> | 30 |
| 12 | <i>Percentage of edited measurements by radiometer wet troposphere criterion. Left: Daily statistics for Saral/AltiKa (all latitudes: black, limited to 66° latitude: red) and Jason-2 (blue). Green vertical lines indicate days with maneuvers on Saral/AltiKa and gold band indicates the safe-hold mode on Saral/AltiKa. Right: Map since beginning of mission (cycles 1 to 18).</i> | 30 |
| 13 | <i>Percentage of edited measurements by square off-nadir angle criterion. Left: Daily statistics for Saral/AltiKa (all latitudes: black, limited to 66° latitude: red) and Jason-2 (blue). Green vertical lines indicate days with maneuvers on Saral/AltiKa and gold band indicates the safe-hold mode on Saral/AltiKa. Right: Map since beginning of mission (cycles 1 to 18).</i> | 31 |
| 14 | <i>Percentage of edited measurements by sea state bias criterion. Left: Daily statistics for Saral/AltiKa (all latitudes: black, limited to 66° latitude: red) and Jason-2 (blue). Green vertical lines indicate days with maneuvers on Saral/AltiKa and gold band indicates the safe-hold mode on Saral/AltiKa. Right: Map since beginning of mission (cycles 1 to 18).</i> | 32 |
| 15 | <i>Percentage of edited measurements by altimeter wind speed criterion. Left: Cycle per cycle monitoring. Green vertical lines indicate days with maneuvers on Saral/AltiKa and gold band indicates the safe-hold mode on Saral/AltiKa. Right: Map since beginning of mission (cycles 1 to 18).</i> | 33 |
| 16 | <i>Percentage of edited measurements by ocean tide criterion. Left: Daily statistics for Saral/AltiKa (all latitudes: black, limited to 66° latitude: red) and Jason-2 (blue). Gold band indicates the safe-hold mode on Saral/AltiKa. Right: Map since beginning of mission (cycles 1 to 18).</i> | 34 |
| 17 | <i>Percentage of edited measurements by sea surface height criterion. Left: Daily statistics for Saral/AltiKa (all latitudes: black, limited to 66° latitude: red) and Jason-2 (blue). Gold band indicates the safe-hold mode on Saral/AltiKa. Right: Map since beginning of mission (cycles 1 to 18).</i> | 35 |

.....

| | | |
|----|--|----|
| 18 | <i>Percentage of edited measurements by sea level anomaly criterion. Left: Daily statistics for Saral/AltiKa (all latitudes: black, limited to 66° latitude: red) and Jason-2 (blue). Green vertical lines indicate days with maneuvers on Saral/AltiKa and gold band indicates the safe-hold mode on Saral/AltiKa. Right: Map since beginning of mission (cycles 1 to 18).</i> | 35 |
| 19 | <i>Daily monitoring of mean of number of elementary Saral/AltiKa 40 Hz (left ordinate) and Jason-2 20 Hz (right ordinate) range measurements. The gold band indicates the safe hold mode on Saral/AltiKa.</i> | 38 |
| 20 | <i>Average map of number of Saral/AltiKa elementary 40 Hz range measurements (left) and Jason-2 elementary 20 Hz range measurement (right) over cycles 1 to 18.</i> | 38 |
| 21 | <i>Cyclic monitoring of rms of elementary 40/20 Hz range measurements for Saral/AltiKa and Jason-2 (left), computing latitude weighted box statistics. Daily mean of rms of elementary Saral/AltiKa 40 Hz and Jason-2 20 Hz range measurements (right). GDR data are plotted with plain lines, IGDR with dotted lines. The gold band indicates the safe hold mode on Saral/AltiKa.</i> | 39 |
| 22 | <i>Average map of rms of Saral/AltiKa elementary 40 Hz range measurements (left) and Jason-2 elementary 20 Hz range measurement (right) over cycles 1 to 18.</i> | 39 |
| 23 | <i>Daily monitoring of mean (left) and standard deviation (right) of Saral/AltiKa and Jason-2 off-nadir angle from waveforms. GDR data are in plain lines, IGDR data in dotted lines. The vertical green line indicates the day where the PF/RF alignment (alignment between the platform and the radio-frequency axis) was corrected. The gold band indicates the safe hold mode on Saral/AltiKa.</i> | 40 |
| 24 | <i>Average map of off-nadir angle from waveforms for Saral/AltiKa (left) and Jason-2 (right) after the correction of the PF/RF alignment over cycles 3 to 18.</i> | 41 |
| 25 | <i>Histogram (of along-track data) of off-nadir angle from waveforms for Saral/AltiKa and Jason-2 (computed for Saral/AltiKa cycle 14).</i> | 42 |
| 26 | <i>Daily monitoring of mean and standard deviation of Saral/AltiKa and Jason-2 backscattering coefficient (top) and cycle per cycle monitoring of latitude weighted box mean for both missions on the bottom. The gold band indicates the safe hold mode on Saral/AltiKa.</i> | 43 |
| 27 | <i>Average map of backscattering coefficient for Saral/AltiKa (left) and Jason-2 (right) cycles 1 to 18. Difference map of gridded Saral and Jason-2 backscattering coefficient for cycles 1 to 18.</i> | 44 |
| 28 | <i>Dispersion diagram of backscattering coefficient between Saral/AltiKa and Jason-2 at 3h crossover points (computed for cycles 1 to 18) on the left and histogram (of along-track data) computed for Saral/AltiKa cycle 14 on the right.</i> | 45 |
| 29 | <i>Daily monitoring of mean and standard deviation significant wave height for Saral/AltiKa and Jason-2 (top) and cycle per cycle monitoring of latitude weighted box mean for both missions on the bottom. The gold band indicates the safe hold mode on Saral/AltiKa.</i> | 46 |
| 30 | <i>Average map of significant wave height for Saral/AltiKa (left) and Jason-2 (right) cycles 1 to 18. Difference map of gridded Saral and Jason-2 significant wave height for cycles 1 to 18.</i> | 47 |
| 31 | <i>Dispersion diagram of significant wave height between Saral/AltiKa and Jason-2 at 3h crossover points (computed for cycles 1 to 18) on the left and histogram (of along-track data) computed for Saral/AltiKa cycle 14 on the right.</i> | 48 |

.....

| | | |
|----|--|----|
| 32 | <i>Daily monitoring of mean and standard deviation ionosphere correction for Saral/AltiKa (GIM) and Jason-2 (filtered dual-frequency ionosphere correction with scale factor 0.14418 for mean computation) on top and cycle per cycle monitoring of latitude weighted box mean for both missions (without the scale factor for Jason-2) on the bottom. The gold band indicates the safe hold mode on Saral/AltiKa.</i> | 49 |
| 33 | <i>Average map of ionosphere correction for Saral/AltiKa (GIM, left) and Jason-2 (filtered dual-frequency ionosphere correction, right) cycles 1 to 18. Note that color scales are different for Saral and Jason-2</i> | 50 |
| 34 | <i>Dispersion diagram of ionosphere correction between Saral/AltiKa (GIM) and Jason-2 (filtered dual-frequency with scale factor of 0.14418 for Jason-2) at 3h crossover points (computed for cycles 1 to 18) on the left and histogram of along-track data (without scale factor for Jason-2) computed for Saral/AltiKa cycle 14 on the right.</i> | 51 |
| 35 | <i>Daily monitoring of mean and standard deviation of radiometer wet troposphere correction for Jason-2 (blue) and Saral/AltiKa (black all latitudes, red latitudes limited to $\pm 66^\circ$). The gold band indicates the safe hold mode on Saral/AltiKa.</i> | 52 |
| 36 | <i>Daily monitoring of mean and standard deviation of radiometer minus model wet troposphere correction for Saral/AltiKa and Jason-2. The gold band indicates the safe hold mode on Saral/AltiKa.</i> | 53 |
| 37 | <i>Average map of radiometer minus ECMWF model wet troposphere correction for Saral/AltiKa (left) and Jason-2 (right) cycles 1 to 18.</i> | 53 |
| 38 | <i>Histogram (of along-track data) of radiometer minus ECMWF model wet troposphere correction between Saral/AltiKa and Jason-2 computed for Saral/AltiKa cycle 14.</i> | 54 |
| 39 | <i>Daily monitoring of mean and standard deviation of altimeter wind speed for Saral/AltiKa and Jason-2. The gold band indicates the safe hold mode on Saral/AltiKa.</i> | 55 |
| 40 | <i>Average map of altimeter wind speed for Saral/AltiKa (left) and Jason-2 (right) cycles 1 to 18.</i> | 55 |
| 41 | <i>Dispersion diagram of altimeter wind speed between Saral/AltiKa and Jason-2 at 3h crossover points (computed for cycles 1 to 18) on the left and histogram of along-track data (without scale factor for Jason-2) computed for Saral/AltiKa cycle 14 on the right.</i> | 56 |
| 42 | <i>Daily monitoring of mean and standard deviation of (along-track) sea state bias of Saral/AltiKa and Jason-2 on the top and cycle per cycle monitoring of latitude weighted box mean for both missions on the bottom. The gold band indicates the safe hold mode on Saral/AltiKa.</i> | 57 |
| 43 | <i>Average map of sea state bias for Saral/AltiKa (left) and Jason-2 (right) cycles 1 to 18. Difference map of gridded Saral and Jason-2 sea state bias for cycles 1 to 18.</i> | 58 |
| 44 | <i>Dispersion diagram of sea state bias between Saral/AltiKa and Jason-2 at 3h crossover points (computed for cycles 1 to 18) on the left and histogram (of along-track data) computed for Saral/AltiKa cycle 14 on the right.</i> | 59 |
| 45 | <i>Map of mean of SSH crossovers differences for Saral/AltiKa (left) and Jason-2 for Saral cycles 1 to 18. Color scales are between ± 3 cm.</i> | 62 |
| 46 | <i>Map of mean of SSH crossovers differences for Saral/AltiKa for Saral cycles 1 to 18. Color scales are between ± 3 cm. Using FES 2012 ocean tide instead of GOT 4.8 (left) and using model wet troposphere (right).</i> | 62 |
| 47 | <i>Cycle per cycle monitoring of ascending/descending SSH differences at mono-mission crossovers for Saral/AltiKa and Jason-2 for Saral cycles 1 to 18.</i> | 63 |

| | | |
|----|--|----|
| 48 | <i>Monitoring of mean of Saral - Jason-2 differences at crossovers using radiometer wet troposphere correction (black line) or ECMWF model wet troposphere correction (green line) for GDR data with different selections. Statistics are computed on base of Jason-2 cycles.</i> | 63 |
| 49 | <i>Map of mean of SSH crossovers differences between Saral/AltiKa and Jason-2 using either radiometer wet troposphere correction (left) or ECMWF model wet troposphere correction (right) for both missions. The maps are centered around the mean.</i> | 64 |
| 50 | <i>Cycle by cycle standard deviation of SSH crossover differences for Saral/AltiKa using several selections (left), map of standard deviation at crossover points (right), the radiometer wet troposphere correction is used.</i> | 65 |
| 51 | <i>monitoring of the standard deviaton of SSH differences at crossovers for SARAL/AltiKa and Jason-2 for Saral cycles 1 to 18 using radiometer (dotted lines) or model (plain lines) wet troposphere correction</i> | 66 |
| 52 | <i>monitoring of the standard deviaton of SSH differences at crossovers for SARAL/AltiKa and Jason-2 for Saral cycles 1 to 18 using radiometer (dotted lines) or model (plain lines) wet troposphere correction</i> | 67 |
| 53 | <i>Cycle per cycle monitoring of mean and standard deviation of SSH crossover differences for SARAL/AltiKa using radiometer wet troposphere correction and geographical selection ($\text{latitude} < 50^\circ$, bathymetry < -1000 m and ocean variability < 20 cm rms).</i> | 68 |
| 54 | <i>Cyclic monitoring of pseudo time tag bias for SARAL/AltiKa and Jason-2</i> | 69 |
| 55 | <i>Map of SLA differences between SARAL/AltiKa and Jason-2 using the radiometer (left) and modeled (right) wet troposphere correction for the 17 first cycles of SARAL/AltiKa.</i> | 70 |
| 56 | <i>Daily monitoring of mean (top left) and standard deviation (top right) of SLA (using radiometer wet troposphere correction) of GDR data (plain lines) and IGDR data (dotted lines). The statistics are done for valid data with all available latitudes. The gold band indicates the safe hold mode on Saral/AltiKa. Bottom: Difference of daily Saral/AltiKa minus Jason-2 SLA using either radiometer or model wet troposphere correction. The statistics are done for valid data with $\text{latitudes} < 50^\circ$, bathymetry < -1000 m and low ocean variability.</i> | 71 |
| 57 | <i>Daily monitoring of mean and standard deviation of valid Saral/AltiKa SLA (with radiometer wet troposphere correction) for Ogdr, Igdr and Gdr products. No particular selection is used (latitude is not limited).</i> | 72 |
| 58 | <i>SARAL/AltiKa global mean record compared to the reference global mean sea level from TOPEX/Poseidon, Jason-1 and Jason-2, with an without the seasonnal signal</i> | 73 |
| 59 | <i>maps of SARAL/AltiKa mispointing for cycles 7, 16, 17 and 18</i> | 74 |
| 60 | <i>number of mispointed track sections (left) and number of mispointing events after the SHM recovery (right)</i> | 75 |
| 61 | <i>Daily averages of the wet troposphere differences (radiometer - model) for SARAL/AltiKa patch 2 data (red), SARAL/AltiKa after the correction and Jason-2 (green)</i> | 76 |
| 62 | <i>daily monitoring of global SLA for Jason-2 and SARAL/AltiKa, the difference is shown in black (left) and the daliy differences of SLA between Jason-2 and SARAL/AltiKa for years 2013 and 2014 (right)</i> | 77 |
| 63 | <i>Cycle by cycle standard deviation of SSH crossover differences for Saral/AltiKa and Jason-2 using selection on bathymetry, ocean variability and latitude computed with ensemble statistics (left) or box statistics $4^\circ \times 4^\circ$(right).</i> | 83 |
| 64 | <i>Distribution of number of crossovers on Saral/AltiKa cycle 5</i> | 83 |
| 65 | <i>Density of crossovers by latitude</i> | 84 |

66 *Monitoring of standard deviation SSH crossovers differences for SARAL/AltiKa and Jason-2 based on Jason-2 cycles using non weighted ensemble statistics method (left) and weighted by latitude method (right) with latitude < 66° (top) or with selection on bathymetry, ocean variability and latitude (bottom) 85*

List of items to be defined or to be confirmed

Applicable documents / reference documents

Contents

| | |
|--|-----------|
| 1. Introduction | 1 |
| 2. Processing status | 2 |
| 2.1. Processing | 2 |
| 2.2. CAL/VAL status | 3 |
| 2.2.1. Acquisition/tracking modes | 3 |
| 2.2.2. List of events | 4 |
| 2.2.3. Missing measurements | 8 |
| 2.2.4. Edited measurements | 11 |
| 2.3. Models and Standards History | 15 |
| 3. Data coverage and edited measurements | 19 |
| 3.1. Missing measurements | 19 |
| 3.1.1. Over land and ocean | 19 |
| 3.1.2. Over ocean | 20 |
| 3.2. Edited measurements | 22 |
| 3.2.1. Editing criteria definition | 22 |
| 3.2.2. Selection of measurements over ocean and lakes | 23 |
| 3.2.3. Flagging quality criteria: Ice flag | 24 |
| 3.2.4. Threshold criteria: Global | 26 |
| 3.2.5. Threshold criteria: 40-Hz measurements number | 27 |
| 3.2.6. Threshold criteria: 40-Hz measurements standard deviation | 27 |
| 3.2.7. Threshold criteria: Significant wave height | 28 |
| 3.2.8. Backscatter coefficient | 29 |
| 3.2.9. Backscatter coefficient: 40 Hz standard deviation | 29 |
| 3.2.10. Radiometer wet troposphere correction | 30 |
| 3.2.11. Square off-nadir angle | 30 |
| 3.2.12. Sea state bias correction | 32 |
| 3.2.13. Altimeter wind speed | 33 |
| 3.2.14. Ocean tide correction | 34 |
| 3.2.15. Sea surface height | 34 |
| 3.2.16. Sea level anomaly | 35 |
| 4. Monitoring of altimeter and radiometer parameters | 37 |
| 4.1. Methodology | 37 |
| 4.2. 40 Hz Measurements | 37 |
| 4.2.1. 40 Hz measurements number | 37 |
| 4.2.2. 40 Hz measurements standard deviation | 39 |
| 4.3. Off-Nadir Angle from waveforms | 40 |
| 4.4. Backscatter coefficient | 43 |
| 4.5. Significant wave height | 46 |
| 4.6. Ionosphere correction | 49 |
| 4.7. Radiometer wet troposphere correction | 52 |
| 4.7.1. Overview | 52 |
| 4.7.2. Comparison with the ECMWF model | 53 |
| 4.8. Altimeter wind speed | 55 |
| 4.9. Sea state bias | 57 |

.....

| | |
|--|-----------|
| 5. SSH crossover analysis | 60 |
| 5.1. Overview | 60 |
| 5.2. Mean of SSH crossover differences | 61 |
| 5.3. Mean of SSH crossover differences between Saral and other missions | 63 |
| 5.4. Standard deviation of SSH crossover differences | 65 |
| 5.5. Performances at crossover points of the different product types (Ogdr/Igdr/Gdr) | 68 |
| 5.6. Estimation of pseudo time-tag bias | 69 |
| 6. Sea Level Anomalies (SLA) Along-track analysis | 70 |
| 6.1. Overview | 70 |
| 6.2. Along-track performances for Saral/AltiKa (GDR-T Patch1) and Jason-2 | 71 |
| 6.3. Along-track performances of the different product types (Ogdr/Igdr/Gdr) | 72 |
| 6.4. SARAL/AltiKa as part of the GMSL record | 73 |
| 7. Particular Investigations | 74 |
| 7.1. Mispointing | 74 |
| 7.2. Correction of the hot calibration count saturation | 75 |
| 7.3. Checking for any impact of the safe hold mode on SARAL/AltiKa SLA | 76 |
| 8. Conclusion | 78 |
| 9. References | 79 |
| 10. Annex | 81 |
| 10.1. Content of Patch1 | 81 |
| 10.2. Content of Patch2 | 82 |
| 10.3. Weighted averaging method for SSH crossover points | 83 |
| 10.4. SARAL/AltiKa global statistical assessment and cross-calibration with Jason-2 | 85 |

1. Introduction

This document presents the synthesis report concerning validation activities of Saral/AltiKa GDRs in 2014 under SALP contract (N° 104685/00 Lot 1.2A) supported by CNES at the CLS Space Oceanography Division. It covers several points: CAL/VAL Saral/AltiKa activities, Saral/AltiKa / Jason-2 cross-calibration, and particular studies and investigations. **The focus is on GDR products, but results using IGDR products are also shown.** The present report is based exclusively on Patch2 data, details concerning the Patch2 reprocessing of Saral/AltiKa data can be found at chapter 10.2. or in [11].

The ISRO/CNES mission Saral/AltiKa was successfully launched on February, 25th 2013 and reached its operational orbit on March, 13th. However it was not exactly on the same ground track as Envisat (roughly 2 km difference at maximum latitude). After inclination maneuvers, Saral reached the same ground track as Envisat on October, 7th 2013.

Since the beginning of the mission, Saral/AltiKa data have been analyzed and monitored in order to assess the quality of Saral/AltiKa products. Cycle per cycle reports are available through the AVISO web page (<http://www.aviso.altimetry.fr/en/data/calval/systematic-calval/validation-reports.html>).

This report presents the activities undertaken in the framework of the SALP contract to assess and monitor Saral/AltiKa data quality. The percentage of missing and edited measurements are monitored. Relevant parameters derived from instrumental measurements and geophysical corrections are also analyzed, and we provide classical metrics to estimate the quality of Saral/AltiKa sea level measurements.

We also present the results of cross-calibration analysis performed between Saral/AltiKa and Jason-2. Even if both satellites are on different ground tracks, comparison remains possible. Only low order statistics are mainly presented here, but other analysis including histograms, plots and maps are routinely produced and used in the quality assessment process.

Indeed, it is now well recognized that the usefulness of any altimeter data only makes sense in a multi-mission context, given the growing importance of scientific needs and applications, in particular for operational oceanography. One major objective of the Saral/AltiKa mission is to ensure in association with Jason-2 the continuity of ocean observations through high precision altimetry. This kind of comparisons between different altimeter missions flying together provides a large number of estimations and consequently efficient long term monitoring of instrument measurements.

2. Processing status

2.1. Processing

Only about 4 months after launch of the Saral/AltiKa mission, Ogdr and Igdr data were available to all users beginning of July 2013. They were first released with some flaws (unit problem for liquid cloud water,...) or some corrections voluntary disabled (atmospheric attenuation at default value) or with disclaimers (ice_flag, altimeter wind not to use, ...). Some of these issues were addressed by the Patch1 (see table 1 concerning when this patch was used for the several products and 10.1. for its content). Beginning of September 2013 the GDR products were released (using from the beginning the Patch1). A description of the different Saral/AltiKa products and their disclaimers is available in the Saral/AltiKa Products handbook ([4]).

Patch2, containing improvements for Saral/AltiKa data, has been launched on February 2014. It has been applied for Ogdr data from cycle 10 pass 0407, then for Igdr data from cycle 10 pass 0566. Finally, Patch2 has been applied for Gdr data from cycle 8 onwards. Cycles 1 to 7 have also been reprocessed. This Patch contains some improvements described in chapter 10.2. (altimeter wind speed, new radiometer neural algorithm, new Ice-2 retracking algorithm,...).

A Patch3, which will provide an improvement of several standards is foreseen, but there is no delivery date available for this next version of the products yet.

| Data version | Ogdr | Igdr | Gdr |
|---|--|---|--|
| Version T without Patch | till cycle 4 segment 0609 | till cycle 4 pass 394 | - |
| Version T with Patch1 (chapter 10.1.) (L1 library=V3.1p1p2, L2 library=V4.2p1p6p9 Processing Pilot=V3-4-1p2p5p6p7p8p9) | from cycle 4 segment 0611 onwards (2013-07-18 13h44m04) | from cycle 4 pass 0395 onwards (2013-07-10 23h56m18) | from cycle 1 pass 0001 onwards |
| Version T with Patch2 (chapter 10.2.) (L1 library=V4.2p1, L2 library=V5.2p1, Processing Pilot=V4.1) | from cycle 10 segment 0407 onwards (2014-02-06 10h46m58) | from cycle 10 pass 0566 onwards (2014-02-11 23h17m37) | from cycle 8 onwards (cycles 1 to 7 have been reprocessed) |
| .../... | | | |

| | | | |
|--------------|------|------|-----|
| Data version | Ogdr | Igdr | Gdr |
|--------------|------|------|-----|

Table 1: *Product versions*

2.2. CAL/VAL status

In order to improve the visibility, the following tables will be presented in yellow or blue color. Color will switch for each cycle. The red color indicates an important event (safe-hold mode).

2.2.1. Acquisition/tracking modes

The following table shows the acquisition/tracking modes since the beginning of Saral/AltiKa mission.

| cycle | pass | start time | stop time | altimeter mode |
|--------|-----------|------------|------------|-------------------------------------|
| 1 | 0001-0200 | 2013-03-14 | 2013-03-21 | DIODE acquisition / median tracking |
| 1 | 0201-0400 | 2013-03-21 | 2013-03-28 | DIODE acquisition / EDP tracking |
| 1 | 0401-0600 | 2013-03-28 | 2013-04-04 | DIODE acquisition / median tracking |
| 1 | 0601-0800 | 2013-04-04 | 2013-04-11 | DIODE / DEM tracking |
| 1 | 0801-1002 | 2013-04-11 | 2013-04-18 | DIODE acquisition / EDP tracking |
| 2 | 0001-1002 | 2013-04-18 | 2013-05-23 | DIODE acquisition / median tracking |
| 3 | 0001-0400 | 2013-05-23 | 2013-06-06 | DIODE acquisition / median tracking |
| 3 | 0401-0800 | 2013-06-06 | 2013-06-20 | DIODE acquisition / EDP tracking |
| 3 | 0801-1002 | 2013-06-20 | 2013-06-27 | DIODE acquisition / median tracking |
| 4 to 9 | 0001-1002 | 2013-06-27 | 2014-01-23 | DIODE acquisition / median tracking |
| 10 | 0001-0127 | 2014-01-23 | 2014-01-27 | DIODE acquisition / median tracking |
| 10 | 0128-0135 | 2014-01-27 | 2014-01-27 | autonomous DIODE / median tracking |
| | | | | .../... |

| cycle | pass | start time | stop time | altimeter mode |
|-------------------|-----------|------------|------------|-------------------------------------|
| 10 | 0136-1002 | 2014-01-27 | 2014-02-27 | DIODE acquisition / median tracking |
| 11 to 16 | 0001-1002 | 2014-02-27 | 2014-09-25 | DIODE acquisition / median tracking |
| 17 | 0001-0324 | 2014-09-25 | 2014-10-06 | DIODE acquisition / median tracking |
| 17 | 0414-0457 | 2014-10-09 | 2014-10-11 | autonomous DIODE / median tracking |
| 17 | 0457-1002 | 2014-10-11 | 2014-10-30 | DIODE acquisition / median tracking |
| 18 to end of 2014 | 0001-1002 | 2014-10-30 | 2014-12-31 | DIODE acquisition / median tracking |

Table 2: *Events*

2.2.2. List of events

The following table shows the major events during the beginning of Saral/AltiKa mission.

| cycle | pass | start time | stop time | event |
|-------|------------|------------------------|------------|---|
| 1 | | 2013-03-14 | 2013-03-17 | X-band stations acquisition problems (a few missing data) |
| 1 | 0172-0175 | 2013-03-20 05:10:03 | 08:30 | calibration I2+Q2 and I&Q for expertise |
| 1 | 0266 | 2013-03-23 12:13:52 | 12:13:55 | semi major axis maneuver |
| 1 | 0372, 0374 | 2013-03-27 | | CAL2 long calibrations at 04:51 (28min missing data) and 06:40 (11min missing data) |
| 1 | 0801 | 2013-04-11 04:42:00 | 04:59:45 | altimeter gain calibration I2+Q2 (mostly over land) |
| 1 | 0868 | 2013-04-13 12:53:52 | 12:53:54 | station keeping maneuver |
| 1 | 0898 | 2013-04-14 13:42:00 | 13:59:45 | altimeter gain calibration I&Q (mostly over land) |
| | | | | .../... |

| cycle | pass | start time | stop time | event |
|-------|---------------|------------------------|-----------|---|
| 1 | 0984 | 2013-04-17 13:47:00 | 14:04:45 | altimeter gain calibration I2+Q2 (mostly over land) |
| 2 | 0034, 0035 | 2013-04-19 9:37 | 10:25 | cross calibration test over S-band station Biak (Indonesia) |
| 2 | 0057 | 2013-04-20 04:53 | 05:12 | altimeter gain calibration I&Q (over land) |
| 2 | 0127 | 2013-04-22 15:26 | 15:54 | cross calibration maneuver |
| 2 | 0206 | 2013-04-25 9:53 | | pitch maneuver (0.045°) to correct the PF/RF alignment (alignment between the platform and the radiofrequency axis) |
| 2 | 0355 | 2013-04-30 14:35 | 15:03 | cross calibration maneuver |
| 2 | 0782 | 2013-05-15 12:48:23 | 12:48:26 | station keeping maneuver |
| 3 | 0438 | 2013-06-07 12:25:11 | 12:25:13 | station keeping maneuver |
| 3 | 0887- 0890 | 2013-06-23 05:06:55 | 06:56:57 | no O/I/GDR product due to PLTM lost |
| 3 | 0926 | 2013-06-24 13:31:11 | 13:31:13 | station keeping maneuver |
| 4 | 0498 | 2013-07-14 14:42:44 | 14:42:47 | station keeping maneuver |
| 4 | 0556 | 2013-07-16 15:01:01 | 15:19:00 | altimeter gain calibration I&Q (mostly over land) |
| 4 | 0586 | 2013-07-17 16:13:01 | 16:30:45 | altimeter gain calibration I2+Q2 (mostly over land) |
| 4 | 0911 | 2013-07-29 00:54:25 | 00:58:26 | inclination maneuver (1 burn on Y and Z axis) |
| 4 | 0984 | 2013-07-31 14:08:03 | 14:08:11 | station keeping maneuver |
| 5 | 0182 | 2013-08-07 13:48:06 | 13:48:09 | station keeping maneuver |
| 5 | 0726 | 2013-08-26 13:51:02 | 13:51:05 | station keeping maneuver |
| | | | | .../... |

| cycle | pass | start time | stop time | event |
|-------|------|------------------------|-----------|---|
| 5 | 0958 | 2013-09-03 16:02:01 | 16:20:00 | altimeter gain calibration I&Q (mostly over land) |
| 6 | 0038 | 2013-09-06 12:44:01 | 13:01:45 | altimeter gain calibration I2+Q2 (over land) |
| 6 | 0812 | 2013-10-03 13:55:39 | 13:57:17 | 1st inclination maneuver to reach the Envisat ground track (1 burn on Z axis) |
| 6 | 0926 | 2013-10-07 13:29:45 | 13:31:25 | 2nd inclination maneuver to reach the Envisat ground track |
| 6 | 0984 | 2013-10-09 14:07:52 | 14:07:57 | station keeping maneuver |
| 7 | 0526 | 2013-10-28 14:11:24 | 14:11:26 | station keeping maneuver |
| 7 | 0586 | 2013-10-30 16:11 | 16:28:45 | altimeter gain calibration I2+Q2 |
| 7 | 0812 | 2013-11-07 13:57:01 | 13:57:03 | station keeping maneuver |
| 8 | 0326 | 2013-11-25 14:31:29 | 14:31:32 | station keeping maneuver |
| 8 | 0812 | 2013-12-12 13:56:58 | 13:57:01 | station keeping maneuver |
| 9 | 0240 | 2013-12-27 14:25:41 | 14:25:44 | station keeping maneuver |
| 10 | 0128 | 2014-01-27 16:15 | 16:32:45 | altimeter gain calibration I2+Q2 (mostly over land) |
| 10 | 0152 | 2014-01-28 12:38:43 | 12:38:45 | station keeping maneuver |
| 11 | 0126 | 2014-03-03 14:50:53 | 14:50:56 | station keeping maneuver |
| 11 | 0782 | 2014-03-26 12:47:17 | 12:47:20 | station keeping maneuver |
| 12 | 0438 | 2014-04-18 12:24:16 | 12:24:19 | station keeping maneuver |
| 12 | 0728 | 2014-04-28 15:12:55 | 15:30:45 | expertise calibration CAL1 |
| | | | | .../... |

| cycle | pass | start time | stop time | event |
|-------|----------------------|--|----------------------------------|--|
| 13 | 0326-0327 | 2014-05-19 14:31:18 | 14:31:21 | station keeping maneuver with two consecutive mispointing events between 14:38 and 14:43 and between 15:03 and 15:12 |
| 14 | 0782 | 2014-07-09 12:47:10 | 12:47:12 | station keeping maneuver |
| 15 | 0356 | 2014-07-29 15:22:00 | 15:39:45 | altimeter gain calibration I2+Q2 (mostly over land) |
| 15 | 0782 | 2014-08-13 12:47:06 | 12:47:08 | station keeping maneuver |
| 16 | 0539 | 2014-09-09 | | No TM from 01:02:30 to 01:06:16 and from 01:09:25 to 01:14:08 due to the update of MNT onboard parameters |
| 16 | 0640 | 2014-09-12 13:44:34 | 13:44:36 | station keeping maneuver |
| 16 | 0406 0474 0690 | 2014-09-04 09:44:24 2014-09-06 18:38:32 2014-09-14 07:36:44 | 09:47:15 18:41:55 07:38:50 | several platform mispointing events caused by a rise in reaction wheel friction due to movement of lubricant. Only the 3 largest events are shown on the left. |
| 17 | 0324 | 2014-10-06 12:40:00 | 12:40:02 | station keeping maneuver |
| 17 | 0324-0414 | 2014-10-06 13:03:22 | 2014-10-09 16:27:46 | safe hold mode |
| 17 | 0438 | 2014-10-10 12:14:14 | 12:14:34 | station keeping maneuver |
| 17 | 0610 | 2014-10-16 12:26:26 | 12:26:35 | station keeping maneuver |
| 17 | 0958 | 2014-10-28 16:02:00 | 16:19:45 | altimeter gain calibration I2&Q2 |
| 18 | 0152 | 2014-11-04 12:26:39 | 12:26:41 | station keeping maneuver |
| 18 | 0640 | 2014-11-21 13:39:10 | 13:39:12 | station keeping maneuver |
| | | | | .../... |

| cycle | pass | start time | stop time | event |
|-------|------|------------------------|-----------|--------------------------|
| 19 | 0182 | 2014-12-10 13:47:02 | 13:47:04 | station keeping maneuver |
| 19 | 0640 | 2014-12-26 13:44:42 | 13:44:45 | station keeping maneuver |

Table 3: *Events (red lines indicates safe hold mode event)*

2.2.3. Missing measurements

This section presents a summary of major satellite or ground segment events that occurred from cycle 1 to 18 (see also section 3.1.). Table 4 gives a status about the number of missing passes (or partly missing) for GDRs, as well as the associated events for each cycle.

Up to now, Saral/AltiKa had a few little missing measurements caused by station acquisition problems or scheduled events (like altimeter expert calibrations). There was also a three-days safe hold mode during cycle 17 caused by a rise in reaction wheel friction due to movement of lubricant.

| cycle | pass | dates | event |
|---------|-----------|---------------------------------|--|
| 1 | 0007 | 2013-03-14 10:59:58 to 11:01:34 | routine calibration |
| 1 | 0016 | 2013-03-14 18:59:59 to 19:01:34 | routine calibration |
| 1 | 0026 | 2013-03-15 02:59:59 to 03:01:34 | routine calibration |
| 1 | 0032 | 2013-03-15 08:02:51 to 08:14:59 | acquisition problems for X-band stations |
| 1 | 0032-0033 | 2013-03-15 08:23:14 to 09:06:41 | acquisition problems for X-band stations |
| 1 | 0036 | 2013-03-15 10:59:59 to 11:01:34 | routine calibration |
| 1 | 0038 | 2013-03-15 13:08:12 to 13:19:09 | acquisition problems for X-band stations |
| 1 | 0038-0039 | 2013-03-15 13:28:08 to 13:41:00 | acquisition problems for X-band stations |
| 1 | 0039 | 2013-03-15 13:48:43 to 14:06:33 | acquisition problems for X-band stations |
| 1 | 0039-0040 | 2013-03-15 14:09:32 to 14:23:17 | acquisition problems for X-band stations |
| 1 | 0044 | 2013-03-15 18:10:11 to 18:21:11 | acquisition problems for X-band stations |
| 1 | 0044-0045 | 2013-03-15 18:30:11 to 18:40:49 | acquisition problems for X-band stations |
| 1 | 0045 | 2013-03-15 18:59:59 to 19:01:34 | routine calibration |
| .../... | | | |

| cycle | pass | dates | event |
|-------|-----------|---------------------------------|--|
| 1 | 0045-0046 | 2013-03-15 19:12:01 to 19:26:57 | acquisition problems for X-band stations |
| 1 | 0046 | 2013-03-15 19:33:54 to 19:37:18 | acquisition problems for X-band stations |
| 1 | 0047 | 2013-03-15 20:35:25 to 20:57:31 | acquisition problems for X-band stations |
| 1 | 0047-0048 | 2013-03-15 20:57:43 to 21:08:58 | acquisition problems for X-band stations |
| 1 | 0048 | 2013-03-15 21:17:45 to 21:32:56 | acquisition problems for X-band stations |
| 1 | 0048 | 2013-03-15 21:38:34 to 21:49:45 | acquisition problems for X-band stations |
| 1 | 0051 | 2013-03-15 23:40:13 to 23:54:57 | acquisition problems for X-band stations |
| 1 | 0051 | 2013-03-16 00:01:12 to 00:16:57 | acquisition problems for X-band stations |
| 1 | 0051-0052 | 2013-03-16 00:22:49 to 00:37:41 | acquisition problems for X-band stations |
| 1 | 0052 | 2013-03-16 00:43:31 to 00:58:15 | acquisition problems for X-band stations |
| 1 | 0055 | 2013-03-16 02:59:59 to 03:01:34 | routine calibration |
| 1 | 0062-0063 | 2013-03-16 09:02:22 to 09:57:57 | acquisition problems for X-band stations |
| 1 | 0063 | 2013-03-16 09:58:29 to 10:09:01 | acquisition problems for X-band stations |
| 1 | 0063 | 2013-03-16 10:10:16 to 10:12:42 | acquisition problems for X-band stations |
| 1 | 0063 | 2013-03-16 10:19:18 to 10:23:46 | acquisition problems for X-band stations |
| 1 | 0064 | 2013-03-16 10:30:42 to 10:33:07 | acquisition problems for X-band stations |
| 1 | 0064 | 2013-03-16 10:53:38 to 10:56:45 | acquisition problems for X-band stations |
| 1 | 0064 | 2013-03-16 10:59:59 to 11:01:34 | routine calibration |
| 1 | 0064-0065 | 2013-03-16 11:03:40 to 11:20:13 | acquisition problems for X-band stations |
| 1 | 0066 | 2013-03-16 12:25:28 to 12:36:38 | acquisition problems for X-band stations |
| 1 | 0066-0067 | 2013-03-16 12:45:31 to 13:01:03 | acquisition problems for X-band stations |
| 1 | 0067-0068 | 2013-03-16 13:06:18 to 13:52:01 | acquisition problems for X-band stations |
| 1 | 0074 | 2013-03-16 19:00:00 to 19:01:34 | routine calibration |
| 1 | 0083 | 2013-03-17 02:59:59 to 03:01:34 | routine calibration |
| | | | .../... |

| cycle | pass | dates | event |
|-------|-----------|---------------------------------|---|
| 1 | 0102 | 2013-03-17 18:59:59 to 19:01:34 | routine calibration |
| 1 | 0172-0175 | 2013-03-20 05:10 to 08:30 | expertise calibrations → small data gaps every 10 minutes |
| 1 | 0372 | 2013-03-27 04:50:59 to 05:18:19 | CAL2 long calibration |
| 1 | 0374 | 2013-03-27 06:39:59 to 06:51:29 | CAL2 long calibration |
| 1 | 0801 | 2013-04-11 04:41:59 to 04:59:46 | altimeter gain calibration I2+Q2 |
| 1 | 0898 | 2013-04-14 13:41:59 to 13:59:46 | altimeter gain calibration I&Q |
| 1 | 0984 | 2013-04-17 13:46:59 to 14:04:46 | altimeter gain calibration I2+Q2 |
| 2 | 0057 | 2013-04-20 04:52:59 to 05:10:45 | altimeter gain calibration I&Q |
| 3 | 0887-0890 | 2013-06-23 05:06:56 to 06:56:58 | PLTM loss |
| 4 | 0556 | 2013-07-16 15:01:00 to 15:19:01 | altimeter gain calibration I&Q |
| 4 | 0586 | 2013-07-17 16:13:00 to 16:30:46 | altimeter gain calibration I2+Q2 |
| 4 | 0929 | 2013-07-29 15:45:56 to 15:55:23 | downlink acquisition problem |
| 4 | 0929 | 2013-07-29 16:05:23 to 16:25:34 | downlink acquisition problem |
| 4 | 0931 | 2013-07-29 17:33:54 to 17:44:14 | downlink acquisition problem |
| 4 | 0931 | 2013-07-29 17:54:13 to 18:06:33 | downlink acquisition problem |
| 4 | 0932 | 2013-07-29 18:06:52 to 18:11:01 | downlink acquisition problem |
| 4 | 0933 | 2013-07-29 19:08:07 to 19:15:03 | downlink acquisition problem |
| 4 | 0933 | 2013-07-29 19:17:09 to 19:27:49 | downlink acquisition problem |
| 4 | 0933 | 2013-07-29 19:28:29 to 19:36:07 | downlink acquisition problem |
| 4 | 0933 | 2013-07-29 19:38:00 to 19:43:44 | downlink acquisition problem |
| 4 | 0938 | 2013-07-29 23:20:23 to 23:26:59 | downlink acquisition problem |
| 4 | 0939 | 2013-07-30 00:16:30 to 00:30:48 | downlink acquisition problem |
| 4 | 0940 | 2013-07-30 01:11:00 to 01:13:59 | downlink acquisition problem |
| 4 | 0940 | 2013-07-30 01:31:06 to 01:32:49 | downlink acquisition problem |
| 4 | 0941 | 2013-07-30 01:42:43 to 01:47:35 | downlink acquisition problem |
| 4 | 0941 | 2013-07-30 02:12:17 to 02:18:29 | downlink acquisition problem |
| 4 | 0942 | 2013-07-30 02:34:08 to 02:40:27 | downlink acquisition problem |
| | | | .../... |

| cycle | pass | dates | event |
|-------|-----------|--|--|
| 4 | 0942 | 2013-07-30 02:49:30 to 03:09:18 | downlink acquisition problem |
| 4 | 0942-0943 | 2013-07-30 03:10:08 to 03:21:43 | downlink acquisition problem |
| 4 | 0943-0944 | 2013-07-30 03:30:41 to 04:13:16 | downlink acquisition problem |
| 5 | 0958 | 2013-09-03 16:02:00 to 16:20:01 | altimeter gain calibration I&Q |
| 6 | 0038 | 2013-09-06 12:44:01 to 13:01:45 | altimeter gain calibration I2+Q2 |
| 6 | 0940 | 2013-10-08 01:17:00 to 01:23:48 | station tracking issue |
| 6 | 0941 | 2013-10-08 01:46:59 to 01:57:43 | station tracking issue |
| 6 | 0941 | 2013-10-08 02:06:46 to 02:18:50 | station tracking issue |
| 7 | 0089 | 2013-10-13 07:58:24 to 08:01:35 | missing TM (which had not been filled by PLTM GAP files) |
| 7 | 0352 | 2013-10-22 12:13:04 to 12:15:45 | modification of onboard radiometer database values |
| 7 | 0586 | 2013-10-30 16:11:00 to 16:28:45 | altimeter gain calibration I2+Q2 |
| 8 | 0391 | 2013-11-27 20:49:23 to 21:01:42 | PLTM loss |
| 9 | 0143-0146 | 2013-12-24 05:31:16 to 07:11:52 | PLTM loss |
| 10 | 0128 | 2014-01-27 16:15 to 16:32:45 | altimeter gain calibration I2+Q2 |
| 11 | 0126 | 2014-03-03 14:51:34 to 14:52:30 | maneuver |
| 12 | 0728 | 2014-04-28 15:12:55 to 15:30:45 | expertise calibration CAL1 |
| 13 | 0326 | 2014-05-19 14:38:24 to 14:42:53 | maneuver |
| 15 | 0356 | 2014-07-29 15:22:00 to 15:39:45 | altimeter gain calibration I2&Q2 |
| 16 | 0539 | 2014-09-09 01:02:30 to 01:06:16 | update of onboard DEM parameters |
| 16 | 0539 | 2014-09-09 01:09:25 to 01:14:08 | update of onboard DEM parameters |
| 17 | 0324-0414 | 2014-10-06 13:03:22 to 2014-10-09 16:27:46 | safe hold mode |
| 17 | 0958 | 2014-10-28 16:02:00 to 16:19:45 | altimeter gain calibration I2&Q2 |

Table 4: *Missing pass status***2.2.4. Edited measurements**

Table 5 indicates particular high editing periods (see section 3.2.). Most of the occurrences correspond to maneuvers.

| cycle | pass | date | comments |
|-------|------|------------|---|
| 1 | 0266 | 2013-03-23 | Partly edited by several parameters out of threshold (semi major axis maneuver) |
| 1 | 0868 | 2013-04-13 | Partly edited by several parameters out of threshold (maneuver) |
| 2 | 0728 | 2013-05-15 | Partly edited by several parameters out of threshold (station keeping maneuver) |
| 3 | 0438 | 2013-06-07 | Partly edited by several parameters out of threshold (station keeping maneuver) |
| 3 | 0926 | 2013-06-24 | Partly edited by several parameters out of threshold (station keeping maneuver) |
| 4 | 0498 | 2013-07-14 | Partly edited by several parameters out of threshold (station keeping maneuver) |
| 4 | 0911 | 2013-07-29 | Partly edited by several parameters out of threshold (inclination maneuver) |
| 4 | 0941 | 2013-07-30 | about 3 minutes of this pass have two 1-Hz data per second, instead of one |
| 4 | 0984 | 2013-07-31 | Partly edited by several parameters out of threshold (inclination maneuver) |
| 5 | 0182 | 2013-08-07 | Partly edited by several parameters out of threshold (station keeping maneuver) |
| 5 | 0726 | 2013-08-26 | Partly edited by several parameters out of threshold (station keeping maneuver) |
| 6 | 0812 | 2013-10-03 | Partly edited by several parameters out of threshold (inclination maneuver) |
| 6 | 0926 | 2013-10-07 | Partly edited by several parameters out of threshold (inclination maneuver) |
| 6 | 0984 | 2013-08-26 | Partly edited by several parameters out of threshold (station keeping maneuver) |
| 7 | 0526 | 2013-10-28 | Partly edited by several parameters out of threshold (station keeping maneuver) |
| 7 | 0812 | 2013-11-07 | Partly edited by several parameters out of threshold (station keeping maneuver) |
| | | | .../... |

| cycle | pass | date | comments |
|-------|-----------|------------|--|
| 8 | 0326 | 2013-11-25 | Partly edited by several parameters out of threshold (station keeping maneuver) |
| 8 | 0812 | 2013-12-12 | Partly edited by several parameters out of threshold (station keeping maneuver) |
| 9 | 0240 | 2013-12-27 | Partly edited by several parameters out of threshold (station keeping maneuver) |
| 9 | - | - | Few passes partly edited by significant wave height values out of maximum threshold (geophysical conditions) |
| 10 | 0152 | 2014-01-28 | Partly edited by several parameters out of threshold (station keeping maneuver) |
| 11 | 0126 | 2014-03-03 | Partly edited by several parameters out of threshold (station keeping maneuver) |
| 11 | 0782 | 2014-03-26 | Partly edited by several parameters out of threshold (station keeping maneuver) |
| 12 | 0438 | 2014-04-18 | Partly edited by several parameters out of threshold (station keeping maneuver) |
| 13 | 0326-0327 | 2014-05-19 | Partly edited by several parameters out of threshold (maneuver followed by a perturbation on the satellite pointing) |
| 14 | 0782 | 2014-07-09 | Partly edited by several parameters out of threshold (station keeping maneuver) |
| 15 | 0782 | 2014-08-13 | Partly edited by several parameters out of threshold (station keeping maneuver) |
| 16 | 0640 | 2014-09-12 | Partly edited by several parameters out of threshold (station keeping maneuver) |
| 16 | - | - | Several passes partly edited by mispointing values out of maximum threshold (wheel friction) |
| 16 | - | - | Several passes partly edited by significant wave height values out of maximum threshold (geophysical reasons) |
| 17 | 0324 | 2014-10-06 | Fully edited on SLA statistics per pass criteria (maneuver before SHM) |
| 17 | 0441 | 2014-10-10 | Fully edited on SLA statistics per pass criteria (high SLA values along the southern coast of Alaska – geophysical conditions) |
| 17 | - | - | Several passes partly edited by several parameters out of threshold (mispointing events) |
| | | | .../... |

| cycle | pass | date | comments |
|-------|------|------------|--|
| 18 | 0640 | 2014-11-21 | Partly edited by several parameters out of threshold (station keeping maneuver) |
| 18 | - | - | Several passes partly edited by mispointing values out of maximum threshold (mispointing events after SHM) |

Table 5: Edited measurement status

2.3. Models and Standards History

During 2013 only GDR products in version T were available for cycles 1 to 7. These products were homogeneous and used all the Patch1 (see content of Patch 1 in chapter 10.1.).

At the beginning of 2014, improvements to Saral/AltiKa data have been applied with the Patch 2. This Patch 2 was applied from cycle 8 onwards and cycles 1 to 7 were reprocessed to provide a homogeneous GDR dataset. The content of Patch 2 is given in appendix 10.2., and the comparisons between Patch 1 and Patch 2 data can be found in [11]). The standards used in the GDR products version "T" Patch2 are listed in table 6.

| Model | Product version "T" Patch2 |
|----------------------|--|
| Orbit | Based on Doris onboard navigator solution for OGDRS. DORIS tracking data for IGDRs DORIS+SLR tracking data for GDRs. Using POE-D |
| Altimeter Retracking | <p>"Ocean MLE4" retracking: MLE4 fit from 2nd order Brown analytical model: MLE4 simultaneously retrieves 4 parameters from the altimeter waveforms:</p> <ul style="list-style-type: none"> • Epoch (tracker range offset) → altimeter range • Composite Sigma → SWH • Amplitude → Sigma0 • Square of mispointing angle <p>"Ice 1" retracking: Geometrical analysis of the altimeter waveforms, which retrieves the following parameters:</p> <ul style="list-style-type: none"> • Epoch (tracker range offset) → altimeter range • Amplitude → Sigma0 <p style="text-align: right;">.../...</p> |

| Model | Product version "T" Patch2 |
|------------------------------------|--|
| | <p>"Ice 2" retracking: The aim of the ice2 retracking algorithm is to make the measured waveform coincide with a return power model, according to Least Square estimators. Retrieval of the following parameters:</p> <ul style="list-style-type: none"> • Epoch → altimeter range • Width of the leading edge → SWH/ • Amplitude → Sigma0 • Slope of the logarithm of the waveform at the trailing edge → Mispointing angle/surface slope • the thermal noise level (to be removed from the waveform samples) <p>"Sea Ice" retracking: In this algorithm, waveform parameterization based on peak threshold retracking is applied to the Ka-band waveform. From this parameterization, a tracking offset and backscatter estimate are determined. Tests are made on the extent of the tracking offset, and extreme values are flagged as retracking failures. The sea-ice waveform amplitude is determined by finding the maximum value of the waveform samples and the tracking offset is determined by finding the point on the waveform (by interpolation) where the waveform amplitude exceeds a threshold determined from the above sea-ice amplitude. A tracking offset is determined. The Centre Of Gravity offset correction must be included in the range measurement as the correction is not available separately in the L2 product.</p> <ul style="list-style-type: none"> • Amplitude → Sigma0 • Tracking offset → altimeter range • Centre Of Gravity offset correction → correction to altimeter range measurement <p>N.B.: the Ice2 retracking algorithm have been tuned to Ka-band since Patch2, but ont the Ice1 not Sea Ice algorithms</p> |
| Altimeter Instrument Corrections | consistent with MLE4 retracking |
| Saral/AltiKa Radiometer Parameters | Using on-board calibration |
| .../... | |

| Model | Product version "T" Patch2 |
|---|---|
| Dry Troposphere Range Correction | From ECMWF atmospheric pressures and model for S1 and S2 atmospheric tides |
| Wet Troposphere Range Correction from Model | From ECMWF model |
| Ionosphere correction | Based on Global Ionosphere TEC Maps from JPL |
| Sea State Bias Model | Hybrid SSB model from [12] |
| Mean Sea Surface | MSS_CNES-CLS11 |
| Mean Dynamic Topography | MDT_CNES-CLS09 |
| Geoid | EGM96 |
| Bathymetry Model | DTM2000.1 |
| Inverse Barometer Correction | Computed from ECMWF atmospheric pressures after removing S1 and S2 atmospheric tides |
| Non-tidal High-frequency De-aliasing Correction | Mog2D high resolution ocean model on (I)GDRs. None for OGDRs. Ocean model forced by ECMWF atmospheric pressures after removing S1 and S2 atmospheric tides. |
| Tide Solution 1 | GOT4.8 |
| Tide Solution 2 | FES2012 + S1 and M4 ocean tides. S1 and M4 load tides ignored |
| Equilibrium long-period ocean tide model. | From Cartwright and Taylor tidal potential. |
| Non-equilibrium long-period ocean tide model. | Mm, Mf, Mtm, and Msqm from FES2004 |
| Solid Earth Tide Model | From Cartwright and Taylor tidal potential. |
| Pole Tide Model | Equilibrium model |
| Wind Speed from Model | ECMWF model |
| Altimeter Wind Speed | wind speed model from [9] |
| Trailing edge variation Flag | Derived from Matching Pursuit algorithm (from J. Tournadre, IFREMER) |
| .../... | |

| Model | Product version "T" Patch2 |
|----------|--|
| Ice flag | Initialized in climatological areas based on wind speed values and updated by comparing the model wet tropospheric correction and the dual-frequency wet tropospheric correction retrieved from radiometer brightness temperatures |

Table 6: Models and standards adopted for the Saral/AltiKa version "T" products (using Patch 2). Adapted from [4]

3. Data coverage and edited measurements

3.1. Missing measurements

3.1.1. Over land and ocean

Determination of missing measurements relative to the theoretically expected orbit ground pattern is an essential tool to detect missing telemetry or satellite events for instance. Applying the same procedure for Saral/AltiKa and Jason-2, the comparison of the percentage of missing measurements has been performed.

AltiKa can use several on board tracking modes: Median, EDP (Earliest Detectable Part) and Diode/DEM (see chapter 2.2.1.). Median mode is similar to the one used by Envisat and for most cycles of Jason-2. EDP tracker should improve the tracker behavior above continental ice surfaces and hydrological zones. Finally, Diode/DEM mode is a technique using information coming from Diode and a digital elevation model available on board. It was already tested on Jason-2. For more information about the different on board tracker algorithms see [6]. The information about the acquisition / tracking mode used is available in the GDR (fields `alt_state_flag_acq_mode_40hz` and `alt_state_flag_tracking_mode_40hz`).

Saral/AltiKa usually uses the **DIODE acquisition / median tracking mode**.

Considering all surface types, Saral/AltiKa has more data available than Jason-2 (which also uses most of the time the median tracker), independently from the tracker mode used for Saral. Figure 1 shows the percentage of available measurements for Saral/AltiKa and Jason-2 (all surfaces) computed with respect to a theoretical possible number of measurements. As long as a record exists for a given date, the measurement is accounted as present (though it may be that there is no useful science data). Differences appear on land surfaces as shown in figure 2. The missing data are highly correlated with the mountains location. Note that the routine calibrations for Saral/AltiKa are done over desert regions, such as Sahara, over Australia, in the south of Africa and over Asia (Mongolia). Therefore the percentage of available data is low in these regions. Otherwise Saral has more available data over land surface than Jason-2. This is probably due to the reduced footprint of Saral compared to Jason-2.

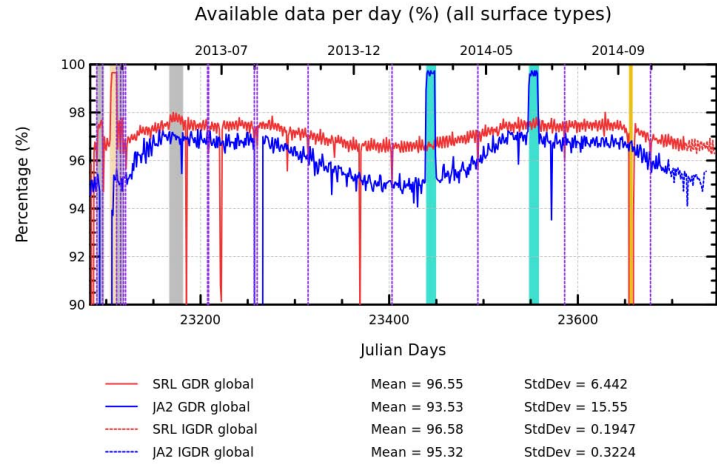


Figure 1: Percentage of available measurements over all types of surfaces for SRL and JA2. Gray bands indicate when Saral/AltiKa uses EDP tracking, wheat color band indicates when Saral/AltiKa used Diode/DEM tracking, turquoise color band indicates when Jason-2 used Diode/DEM tracking, gold color band indicates when Saral/AltiKa is on safe-hold mode. Vertical dotted lines in lilac indicate days with special calibrations.

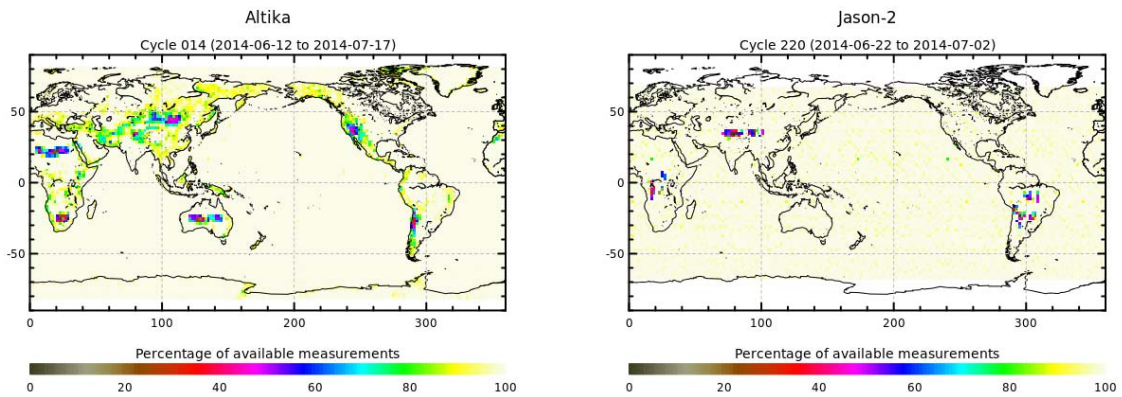


Figure 2: Map of percentage of available measurements over land for Saral/AltiKa on cycle 14 and for Jason-2 on cycle 220 (right).

3.1.2. Over ocean

When considering ocean surface, the same analysis method leads generally to slightly less available data for Saral/AltiKa compared to Jason-2 data coverage, as plotted on the left of figure 3. It represents the percentage of available measurements relative to the theory, when limited to ocean surfaces. Over the shown period, the mean value is about 97.1% for Jason-2, and 99.2% for Saral/AltiKa. Note that Jason-2 has two safe-hold mode periods and Saral/AltiKa one safe-hold mode period, which explains the globally lower value for Jason-2. Saral/AltiKa had other periods with reduced data availability. All these events are described on table 4.

On the right of figure 3, the percentage of available measurements is plotted without taking into account the days where instrumental events or other big anomalies occurred. The mean value of available measurements increased to 99.98% for Jason-2 and 99.88% for Saral/AltiKa. These 0.1% of fewer data over ocean for Saral/AltiKa compared to Jason-2 are likely due to the impact of rain due to the Ka-band frequency. This exceeds largely the specifications for Saral/AltiKa, which were (see [14]) 95% of all possible over-ocean data during a 3-year period with no systematic gaps plus the specific Ka-band limitation (5% of measurements may be not achieved due to rain rate > 1.5 mm/h according to geographic areas).

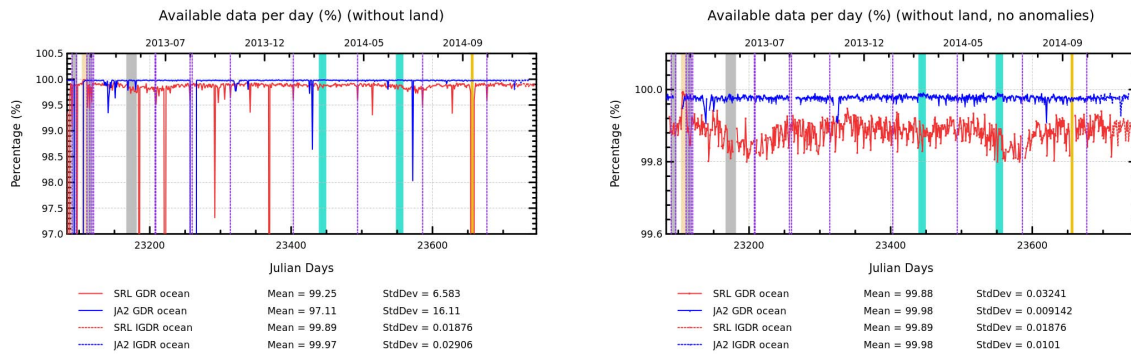


Figure 3: *Cycle per cycle percentage of available measurements over ocean (left) and without anomalies (right) for Saral/AltiKa and Jason-2. Gray bands indicate when Saral/AltiKa uses EDP tracking, wheat color band indicates when Saral/AltiKa used Diode/DEM tracking, turquoise color band indicates when Jason-2 used Diode/DEM tracking, gold color band indicates when Saral/AltiKa is on safe-hold mode. Lilac vertical lines, indicate days with special calibrations, which can be over ocean.*

3.2. Edited measurements

3.2.1. Editing criteria definition

Editing criteria are used to select valid measurements over ocean. The editing process is divided into 4 parts. First, only measurements over ocean and lakes are kept (see section 3.2.2.). Second, some flags are used as described in section 3.2.3.. Note that the rain flag is not usable yet in the GDR products (always set to zero). But most measurements corrupted by rain are well detected by other altimeter parameter criteria. Then, threshold criteria are applied on altimeter, radiometer and geophysical parameters and are described in the table 7. Moreover, a spline criterion is applied to remove the remaining spurious data. For each criterion, the day per day percentage of edited measurements has been monitored. This allows detection of anomalies in the number of removed data, which could come from instrumental, geophysical or algorithmic changes. Cycle per cycle statistics of edited data are also routinely monitored, but not shown here, as only a few cycles are available.

Note that the altimeter wind speed is usable since the GDR-T Patch2 has been applied.

| Parameter | Min thresholds | Max thresholds | mean edited |
|---------------------------------------|-----------------------|-------------------------|-------------|
| Sea surface height | -130 m | 100 m | 0.47% |
| Sea level anomaly | -2 m | 2 m | 0.80% |
| Number measurements of range | 20 | <i>Not applicable</i> | 1.10% |
| Standard deviation of range | 0 | 0.2 m | 1.51% |
| Squared off-nadir angle | -0.2 deg ² | 0.0625 deg ² | 0.42% |
| Dry troposphere correction | -2.5 m | -1.9 m | 0.00% |
| Inverted barometer correction | -2 m | 2 m | 0.00% |
| Radiometer wet troposphere correction | -0.5m | 0 m | 0.06% |
| Significant wave height | 0 m | 11 m | 0.42% |
| Sea State Bias | -0.5 m | 0.0025 m | 0.29% |
| Number measurements of Ka-band Sigma0 | 20 | <i>Not applicable</i> | 1.03% |
| Standard deviation of Ka-band Sigma0 | 0 | 1 dB | 0.94% |
| Ka-band Sigma0 | 3 dB | 30 dB | 0.35% |
| Ocean tide | -5 m | 5 m | 0.18% |
| Equilibrium tide | -0.5 m | 0.5 m | 0.17% |
| | | | .../... |

| Parameter | Min thresholds | Max thresholds | mean edited |
|----------------------|----------------|----------------|-------------|
| Earth tide | $-1 m$ | $1 m$ | 0.00% |
| Pole tide | $-0.15 m$ | $0.15 m$ | 0.00% |
| Altimeter wind speed | $0 m.s^{-1}$ | $30 m.s^{-1}$ | 0.29% |
| All together | - | - | 2.60% |

Table 7: *Editing criteria, statistics obtained for cycles 1 to 18*

3.2.2. Selection of measurements over ocean and lakes

In order to remove data over land, a land-water mask is used (surface.type in the GDR products). Only measurements over ocean or lakes are kept. This allows to keep data near the coasts and so to detect potential anomalies in these areas. Furthermore, there is no impact on global performance estimations since the most significant results are derived from analyzes in deep ocean areas. Figure 4 shows the day per day percentage of measurements eliminated by this selection. The curve is quite stable even after the safe-hold mode. But it reveals the impact of the different altimeter tracking modes: when the DIODE/DEM (digital elevation model) tracking mode is used (wheat colored stripe), slightly more data are edited by land flag. This is an expected result: less data are missing in DIODE/DEM mode over land, as a consequence there is a higher percentage of edited data.

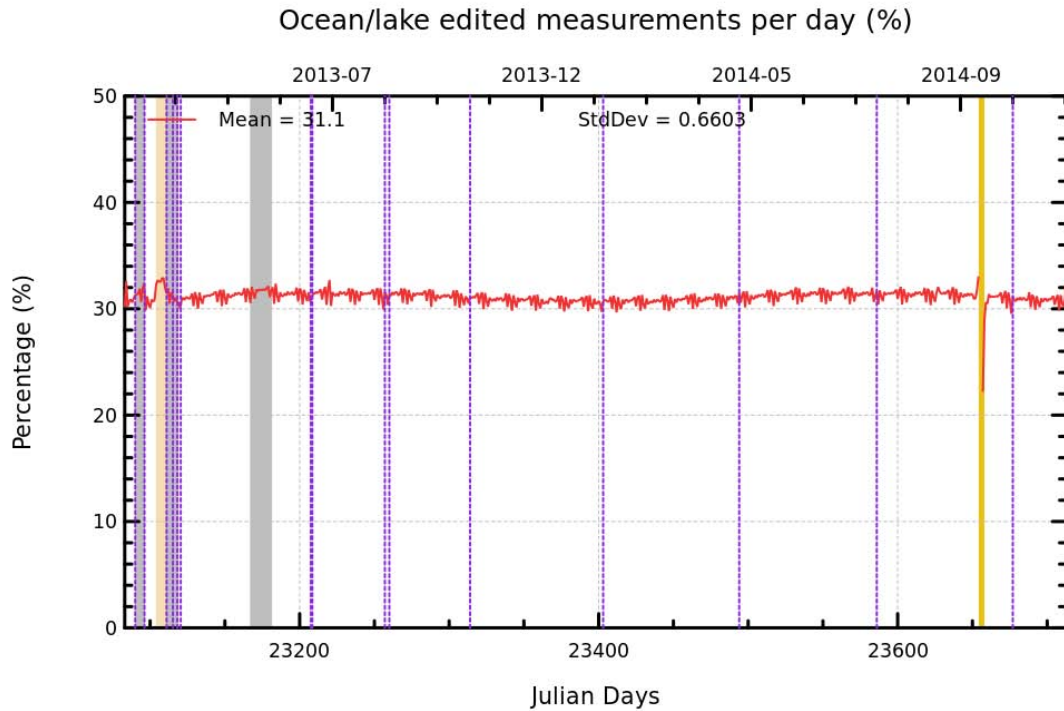


Figure 4: Day per day percentage of eliminated measurements during selection of ocean/lake measurements. Gray bands indicate when Saral/AltiKa uses EDP tracking, wheat color band indicates when Saral/AltiKa used Diode/DEM tracking, elsewhere Median tracking is used. Gold color band indicates when Saral/AltiKa is on safe-hold mode. Vertical dotted lines in lilac indicate days with special calibrations.

3.2.3. Flagging quality criteria: Ice flag

The ice flag (ice_flag in the GDR products) is used to remove the sea ice data. Left of figure 5 shows the day per day percentage of measurements edited by this criterion. Over the shown period, no anomalous trend is detected but the nominal seasonal cycle is visible. Considering the black curve, which indicates the percentage of edited Saral/AltiKa data without geographical selections, the minima ($\sim 16\%$ of edited data) appears yearly in February and September. These are also the periods where the antarctic or arctic sea ice extension are minimum. The maxima ($\sim 20\%$ of edited data) of the curve are around May/June and October/November. These are the periods, where arctic or antarctic sea ice extension have approximately mid-values. When limited to $|\text{latitude}| < 66^\circ$, Saral/AltiKa and Jason-2 percentage of data edited by sea ice have a similar annual cycle, which is correlated to the antarctic sea ice extension. Indeed, the maximum number of points over ice is reached during the southern winter (ie. August - October). When limiting measurements between 66° north and south, thawing of sea ice, which takes place especially in northern hemisphere over 66°N , can not be detected. The percentage of measurements edited by ice flag is plotted in the right of figure 5 for all the period since the beginning of mission. White color indicates when the flag is set to 0 (no ice).

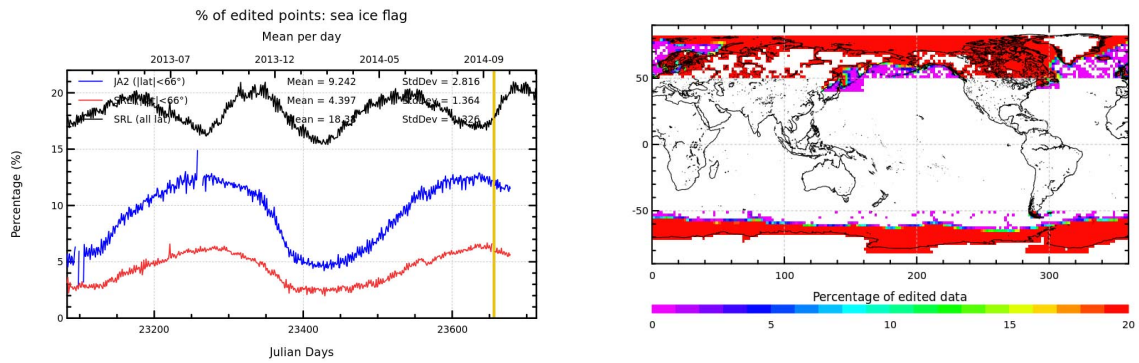


Figure 5: Percentage of edited measurements by ice flag criterion. Left: Daily statistics for GDR Saral/AltiKa (all latitudes: black, limited to 66° latitude: red) and Jason-2 (blue). Gold color band indicates when Saral/AltiKa is on safe-hold mode. Right: Map since beginning of mission (cycles 1 to 18).

3.2.4. Threshold criteria: Global

Instrumental parameters have also been analyzed concerning their quality from comparison with thresholds, after having selected only ocean/lakes measurements and removing sea ice with the ice flag. Note that no measurement is edited by the following corrections : dry troposphere correction, inverted barometer correction (including DAC), equilibrium tide, earth and pole tide. Indeed these parameters are only verified in order to detect data at default values, which might happen during a processing anomaly.

The percentage of edited measurements using each criterion is monitored on a day per day basis (figure 6). The mean percentage of edited measurements is about 2.6% (2.4% when $|\text{latitude}|$ is limited to 66°). This is about 1% below the Jason-2 figure. Some weak variation is visible.

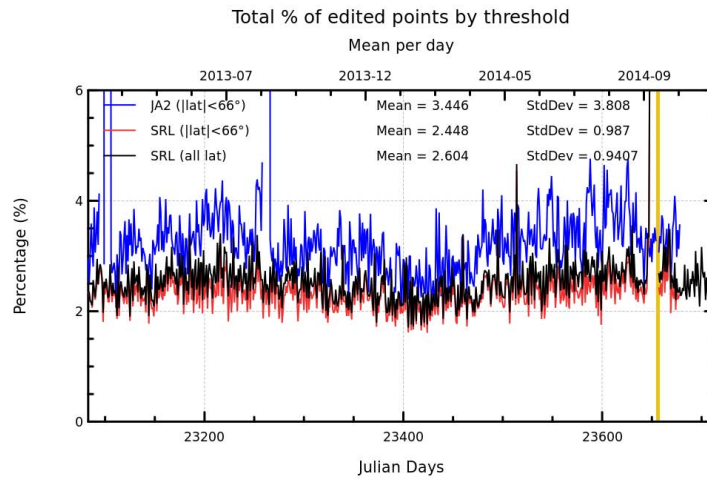


Figure 6: Daily statistics of percentage of edited measurements by threshold criteria for GDR Saral/AltiKa (all latitudes: black, limited to 66° latitude: red) and Jason-2 (blue). Gold color band indicates when Saral/AltiKa is on safe-hold mode.

3.2.5. Threshold criteria: 40-Hz measurements number

The percentage of edited measurements because of a too low number of 40-Hz measurements is represented on the left side of figure 7. No trend nor any anomaly has been detected. The statistics, when limiting the latitude to less than 66° are slightly reduced. The percentage of edited data is similar for Saral/AltiKa and Jason-2.

The map of measurements edited by 40-Hz measurements number criterion is plotted on right side of figure 7 and shows correlation with heavy rain and wet areas (in general regions with disturbed sea state), as well as regions close to sea ice. Indeed waveforms are distorted by rain cells or sigma bloom events, which makes them often meaningless for SSH calculation. As a consequence, edited measurements due to several altimetric criteria are often correlated with wet areas (rain cells/sigma bloom events).

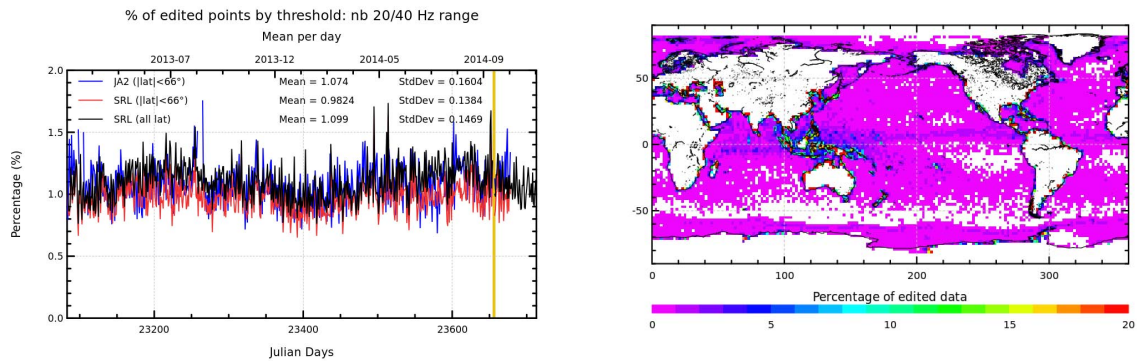


Figure 7: Percentage of edited measurements by 40-Hz measurements number criterion (20-Hz for Jason-2). Left: Daily statistics for Saral/AltiKa (all latitudes: black, limited to 66° latitude: red) and Jason-2 (blue). Gold color band indicates when Saral/AltiKa is on safe-hold mode. Right: Map since beginning of mission (cycles 1 to 18).

3.2.6. Threshold criteria: 40-Hz measurements standard deviation

The percentage of edited measurements due to 40-Hz measurements standard deviation criterion ($\sim 1.5\%$) is shown in figure 8 (left). For some days, more data are edited by this criterion. This is mostly due to safe-hold mode or to maneuver burns (see also table 3), indicated by green vertical lines. In this case, the data a few minutes before and after the maneuver are edited (in general several parameters are out of thresholds) as a consequence of the lower platform pointing accuracy. The right side of figure 8 shows a map of measurements edited by the 40-Hz measurements standard deviation criterion. As in section 3.2.5., edited measurements are correlated with wet areas.

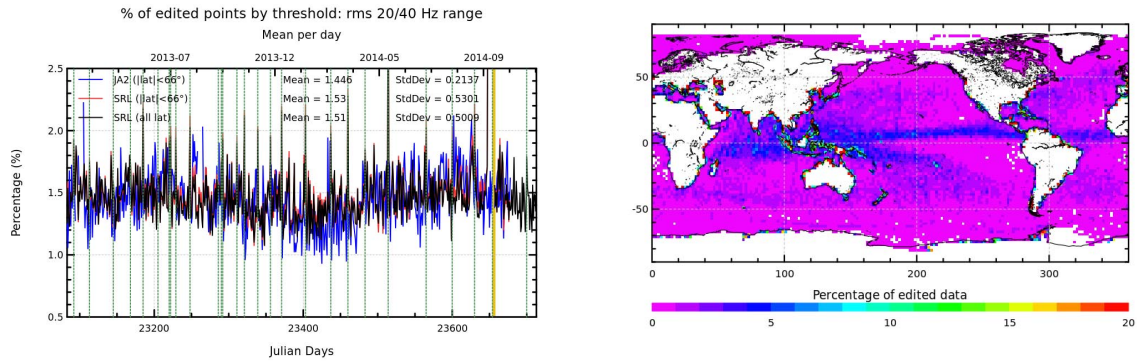


Figure 8: Percentage of edited measurements by 40-Hz measurements standard deviation criterion (20-Hz for Jason-2). Left: Daily statistics for Saral/AltiKa (all latitudes: black, limited to 66° latitude: red) and Jason-2 (blue). Green vertical lines indicate days with maneuvers on Saral/AltiKa and gold band indicates the safe-hold mode on Saral/AltiKa. Right: Map since beginning of mission (cycles 1 to 18).

3.2.7. Threshold criteria: Significant wave height

The percentage of edited measurements due to significant wave height criterion is represented in figure 9. It is about 0.42%. As for standard deviation of 40-Hz data, more data are edited by this criterion for some days. This is mostly due to safe-hold mode and maneuver burns (see also table 3), indicated by green vertical lines. In this case, the data a few minutes before and after the maneuver are edited. Note that for Jason-2, roughly 0.66% of data are edited by SWH out of thresholds. This is mainly due to Jason-2 having almost twice as much SWH data at default values than Saral/AltiKa. Figure 9 (right part) shows that measurements edited by SWH criterion are especially found in wet regions where heavy rains and sigma bloom events can occur.

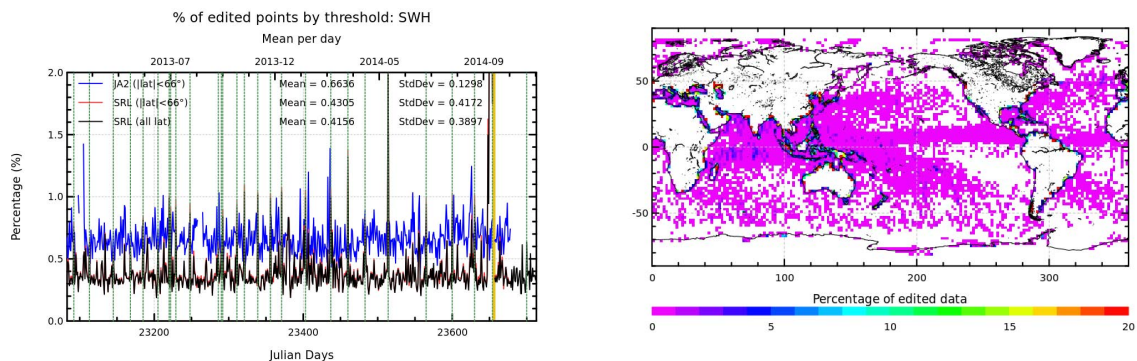


Figure 9: Percentage of edited measurements by SWH criterion. Left: Daily statistics for GDR Saral/AltiKa and Jason-2 (blue). Green vertical lines indicate days with maneuvers on Saral/AltiKa and gold band indicates the safe-hold mode on Saral/AltiKa. Right: Map since beginning of mission (cycles 1 to 18).

3.2.8. Backscatter coefficient

The percentage of edited measurements due to backscatter coefficient criterion is represented in figure 10. It is about 0.35% (whether considering all latitudes or limiting to 66°), compared to 0.61% for Jason-2. It is also impacted by the safe-hold mode and most of the maneuvers (see vertical green lines). As for SWH, Jason-2 has almost twice as much backscattering values at default values than Saral/AltiKa. The right part of figure 10 shows that measurements edited by backscatter coefficient criterion are especially found in wet regions where measurements are impacted by rain events or by sigma bloom events.

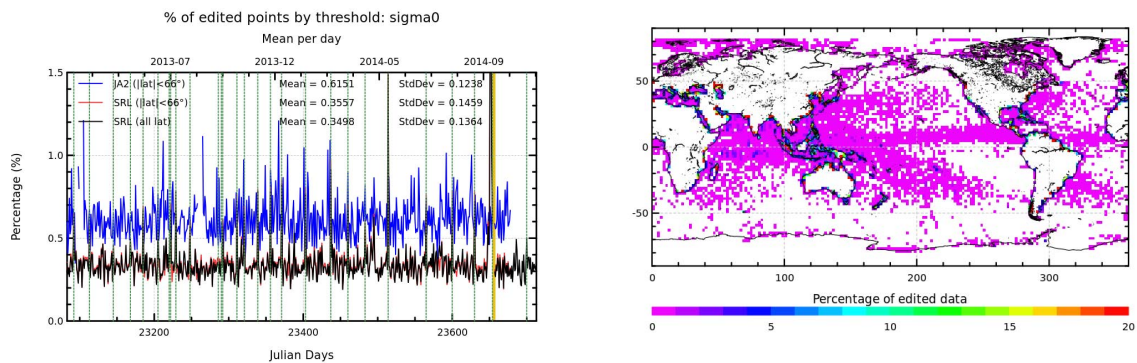


Figure 10: Percentage of edited measurements by $\text{Sigma}0$ criterion. Left: Daily statistics for Saral/AltiKa (all latitudes: black, limited to 66° latitude: red) and Jason-2 (blue). Green vertical lines indicate days with maneuvers on Saral/AltiKa and gold band indicates the safe-hold mode on Saral/AltiKa. Right: Map since beginning of mission (cycles 1 to 18).

3.2.9. Backscatter coefficient: 40 Hz standard deviation

The percentage of edited measurements due to 40 Hz backscatter coefficient standard deviation criterion is represented in figure 11. It is about 0.94%, compared to 1.99% for Jason-2. It is also impacted by the safe-hold mode and some of the maneuvers (see vertical green lines). The right part of figure 10 shows that measurements edited by 40 Hz backscatter coefficient standard deviation criterion are mostly found in wet regions.

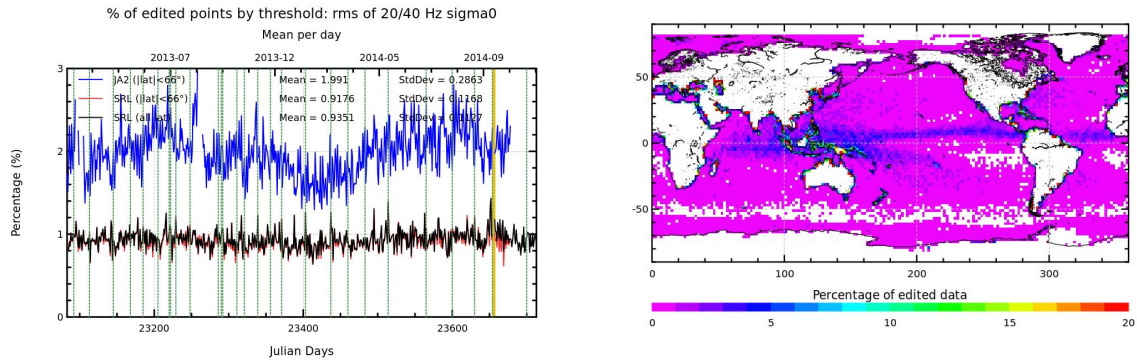


Figure 11: Percentage of edited measurements by 40 Hz Sigma0 standard deviation criterion. Left: Daily statistics for Saral/AltiKa (all latitudes: black, limited to 66° latitude: red) and Jason-2 (blue). Green vertical lines indicate days with maneuvers on Saral/AltiKa and gold band indicates the safe-hold mode on Saral/AltiKa. Right: Map since beginning of mission (cycles 1 to 18).

3.2.10. Radiometer wet troposphere correction

The percentage of edited measurements due to radiometer wet troposphere correction criterion is represented in figure 12. It is about 0.06%. Jason-2 edits generally slightly less data (except after safe-hold modes, when the radiometer is switched on some time after the altimeter). The edited data for Saral/AltiKa are generally due to wet troposphere wetter than the -0.5 m threshold.

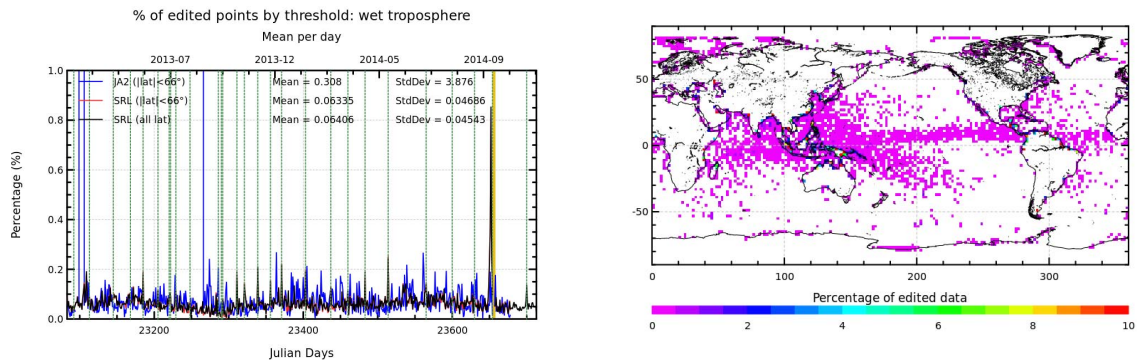


Figure 12: Percentage of edited measurements by radiometer wet troposphere criterion. Left: Daily statistics for Saral/AltiKa (all latitudes: black, limited to 66° latitude: red) and Jason-2 (blue). Green vertical lines indicate days with maneuvers on Saral/AltiKa and gold band indicates the safe-hold mode on Saral/AltiKa. Right: Map since beginning of mission (cycles 1 to 18).

3.2.11. Square off-nadir angle

The percentage of edited measurements due to square off-nadir angle criterion is represented in figure 13. It is about 0.42% (when considering all latitudes, and 0.34% when considering only data

with latitudes up to 66°). As for other parameters, maneuvers have an impact on the number of edited data. The daily mean increases a few weeks before the safe-hold mode and stays high after the safe-hold mode. These high values are caused by a rise in reaction wheel friction due to movement of lubricant (see section 7.1. for more details). The map 13 shows that edited measurements are mostly found in wet regions or places, where the maneuvers take place (Indian Ocean).

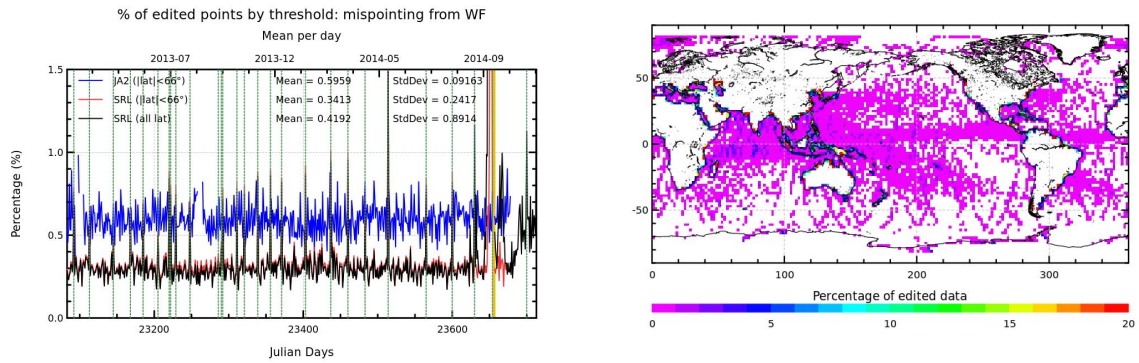


Figure 13: *Percentage of edited measurements by square off-nadir angle criterion. Left: Daily statistics for Saral/AltiKa (all latitudes: black, limited to 66° latitude: red) and Jason-2 (blue). Green vertical lines indicate days with maneuvers on Saral/AltiKa and gold band indicates the safe-hold mode on Saral/AltiKa. Right: Map since beginning of mission (cycles 1 to 18).*

3.2.12. Sea state bias correction

The percentage of edited measurements due to sea state bias correction criterion is represented in figure 14. The percentage of edited measurements is about 0.29% and increases when maneuver take place. The percentage of edited Jason-2 by sea state bias criteria is around twice as high, mainly due to more data at default value as a consequence of SWH and σ_0 values at default. The map 14 shows that edited measurements are mostly found in wet regions and Artic.

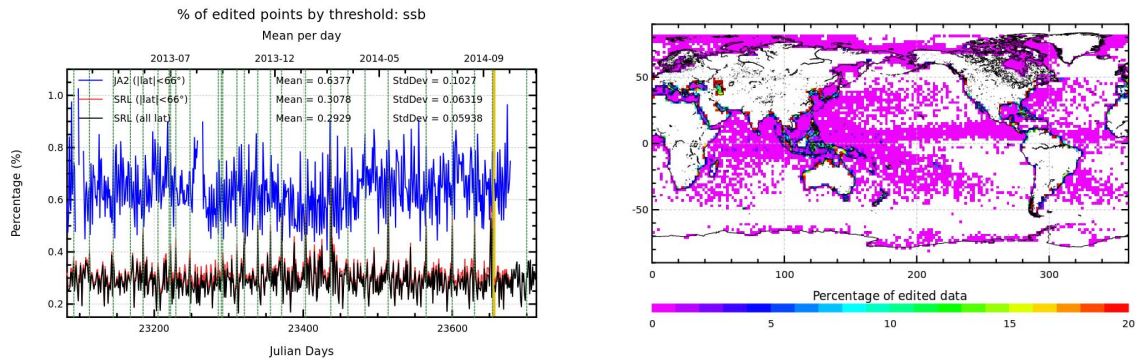


Figure 14: Percentage of edited measurements by sea state bias criterion. Left: Daily statistics for Saral/AltiKa (all latitudes: black, limited to 66° latitude: red) and Jason-2 (blue). Green vertical lines indicate days with maneuvers on Saral/AltiKa and gold band indicates the safe-hold mode on Saral/AltiKa. Right: Map since beginning of mission (cycles 1 to 18).

3.2.13. Altimeter wind speed

The percentage of edited measurements due to altimeter wind speed criterion is represented in figure 15. It is about 0.29%. The measurements are mostly edited when sigma0 shows very high values (higher than 25 dB) or default values, which occur during sigma bloom and also over sea ice. Indeed, the wind speed algorithm (which uses backscattering coefficient and significant wave height) can not retrieve values for sigma0 higher than 25 dB. For such backscattering values, wind speeds would in any case be very low.

Wind speed is also edited during maneuvers, or when it has negative values, which can occur in GDR products. Therefore, the percentage of edited altimeter wind speed is similar to the percentage of edited sea state bias.

The map 15 showing percentage of measurements edited by altimeter wind speed criterion is correlated with maps 14 and 9.

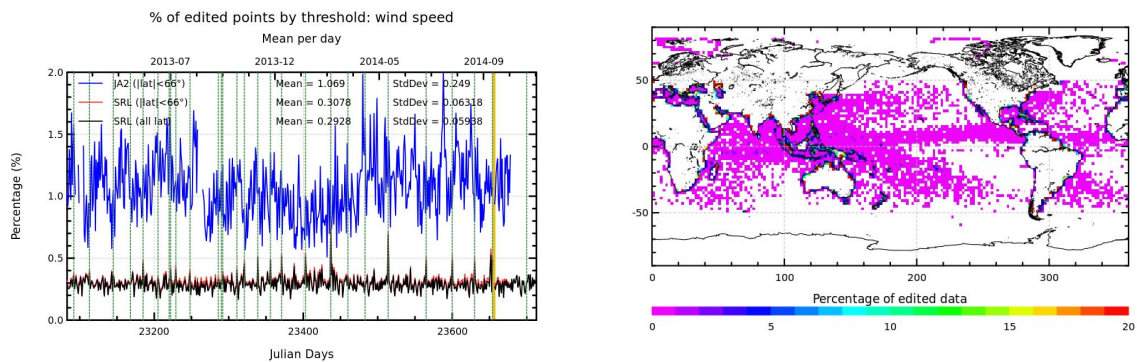


Figure 15: Percentage of edited measurements by altimeter wind speed criterion. Left: Cycle per cycle monitoring. Green vertical lines indicate days with maneuvers on Saral/Altika and gold band indicates the safe-hold mode on Saral/Altika. Right: Map since beginning of mission (cycles 1 to 18).

3.2.14. Ocean tide correction

The percentage of edited measurements due to ocean tide correction criterion is represented in figure 16. It is about 0.18% which is greater than the percentage edited by Jason-2 (0.009%). Since the launching of the GDR-T Patch2 version, the geocentric ocean tide (GOT4.8) has no data over land, including enclosed water bodies such as Caspian Sea. Furthermore this impacts some data near coasts. This is due to the equilibrium long-period tide height (included in the global ocean tide) which, for Patch2, is computed with FES2012 algorithm, which tests previously if the grid of the FES2012 tide atlas is defined or not. Consequently, the equilibrium tide is set to default values over land (and therefore also the geocentric ocean tide).

That explains the presence of edited data (map 16) near coasts and in Caspian Sea.

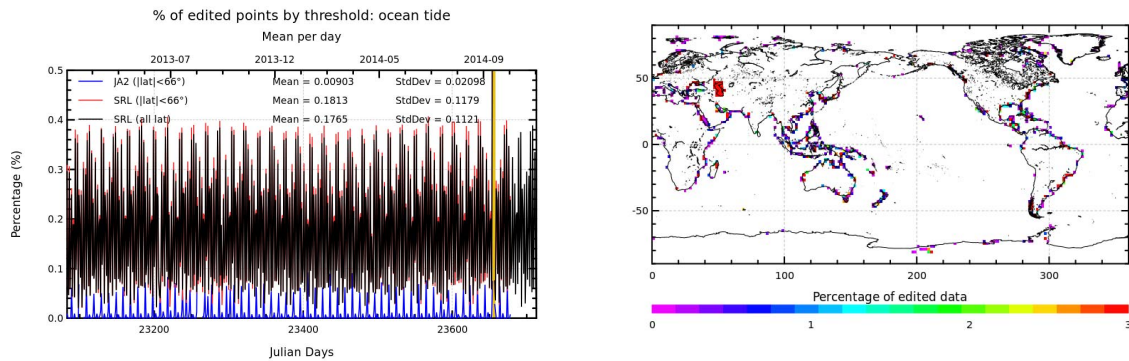


Figure 16: *Percentage of edited measurements by ocean tide criterion. Left: Daily statistics for Saral/AltiKa (all latitudes: black, limited to 66° latitude: red) and Jason-2 (blue). Gold band indicates the safe-hold mode on Saral/AltiKa. Right: Map since beginning of mission (cycles 1 to 18).*

3.2.15. Sea surface height

The percentage of edited measurements due to sea surface height (orbit - Ka-band range) criterion is represented in figure 17. It is about 0.47% (considering all latitudes and 0.49% considering only data with latitudes up to 66°). The measurements edited by sea surface height criterion are mostly found near coasts in equatorial and mid-latitude regions, as well as for regions with low significant wave heights (see map 17). The majority of the edited measurements has defaulted range values, due to default values of the sea state bias and the ocean tide correction.

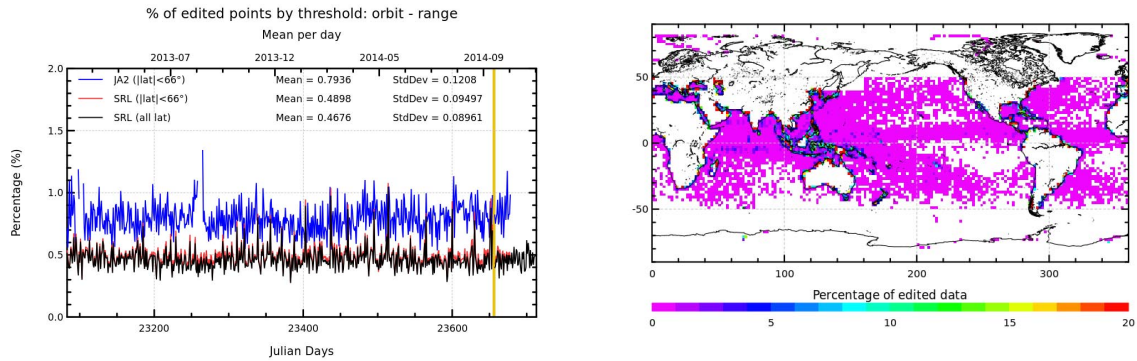


Figure 17: Percentage of edited measurements by sea surface height criterion. Left: Daily statistics for Saral/AltiKa (all latitudes: black, limited to 66° latitude: red) and Jason-2 (blue). Gold band indicates the safe-hold mode on Saral/AltiKa. Right: Map since beginning of mission (cycles 1 to 18).

3.2.16. Sea level anomaly

The percentage of edited measurements due to sea level anomaly criterion is represented in figure 18. It is about 0.80% (considering all latitudes and 0.76% considering only data with latitudes up to 66°). During maneuvers, the percentage of edited data is generally slightly increased as well as before safe-hold mode.

Whereas the map in figure 18 allows us to plot the measurements edited due to sea level anomaly out of thresholds (after applying all other threshold criteria). There are only very few measurements, mostly located near Antarctic, when data were neither edited by surface type flag nor by ice flag.

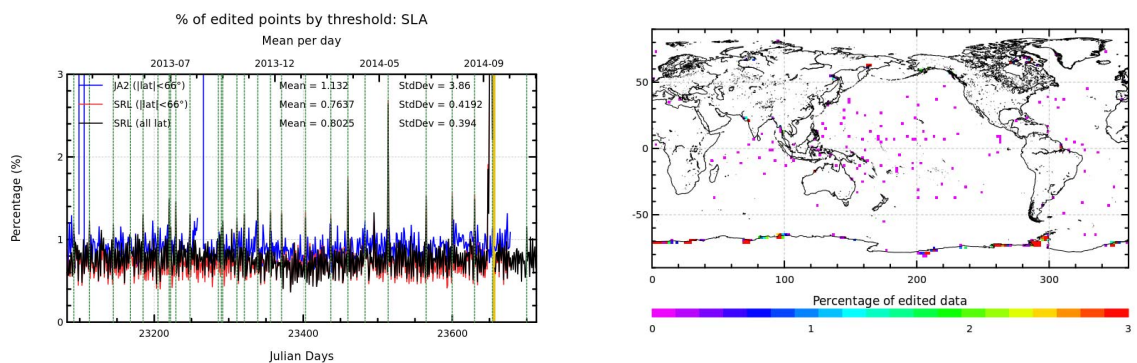


Figure 18: Percentage of edited measurements by sea level anomaly criterion. Left: Daily statistics for Saral/AltiKa (all latitudes: black, limited to 66° latitude: red) and Jason-2 (blue). Green vertical lines indicate days with maneuvers on Saral/AltiKa and gold band indicates the safe-hold mode on Saral/AltiKa. Right: Map since beginning of mission (cycles 1 to 18).

compared to Envisat data seems figure ?? this value is shown for the 3 missions in function of 4° latitude bands. In addition to valid points, only data fulfilling the following selections were

chosen: $|\text{latitude}| < 50^\circ$, bathymetry less than -1000 m and ocean variability less than 0.2 m. The performance of the three missions is similar, showing that editing criteria chosen for Saral/AltiKa allows the mission to obtain similar results as Jason-2 and Envisat. Note also that some algorithms for Saral/AltiKa are not yet tuned (for example sea state bias, radiometer wet troposphere correction, altimeter wind speed). Results using the future Patch2 version of Saral/AltiKa GDR-T (see also chapter ??) will show even better results.

4. Monitoring of altimeter and radiometer parameters

4.1. Methodology

Both mean and standard deviation of the main parameters of **valid** Saral/AltiKa (GDR-T Patch2) data have been monitored since the beginning of the mission. Therefore ordinary daily statistics have been computed, but also box statistics with weighting of latitude. Indeed, as the measurement distribution is not homogeneous with latitude, this can skew the statistics to values of the data in data-rich latitudes. Moreover, a comparison with Jason-2 parameters has also been performed. As both satellites are on different ground tracks no point-to-point comparisons (as it was possible during flight formation phase between Jason-1 and Jason-2) are feasible. Comparisons are done by superposing monitoring of daily or cycle per cycle statistics or histograms. Furthermore, parameters are averaged on a grid-structure for both satellites, which are then subtracted one from the other. Another mean of comparison are dispersion diagrams between Saral/AltiKa and Jason-2 data at 3h-crossover points.

Note that for daily monitoring, there are some gaps end of March/ early April and in September 2013 for Jason-2 and in October 2014 (from October 6 to 9) for Saral/AltiKa. This is due to safe-hold modes.

Most of the following daily monitoring present GDR data in plain lines and are continued with IGDR data in dotted lines.

4.2. 40 Hz Measurements

The monitoring of the number and standard deviation of 40 Hz elementary range measurements used to derive 1 Hz data is presented here. These two parameters are computed during the altimeter ground processing. For both Saral/AltiKa and Jason-2, before performing a regression to derive the 1 Hz range from 40 Hz or 20 Hz data, a MQE (mean quadratic error) criterion is used to select valid 40/20 Hz measurements. This first step of selection consists in verifying that the 40/20 Hz waveforms can be approximated by a Brown echo model (Brown, 1977 [3]) (Thibaut et al. 2002 [15]). Then, through an iterative regression process, elementary ranges too far from the regression line are discarded until convergence is reached. Thus, monitoring the number of 40/20 Hz range measurements and the standard deviation computed among them is likely to reveal changes at instrumental level.

4.2.1. 40 Hz measurements number

Number of elementary 40 Hz range measurements is close to 38.5 (black curve on figure 19). Before the correction of the PF/RF alignment (alignment between the platform and the radiofrequency axis) on 25th of April 2013 this value was slightly higher (around 38.6). Jason-2 has an average close to 19.6 as number of elementary 20 Hz range measurements (which is when multiplied by 2, higher than the value of Saral/AltiKa). It also shows smaller temporal variability. Note that before Patch1 version, the MQE threshold was not applied during the 40 Hz to 1 Hz compression (IGDR data till cycle 4, pass 394), the daily mean of the number of the elementary 40 Hz range measurements was 39.0. So in average 0.5 40 Hz elementary range measurements are removed during the 40 Hz to 1 Hz compression by the MQE criteria. These removed data might be due to perturbations in the footprint (rain, sigma bloom). For both missions, the number of elementary range measurements is correlated with the significant wave height (ann, for SARAL/AltiKa,

with sea ice extent). Figure 20 shows less elementary range measurements around Indonesia, the Mediterranean Sea and close to coasts, which are all regions of low significant wave heights (see also map of SWH 30) and therefore regions where sigma bloom may occur and also rain areas. High latitudes also show a lower number of range elementary measurements, due to the presence of sea-ice.

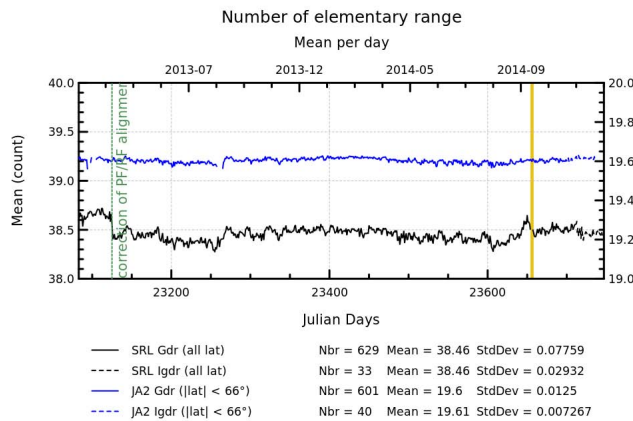


Figure 19: Daily monitoring of mean of number of elementary Saral/AltiKa 40 Hz (left ordinate) and Jason-2 20 Hz (right ordinate) range measurements. The gold band indicates the safe hold mode on Saral/AltiKa.

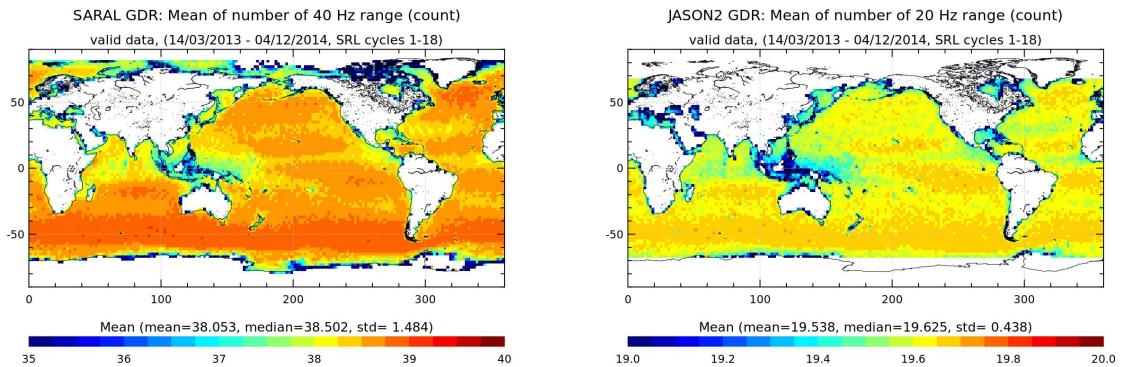


Figure 20: Average map of number of Saral/AltiKa elementary 40 Hz range measurements (left) and Jason-2 elementary 20 Hz range measurement (right) over cycles 1 to 18.

4.2.2. 40 Hz measurements standard deviation

Saral/AltiKa standard deviation of the 40 Hz measurements is 5.7 cm, whereas it is 8.0 cm for Jason-2 (right side of figure 21). Using latitude weighted box statistics (left side of figure 21), these values decrease to respectively 5.6 and 7.7 cm. These values are very close to the ones found when computing the power spectrum. The value of Saral/AltiKa is lower than the one of Jason-2 due to the altimeter band-width, which is 480 MHz for Saral/AltiKa instead of 320 MHz for Jason-2 (see [13]). As for the number of elementary range measurements, the standard deviation of the elementary range measurements are correlated to the significant wave height (see maps on figures 22 and 30).

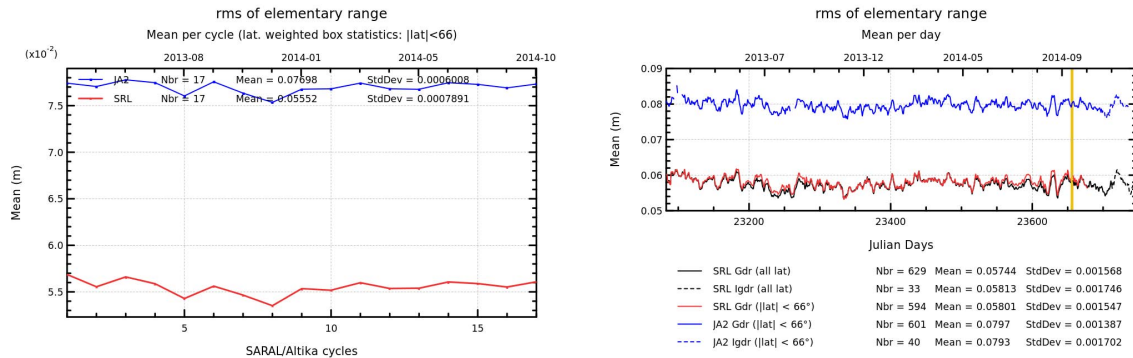


Figure 21: Cyclic monitoring of rms of elementary 40/20 Hz range measurements for Saral/AltiKa and Jason-2 (left), computing latitude weighted box statistics. Daily mean of rms of elementary Saral/AltiKa 40 Hz and Jason-2 20 Hz range measurements (right). GDR data are plotted with plain lines, IGDR with dotted lines. The gold band indicates the safe hold mode on Saral/AltiKa.

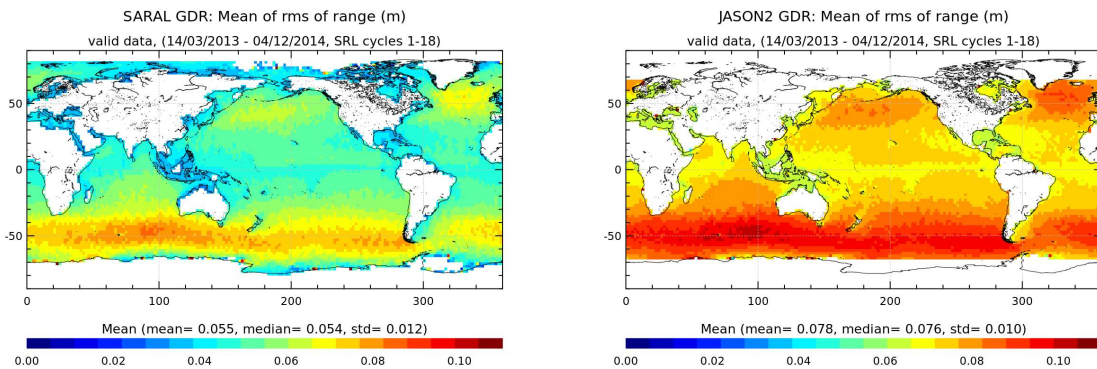


Figure 22: Average map of rms of Saral/AltiKa elementary 40 Hz range measurements (left) and Jason-2 elementary 20 Hz range measurement (right) over cycles 1 to 18.

4.3. Off-Nadir Angle from waveforms

The off-nadir angle is estimated from the waveform shape during the altimeter processing. The off-nadir angle, averaged on a daily basis, has been plotted for Saral/AltiKa and Jason-2 on the left side of figure 23, whereas the right side shows the daily standard deviation of the off-nadir angle from waveforms. In the beginning of the Saral/AltiKa mission the off-nadir angle from waveforms was slightly positive (around 0.003 degrees²), a X-cross calibration maneuver with $+0.3^\circ/-0.3^\circ$ in pitch and than $+0.3^\circ/-0.3^\circ$ in roll was done on 22th of April 2013 (see N. Stenou [13]). This allowed to determine that a correction of -0.045 degree in pitch direction was necessary. It was performed on 25th of April 2013. A last X-cross calibration on 30th of April 2013 showed that the correction was successful. Off-nadir angle from waveforms stayed from this day on close to zero and very stable spatially and temporally. Nevertheless, a few variations appeared during summer 2014 caused by a rise in reaction wheel friction due to movement of lubricant. This event ended with the loss of a wheel and an important increase of the daily mean of the off-nadir angle leading to a safe-hold mode between 6th and 9th of October 2014. After the safe-hold mode, the daily mean of the mispointing is not as stable as it used to be at the beginning of the mission, as illustrated by the slight rise of the daily standard deviation. Though Jason-2 off-nadir angle from waveforms is also close to zero (though mostly slightly negative), it shows more variations. Standard deviation of the off-nadir angle from waveforms is also higher for Jason-2 than for Saral/AltiKa (right of figure 23). This is also visible on the histograms (figure 25). The shape of Saral/AltiKa off-nadir angle from waveforms histogram is much narrower than for Jason-2.

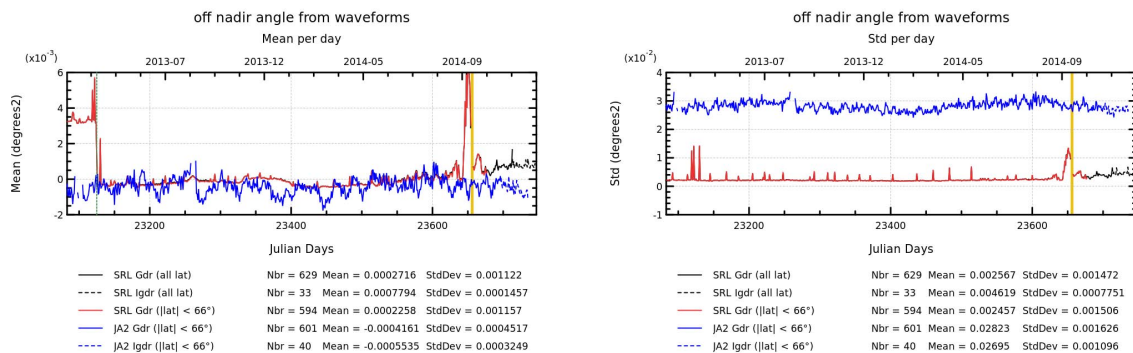


Figure 23: Daily monitoring of mean (left) and standard deviation (right) of Saral/AltiKa and Jason-2 off-nadir angle from waveforms. GDR data are in plain lines, IGDR data in dotted lines. The vertical green line indicates the day where the PF/RF alignment (alignment between the platform and the radio-frequency axis) was corrected. The gold band indicates the safe hold mode on Saral/AltiKa.

The off-nadir angle from waveforms represents either real mispointing or is due to backscattering properties of the surface, which can modify the slope of the trailing edge of the waveforms. Jason-2 shows more variation for the off-nadir angle from waveforms due to its larger antenna aperture. Jason-2 has an antenna beamwidth of 1.29° , whereas Saral/AltiKa has only 0.6° . In addition Jason-2 is in a higher orbit. The Jason-2 footprint is therefore larger (radius of 9.6 km) than the Saral/AltiKa footprint (5.7 km). Therefore the probability of perturbations within the footprint - which modify the backscattering properties of the surface - is higher for Jason-2 than for Saral/AltiKa.

Until cycle 15 of Saral/AltiKa, both missions were stable concerning the platform pointing and had no mispointing. From cycle 15, mispointing events started to appear on Saral/AltiKa at first only affecting few sections of passes. These events got stronger and more regular until safe-hold mode on cycle 17 (see more details at section 7.1.). After the safe-hold mode, mispointing events are still observed regularly but with limited impact on SSH data quality.

The map of Saral/AltiKa off-nadir angle from waveforms (left of figure 24) is not homogeneous. The Indian ocean is impacted by platform mispointing due to maneuvers. High mispointing values are observed at high latitudes close to sea ice. Mispointing is slightly positive around Indonesia and equator and close to coasts. On the other hand, the region around 50°S has slightly negative values. The map of Jason-2 (right of figure 24) is generally slightly negative, except for regions around Indonesia, and close to coasts (especially in the northern hemisphere), the amplitudes of the off-nadir angle from waveforms are greater for Jason-2 than for Saral/AltiKa. Because of platform mispointing events, Saral/AltiKa map is now less correlated to the map of backscattering coefficient (figure 27).

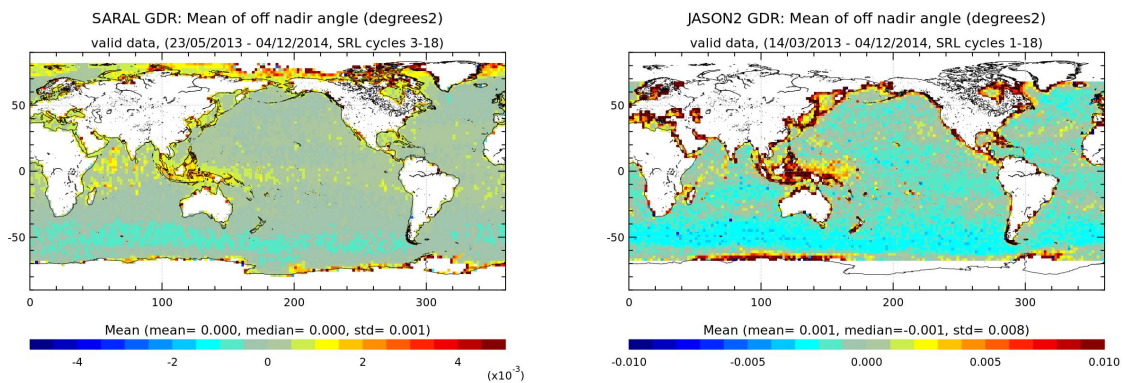


Figure 24: Average map of off-nadir angle from waveforms for Saral/AltiKa (left) and Jason-2 (right) after the correction of the PF/RF alignment over cycles 3 to 18.

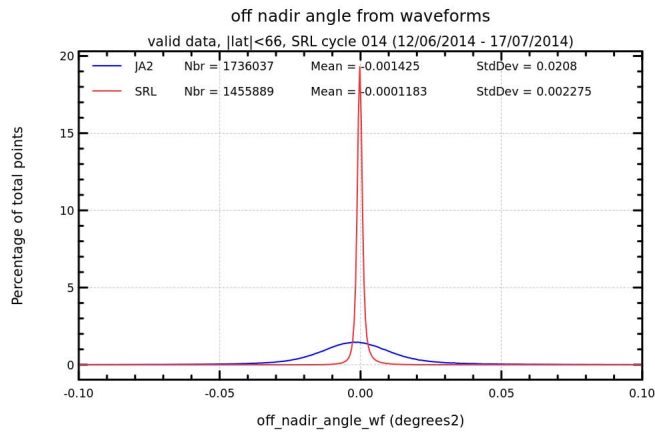


Figure 25: Histogram (of along-track data) of off-nadir angle from waveforms for Saral/AltiKa and Jason-2 (computed for Saral/AltiKa cycle 14).

4.4. Backscatter coefficient

Saral/AltiKa is the first altimeter mission using the Ka-band frequency. It has therefore a different behavior than altimeters using Ku-band frequency. Several studies were done to prepare the Saral/AltiKa mission. They found that the Ka-band backscattering coefficient will be about 3.5 dB smaller than the Ku-band backscattering coefficient (see [13]). Concerning the real Saral/AltiKa data, the difference to Ku-band backscattering coefficient is smaller: 2.5 dB in average (see bottom of figure 26). The daily evolution of Saral/AltiKa backscattering coefficient shows the same signals as the one of Jason-2 (top left of figure 26) and the dispersion diagram of backscattering coefficients at 3h crossover points (28) shows also a good correlation.

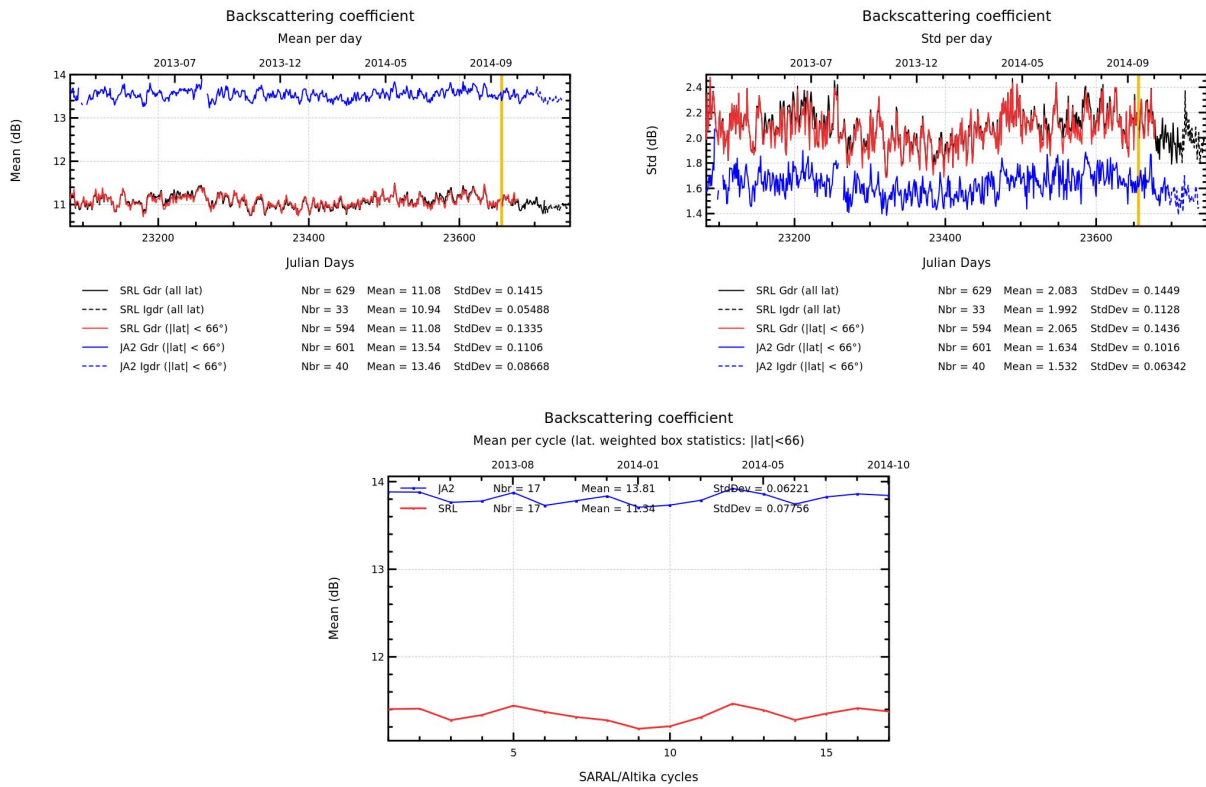


Figure 26: Daily monitoring of mean and standard deviation of Saral/AltiKa and Jason-2 backscattering coefficient (top) and cycle per cycle monitoring of latitude weighted box mean for both missions on the bottom. The gold band indicates the safe hold mode on Saral/AltiKa.

Nevertheless there is quite a dispersion, and indeed the daily standard deviation of backscattering coefficient is higher for Saral/AltiKa than for Jason-2 (top right of figure 26). Though the maps (centered around the mean value for better comparison between Saral and Jason-2) of backscattering coefficient show the same structures for both missions (see top of figure 27), the amplitudes of these structures are stronger for Saral/AltiKa than for Jason-2. Also the difference between Ka- and Ku-band backscattering coefficient is not a simple bias, as shown on the difference map (bottom of figure 27).

Furthermore the shape of the histograms is quite different for the Ka- and Ku-band frequencies. The backscattering coefficient is one of the parameters which is quite different for the two frequencies.

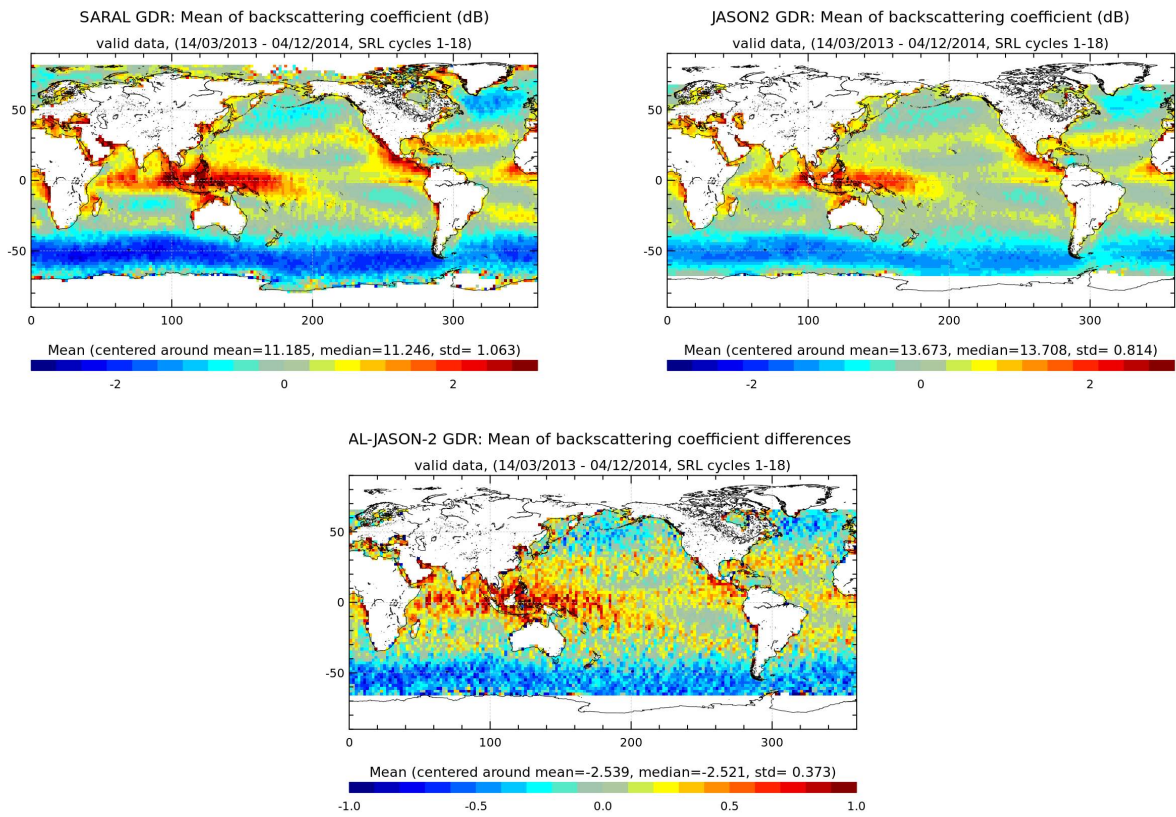


Figure 27: Average map of backscattering coefficient for Saral/AltiKa (left) and Jason-2 (right) cycles 1 to 18. Difference map of gridded Saral and Jason-2 backscattering coefficient for cycles 1 to 18.

RL/JA2 XOvers<3h, cycles 001-016 (2013-03-14 / 2014-09-;

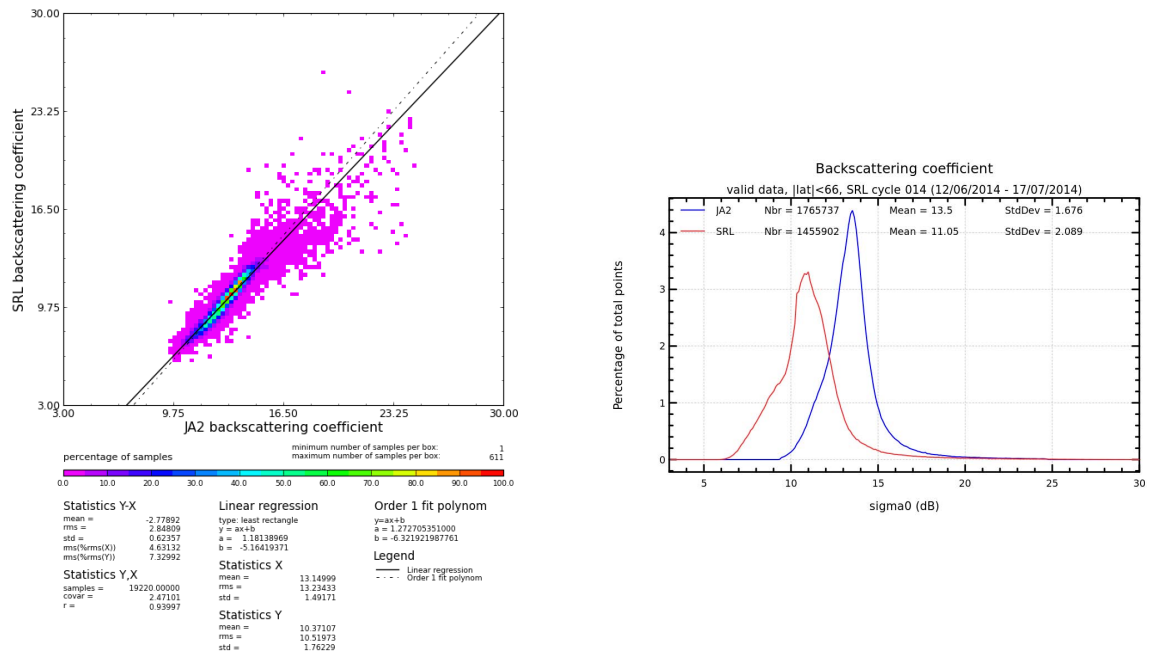


Figure 28: Dispersion diagram of backscattering coefficient between Saral/Altika and Jason-2 at 3h crossover points (computed for cycles 1 to 18) on the left and histogram (of along-track data) computed for Saral/Altika cycle 14 on the right.

4.5. Significant wave height

The significant wave height (SWH) is one of the parameters derived from the waveforms. Daily monitoring of mean and standard deviation of SWH vary temporally, but are very similar for Saral/AltiKa and Jason-2 (see top of figure 29). The mean is very close for both missions when limited to 66° latitude. When taking into account all latitudes, SWH is slightly reduced for Saral/AltiKa as small SWH occur in very high northern latitudes when the sea ice recedes (see also left map of figure 30). The maps of SWH show the same structures: low SWH around Indonesia, in the Mediterranean Sea and the Gulf of Mexico and high SWH around 50°S (as well as in North Atlantic). The difference map between the two satellites (bottom of figure 30) is centered around a difference of 3 to 4 cm, with slightly higher values for Saral/AltiKa. Stronger differences occur in high latitudes (in regions, where SWH is higher than 2-3 m). These differences are probably due to time differences in the sampling. When considering dispersion diagram of Saral/AltiKa and Jason-2 SWH at 3h crossovers (left of figure 31), a strong correlation coefficient of over 0.98 is obtained.

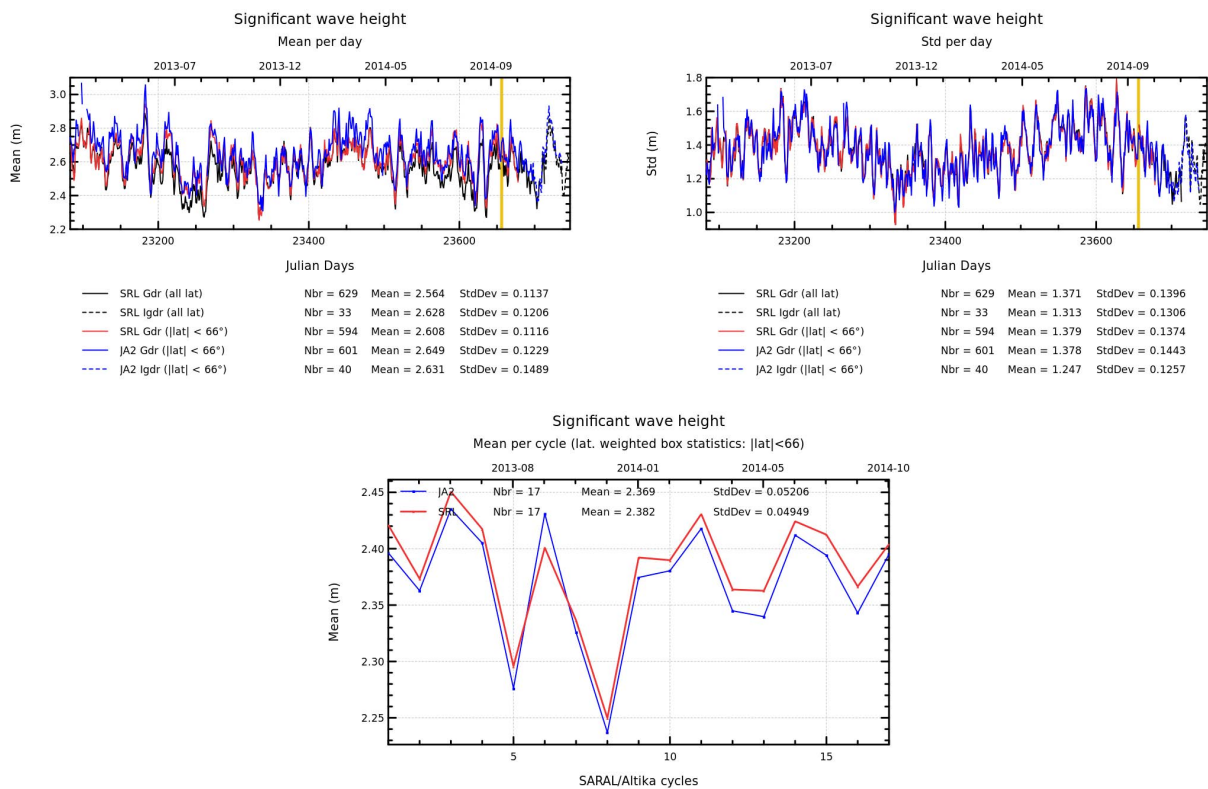


Figure 29: Daily monitoring of mean and standard deviation significant wave height for Saral/AltiKa and Jason-2 (top) and cycle per cycle monitoring of latitude weighted box mean for both missions on the bottom. The gold band indicates the safe hold mode on Saral/AltiKa.

The dispersion diagram shows a mean value for Jason-2 SWH at 3h SRL/JA2 crossover points of 3.06 m and 3.12 m for Saral/AltiKa. This is considerably higher than the mean values of daily along-track SWH (around 2.60 m). This is related to the geographical positions of the 3h crossover points: there are more crossover points in latitudes around 50°, than in low latitudes. And around

50°S the SWH has high values (see also top of figure 30), which skews the mean of SWH computed at 3h crossovers to higher values. Nevertheless, this diagnostic shows that for the same positions (SRL/JA2 3h crossovers) with a time difference less than 3h, Saral/AltiKa SWH is slightly higher than Jason-2. This is also the case when computing latitude weighted box statistics (in order to compensate for uneven data distribution), as shown on bottom of figure 29, where Jason-2 SWH is generally slightly lower than Saral/AltiKa SWH. When considering along-track statistics (top of figure 29), this order is inverted (Jason-2 SWH higher than Saral/AltiKa SWH), as Jason-2 has more data in high latitudes, especially in southern hemisphere, where there is less land. In these regions the SWH is high and skews the mean to higher values.

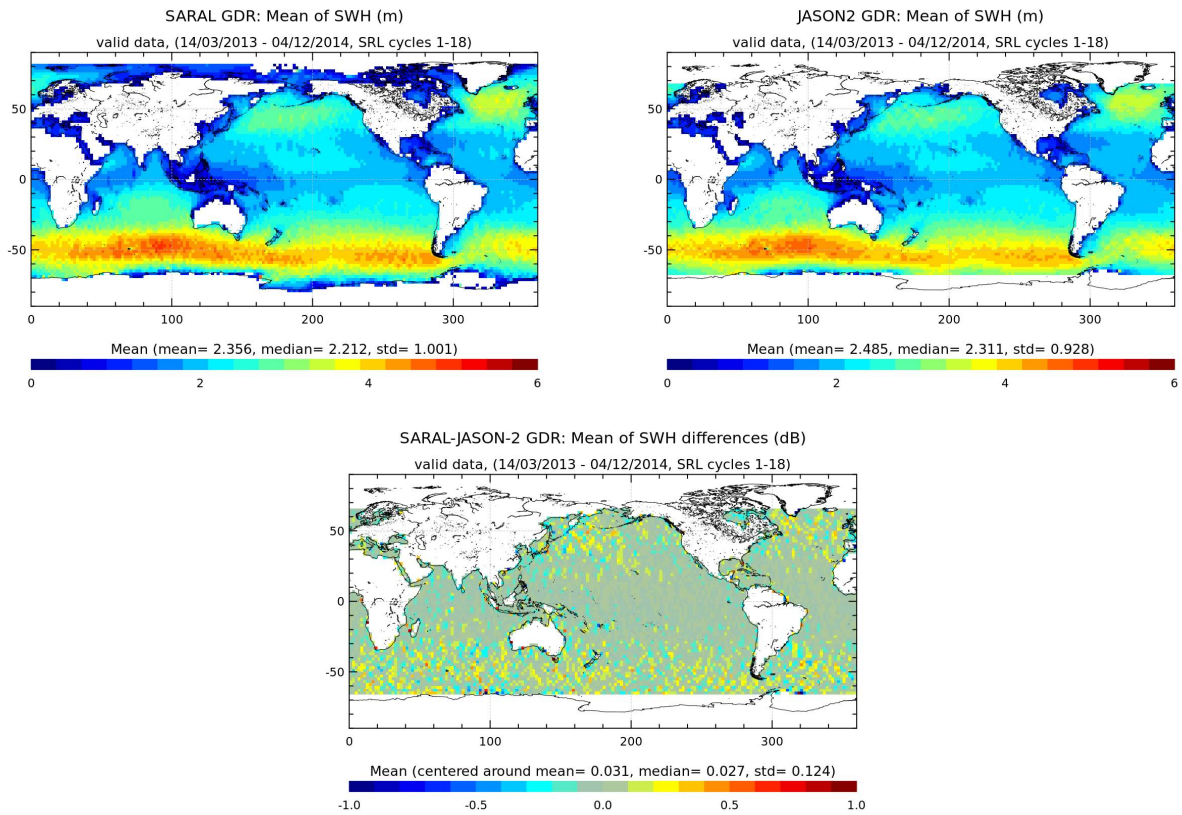


Figure 30: Average map of significant wave height for Saral/AltiKa (left) and Jason-2 (right) cycles 1 to 18. Difference map of gridded Saral and Jason-2 significant wave height for cycles 1 to 18.

The shapes of the histograms are very similar (see right side of figure 31) for Jason-2 and Saral/AltiKa, except for small SWH. The minimum SWH value of Saral/AltiKa SWH is 12.6 cm (related to the look-up table), it is 0 for Jason-2. Nevertheless, small SWH of current Jason-2 or Jason-1 data are not precise (errors of about 15 cm), as the look-up table correction for small SWH is not correct, whereas the Saral/AltiKa look-up tables were updated for Patch2. Furthermore, the histogram for Saral/AltiKa shows a small bump for SWH around 50cm. Note that in the wave forecasting systems of Meteo-France, altimeter significant wave height from Jason-2 and Saral/AltiKa are only assimilated for values higher than 50 cm. According to L. Aouf, the Saral/AltiKa SWH data have a positive impact on the wave analysis and forecast of the Meteo-France wave analysis model ([2]).

RL/JA2 XOvers<3h, cycles 001-016 (2013-03-14 / 2014-09-;

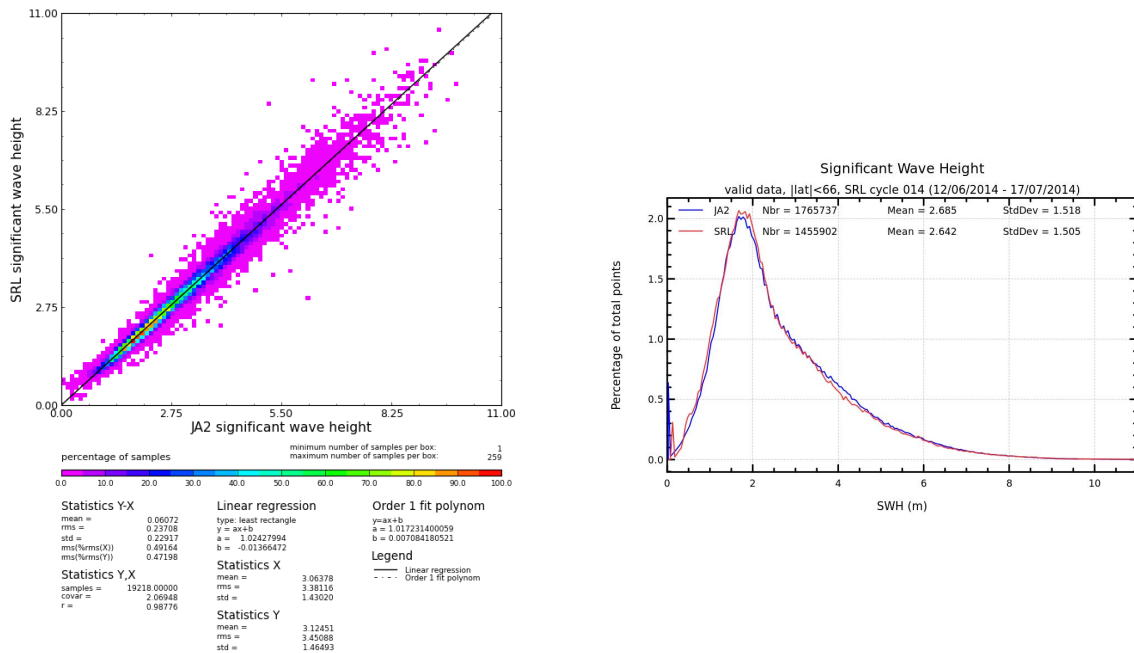


Figure 31: Dispersion diagram of significant wave height between Saral/Altika and Jason-2 at 3h crossover points (computed for cycles 1 to 18) on the left and histogram (of along-track data) computed for Saral/Altika cycle 14 on the right.

4.6. Ionosphere correction

As the Saral/AltiKa altimeter uses a frequency of 35.75 GHz (Ka-band), the ionospheric effects are very small (divided by roughly seven compared to Ku-band frequency). Therefore a mono-frequency altimeter was chosen for the Saral/AltiKa mission, so it is not possible to compute a dual-frequency ionospheric correction such as for Jason-2. Instead, the Saral/AltiKa GDR products contain only the GIM ionosphere correction.

The large differences between Ka-band and Ku-band ionosphere corrections are shown on the latitude weighted box statistics (bottom of figure 32), where Saral/AltiKa GIM ionosphere correction has small values (around 7 mm) and it varies little in time, whereas Jason-2 filtered dual-frequency ionosphere correction has values of around 7 cm, which vary temporally. Also the standard deviation of along-track data is higher for Jason-2 than for Saral/AltiKa (right of figure 32).

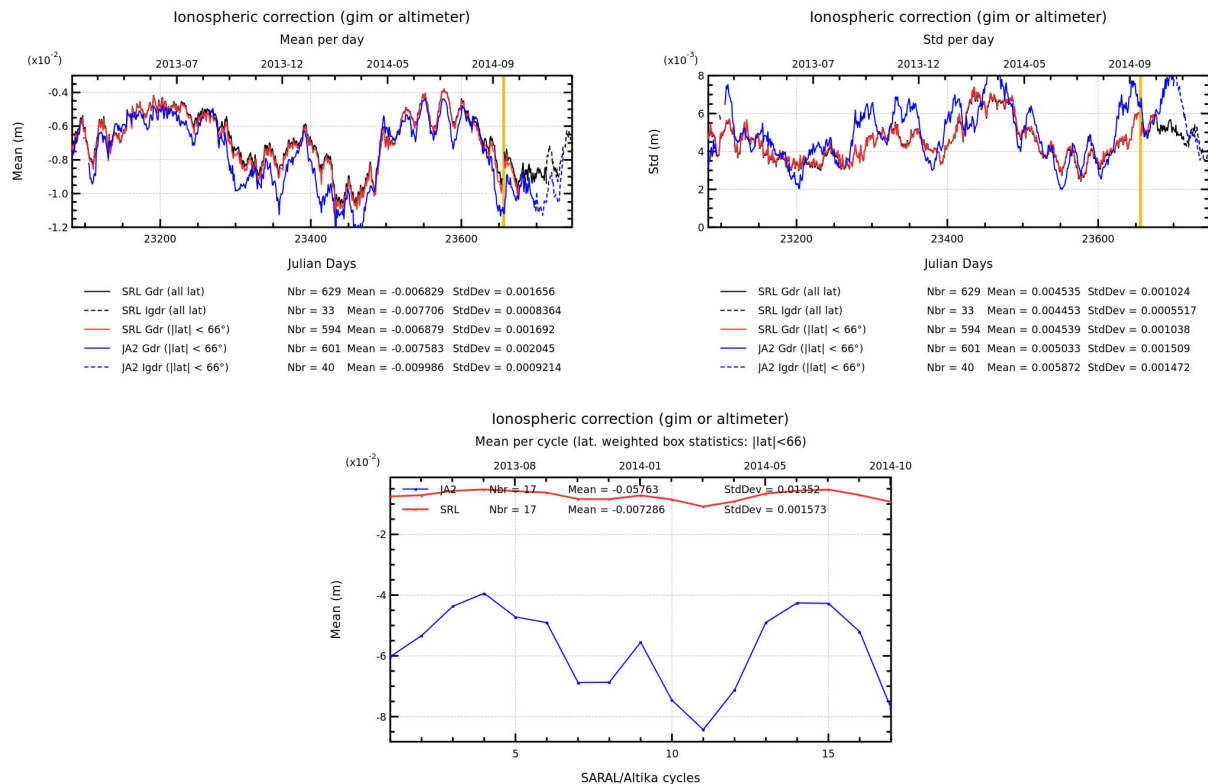


Figure 32: Daily monitoring of mean and standard deviation ionosphere correction for Saral/AltiKa (GIM) and Jason-2 (filtered dual-frequency ionosphere correction with scale factor 0.14418 for mean computation) on top and cycle per cycle monitoring of latitude weighted box mean for both missions (without the scale factor for Jason-2) on the bottom. The gold band indicates the safe hold mode on Saral/AltiKa.

Top left of figure 32 shows the daily mean of ionosphere correction for Saral/AltiKa (GIM ionosphere using all latitudes (black line) or limiting to 66° latitude) and for Jason-2 (filtered dual-frequency ionosphere correction), where a scale factor of 0.14418 is applied in order to set it on the same level as Ka-band frequency ($13.575^2/35.75^2$). Generally the two curves show a similar evolution, but locally differences of around 2 mm may occur (with generally Jason-2 having stronger values).

This may be due to the fact that Saral/AltiKa uses a model ionosphere correction, whereas Jason-2 has a dual-frequency ionosphere correction. It may also be due to the fact that Saral/AltiKa is a sun-synchronous satellite with 6:00 local time for ascending node and 18:00 local time for descending node. As ionosphere correction varies with local time, it is very small for ascending (morning) passes and has absolute values up to 2 cm in the equatorial region for descending (evening) passes. Jason-2 on the other hand is not sun-synchronous and revisits only every 12 cycles the same local hours.

Highest ionosphere correction (absolute values) can be found in the same regions (equatorial region) for Saral/AltiKa and Jason-2 (see maps of figure 33), but the amplitude is of course very different (due to the different frequencies). This can also be seen on the histogram (right of figure 34), where the shape of Saral/AltiKa histogram is very narrow with a strong mode close to zero. The shape of Jason-2 histogram is much more spread out and flatter.

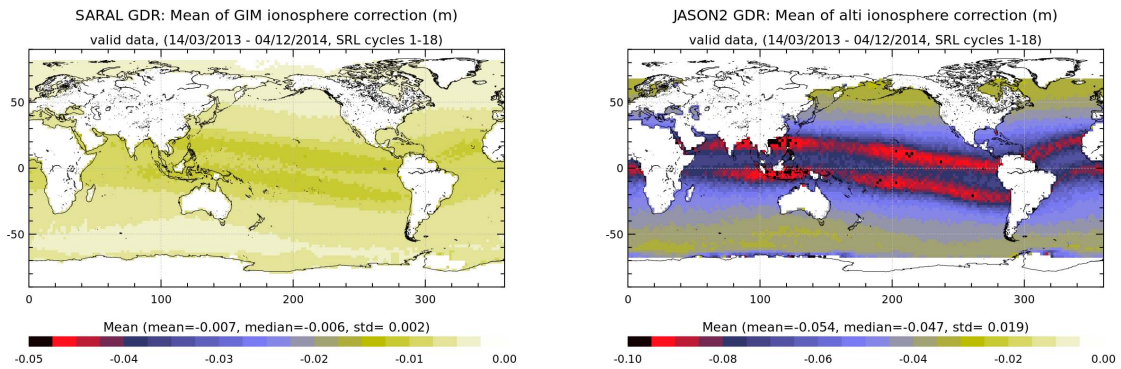


Figure 33: Average map of ionosphere correction for Saral/AltiKa (GIM, left) and Jason-2 (filtered dual-frequency ionosphere correction, right) cycles 1 to 18. Note that color scales are different for Saral and Jason-2

The dispersion diagram of ionosphere corrections (the Jason-2 one is rescaled to Ka-band frequency) at 3h multi-mission crossovers shows correlation, but not very good (with a correlation coefficient of only 0.80).

RL/JA2 XOvers<3h, cycles 001-016 (2013-03-14 / 2014-09-:

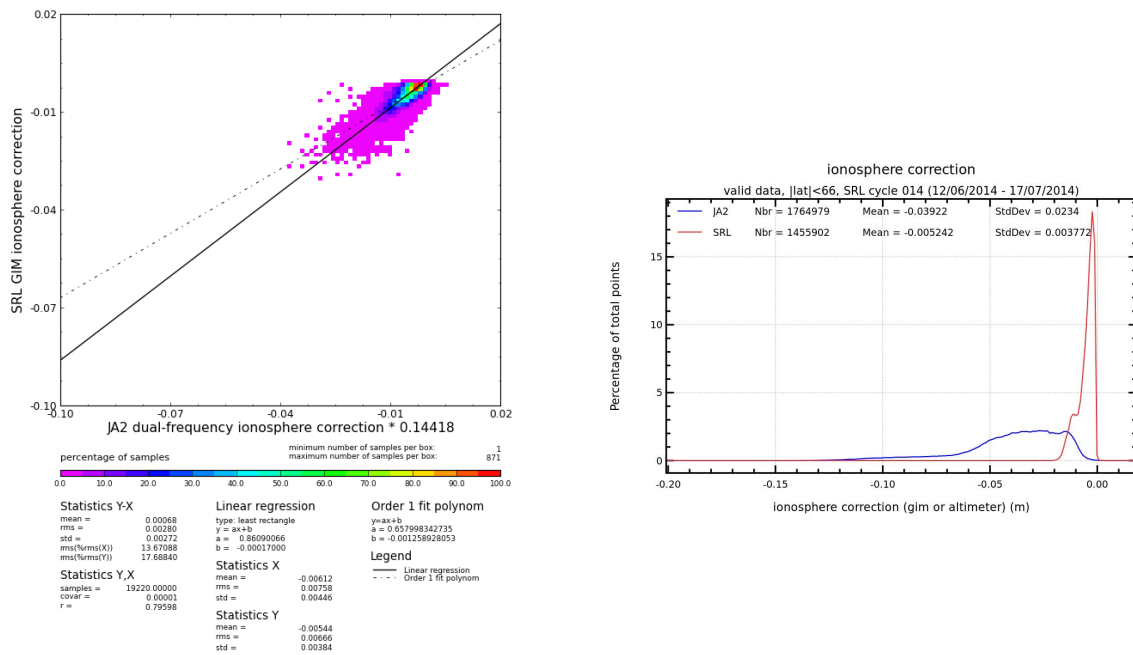


Figure 34: Dispersion diagram of ionosphere correction between Saral/Altika (GIM) and Jason-2 (filtered dual-frequency with scale factor of 0.14418 for Jason-2) at 3h crossover points (computed for cycles 1 to 18) on the left and histogram of along-track data (without scale factor for Jason-2) computed for Saral/Altika cycle 14 on the right.

4.7. Radiometer wet troposphere correction

4.7.1. Overview

In order to have access to radiometer wet troposphere correction, liquid water content, water vapor content and atmospheric attenuation, Saral/AltiKa uses a dual-frequency radiometer (23.8 GHz +/- 200 MHz & 37 GHz +/- 500 MHz), whereas Jason-2 has a three-frequency radiometer (18.7, 23.8 and 34.0 GHz). Figure 35 shows the daily mean and standard deviation of radiometer wet troposphere correction for Saral/AltiKa and Jason-2. Since Patch2, the standard deviation is smaller for Saral/AltiKa than for Jason-2. Concerning the mean of radiometer wet troposphere correction, Jason-2 has dryer values than Saral/AltiKa. This is on the one hand related to different radiometer wet troposphere correction retrieval algorithms, but on the other hand, this can also be related to different local times of the satellites (sun-synchronous 6h/18h for Saral/AltiKa). During several months the radiometer wet troposphere correction of Saral/AltiKa went dryer, this is related to the saturation of the hot calibration counts, which was corrected on 22 October 2013 (explaining the jump of around 5 mm amplitude visible on the monitoring). The safe-hold mode of Saral/AltiKa didn't generate any significant impact on the daily mean.

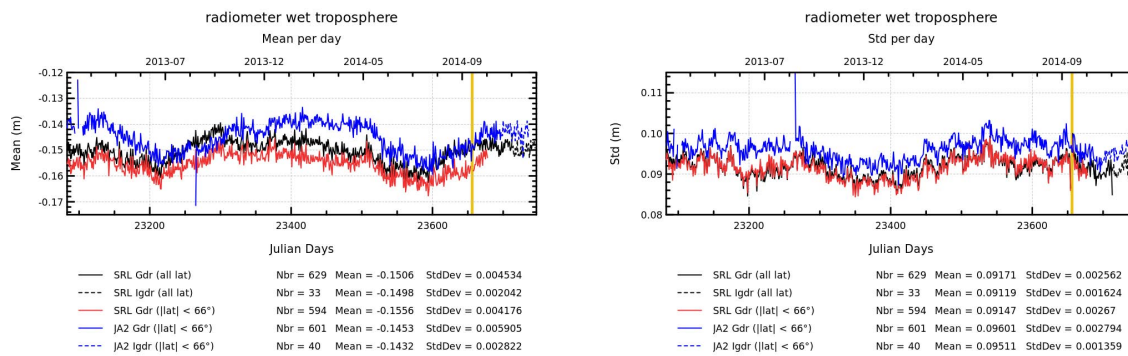


Figure 35: Daily monitoring of mean and standard deviation of radiometer wet troposphere correction for Jason-2 (blue) and Saral/AltiKa (black all latitudes, red latitudes limited to $\pm 66^\circ$). The gold band indicates the safe hold mode on Saral/AltiKa.

4.7.2. Comparison with the ECMWF model

The ECMWF wet troposphere correction has been used to check the Saral/AltiKa and Jason-2 radiometer corrections. Daily differences are calculated and plotted in figure 36. The drift in the radiometer wet troposphere correction of Saral/AltiKa due to the saturation of the hot calibration count is clearly visible on the left part of figure 36. Outside of this drift the difference between radiometer and ECMWF wet troposphere correction for Saral/AltiKa and Jason-2 is around 5 mm. The two ECMWF model updates (June and November 2013) occurred during the observed period, which might have an impact on the model wet troposphere correction, did not show any impact on the data.

The standard deviation of radiometer minus model wet troposphere correction is higher for Saral/AltiKa (around 1.6 cm) compared to Jason-2 (around 1.2 cm), shown on left of figure 36 and also on the histogram on figure 38.

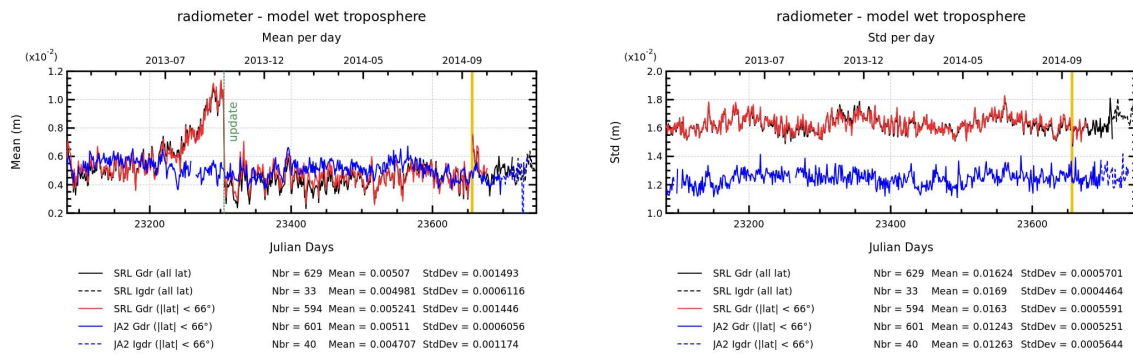


Figure 36: Daily monitoring of mean and standard deviation of radiometer minus model wet troposphere correction for Saral/AltiKa and Jason-2. The gold band indicates the safe hold mode on Saral/AltiKa.

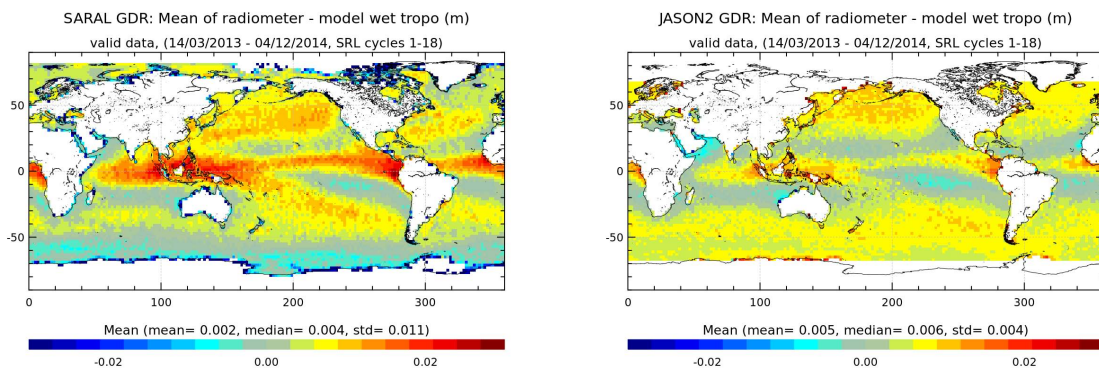


Figure 37: Average map of radiometer minus ECMWF model wet troposphere correction for Saral/AltiKa (left) and Jason-2 (right) cycles 1 to 18.

The maps of radiometer minus ECMWF model wet troposphere correction (figure 37) are centered

around the mean value (5 mm for Jason-2, 2 mm for Saral/AltiKa). The mean of the Saral/AltiKa map is impacted on the one side by the saturation of the hot calibration counts (which tends to overestimate the difference) and on the other side by some boxes near the frontier between sea ice and free water (which tends to underestimate the mean). These boxes with strong negative values are an indication that probably not all sea ice cases are edited. Geographical structures of the radiometer minus model wet troposphere corrections are similar for the two satellites in high latitudes (around $\pm 50^\circ$), but quite different for low latitudes.

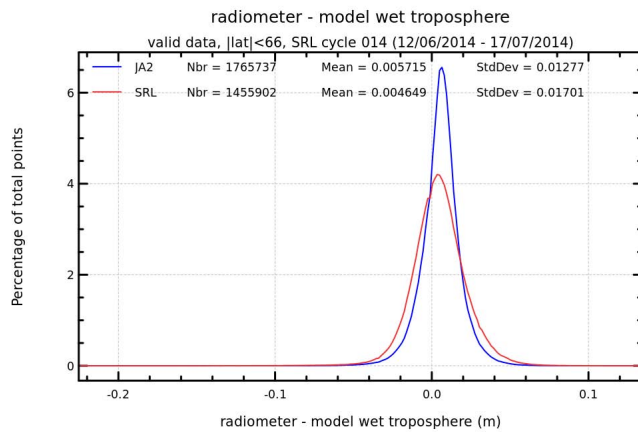


Figure 38: Histogram (of along-track data) of radiometer minus ECMWF model wet troposphere correction between Saral/AltiKa and Jason-2 computed for Saral/AltiKa cycle 14.

4.8. Altimeter wind speed

The altimeter wind speed present in Patch1 was not usable, since the look-up table from Jason-1 was used, but with the Ka-band backscattering coefficient is very different from the Ku-band one. For Patch2 version, the altimeter wind speed algorithm developed by [9] for Ka-band altimetry is used. Figure 39 shows the daily monitoring of the mean and standard deviation of altimeter wind speed for Saral/AltiKa and Jason-2. The Patch2 altimeter wind speed has values similar to the Jason-2 altimeter wind speed.

It should be noted that in the current products, the SARAL/AltiKa wind speed is impacted by the saturation of the radiometer hot calibration counts through the estimation of atmospheric attenuation which is then applied on the backscatter coefficient. The maps of altimeter wind speed for both missions are similar (see 40).

The figure 41 shows a good correlation of wind speed data between the two missions (over 0.95), yet the relationship between Jason-2 and SARAL/AltiKa remains non truly linear.

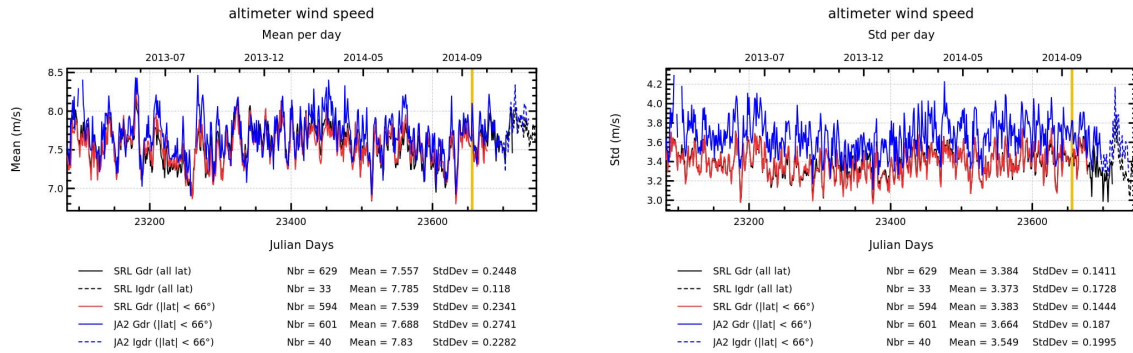


Figure 39: Daily monitoring of mean and standard deviation of altimeter wind speed for Saral/AltiKa and Jason-2. The gold band indicates the safe hold mode on Saral/AltiKa.

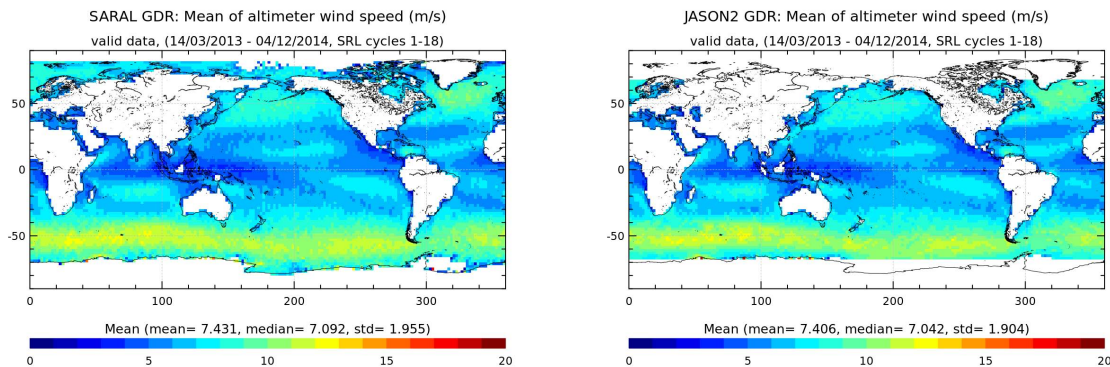


Figure 40: Average map of altimeter wind speed for Saral/AltiKa (left) and Jason-2 (right) cycles 1 to 18.

RL/JA2 XOvers<3h, cycles 001-016 (2013-03-14 / 2014-09-;

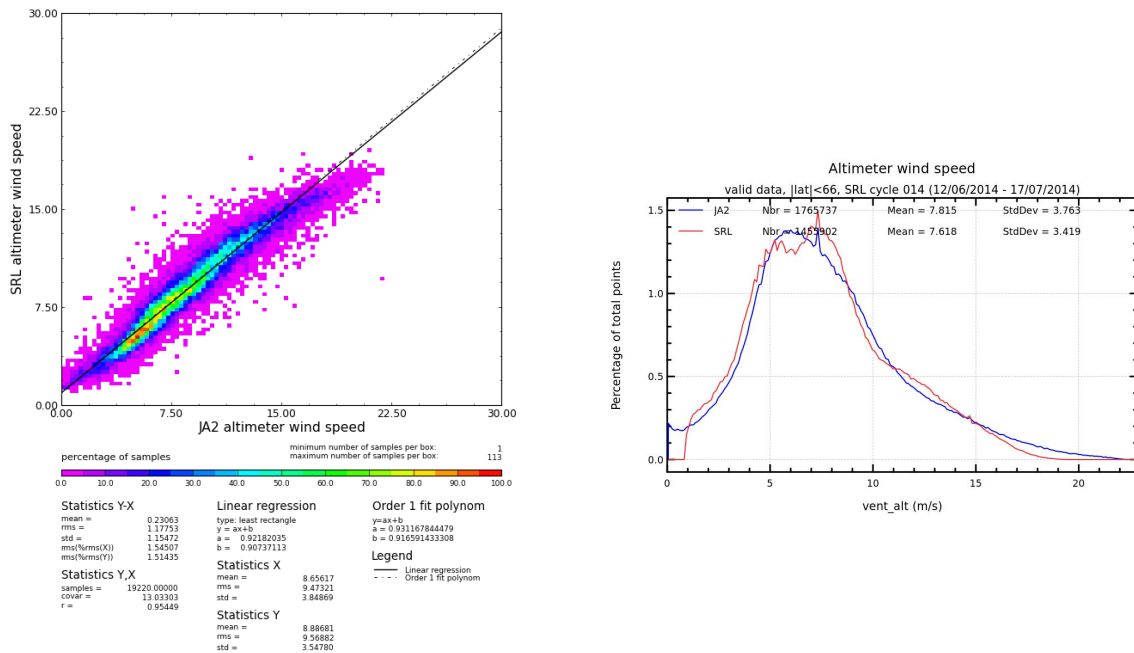


Figure 41: Dispersion diagram of altimeter wind speed between Saral/AltiKa and Jason-2 at 3h crossover points (computed for cycles 1 to 18) on the left and histogram of along-track data (without scale factor for Jason-2) computed for Saral/AltiKa cycle 14 on the right.

4.9. Sea state bias

In Patch1 version, the sea state bias was as a first approximation set equal to -3.5% of SWH. For Patch2 a hybrid SSB solution developed by R. Scharroo was used (this SSB was computed using the same method as in [12]). The Patch2 SSB solution is in absolute values around 1.8cm stronger (which increases the Patch2 SLA) than the Patch1 solution. This is related to the method of SSB computation (hybrid method).

The daily monitoring of the along-track sea state bias for Saral/AltiKa and Jason-2 show similar temporal evolution, but Saral/AltiKa SSB has higher absolute values (around 2.5 cm higher) than Jason-2 (see left side of figure 42). This is also the case when considering latitude weighted box statistics (bottom of figure 42). But this is not a homogeneous bias, it varies geographically, as shown on bottom of figure 43. Furthermore the daily standard deviation is also slightly larger for Saral/AltiKa compared to Jason-2 (see right side of figure 42).

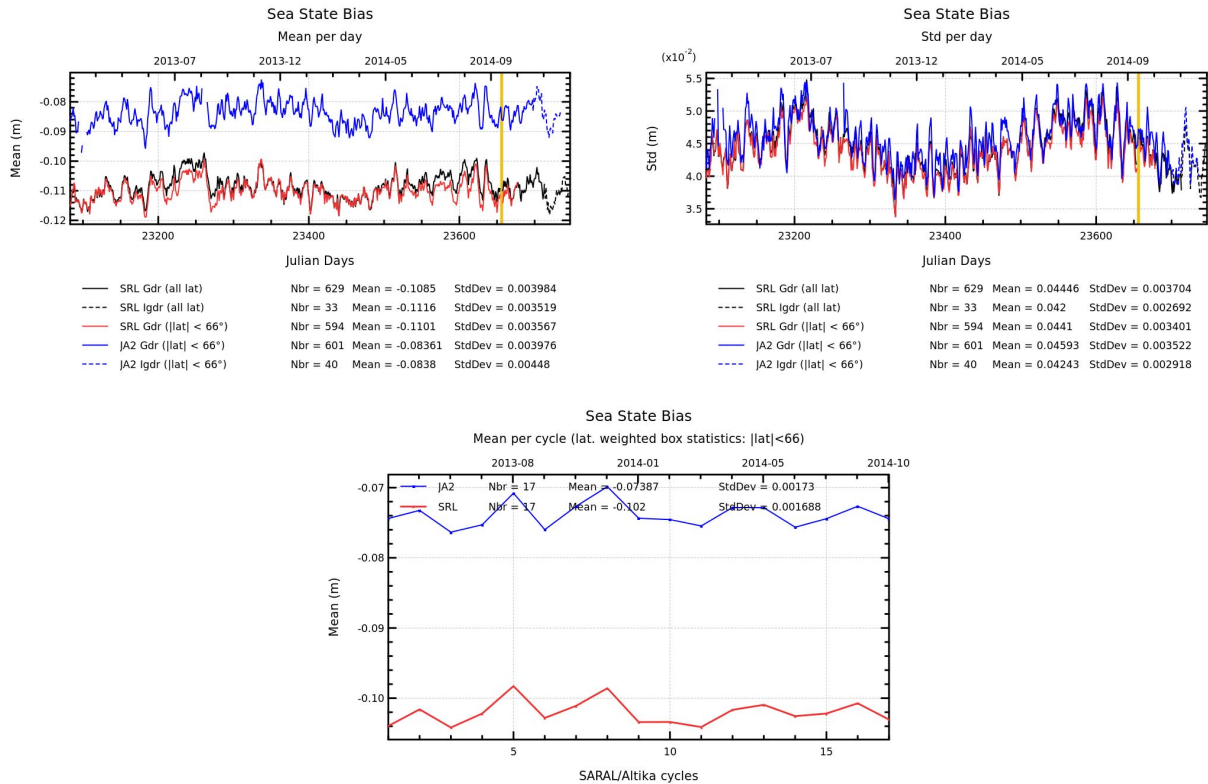


Figure 42: Daily monitoring of mean and standard deviation of (along-track) sea state bias of Saral/AltiKa and Jason-2 on the top and cycle per cycle monitoring of latitude weighted box mean for both missions on the bottom. The gold band indicates the safe hold mode on Saral/AltiKa.

Indeed the map of Saral/AltiKa sea state bias shows higher values in the region of 50°S (where SWH is strong) than the map of Jason-2 (top of figure 43). The dispersion diagram of Saral/AltiKa and Jason-2 sea state bias at 3h multi-mission crossovers confirms that the Saral/AltiKa SSB is overestimated for high SSB (equals high SWH). The different nature of the SSB models used for Saral/AltiKa and Jason-2 (dedicated model) is also visible on the right side of figure 44, showing very different shapes of histograms.

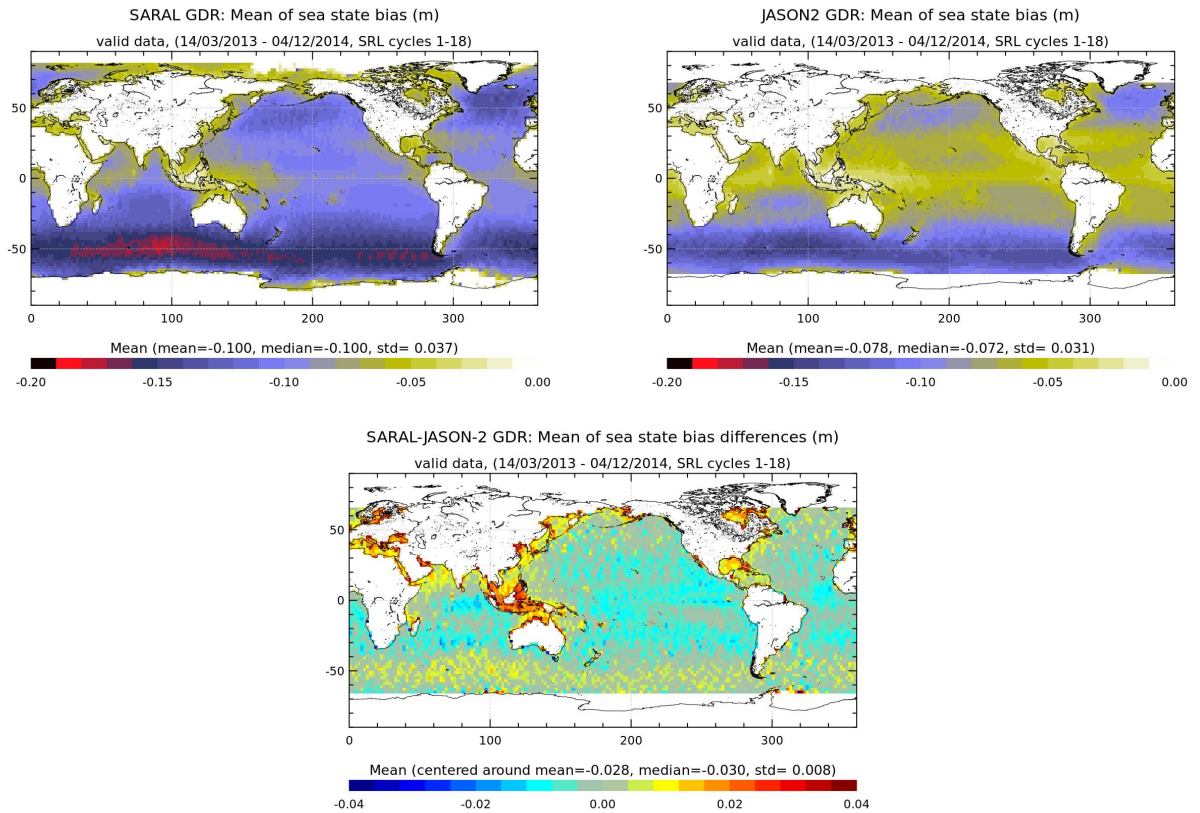


Figure 43: Average map of sea state bias for Saral/AltiKa (left) and Jason-2 (right) cycles 1 to 18. Difference map of gridded Saral and Jason-2 sea state bias for cycles 1 to 18.

This difference in sea state bias between the two missions has also an impact on the geographically correlated biases between the two missions, as shown in chapter 5.3., concerning maps of sea surface height differences at multi-mission crossover points.

RL/JA2 XOvers<3h, cycles 001-016 (2013-03-14 / 2014-09-;

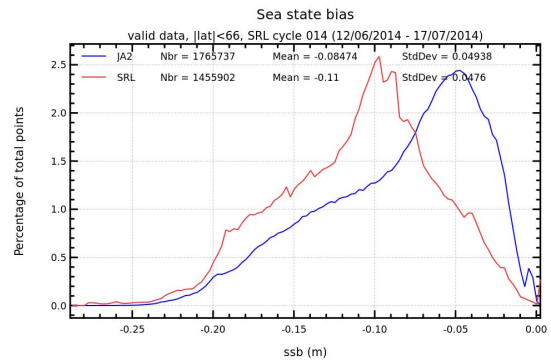
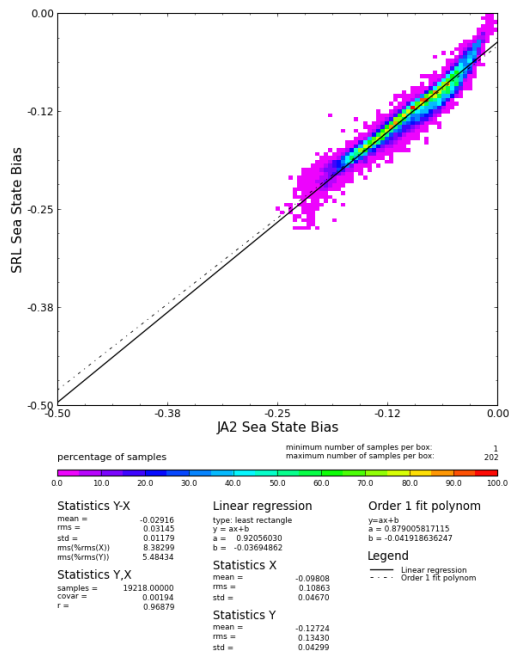


Figure 44: Dispersion diagram of sea state bias between Saral/AltiKa and Jason-2 at 3h crossover points (computed for cycles 1 to 18) on the left and histogram (of along-track data) computed for Saral/AltiKa cycle 14 on the right.

5. SSH crossover analysis

5.1. Overview

SSH crossover differences are the main tool to analyze the whole altimetry system performances. They allow us to analyze the SSH consistency between ascending and descending passes. However in order to reduce the impact of oceanic variability, we select crossovers with a maximum time lag of 10 days. This gives a measure of the performance on mesoscale time and spatial scales. Mean and standard deviation of SSH crossover differences are computed from the valid data set to perform maps or a cycle by cycle monitoring over all the altimeter period. In order to monitor the performances over stable surfaces, additional editing is applied to remove shallow waters (bathymetry above -1000m), areas of high ocean variability (variability above 20 cm rms) and high latitudes ($> |50|deg$). SSH performances are then always estimated with equivalent conditions. The main SSH calculation for SARAL/AltiKa and Jason-2 are defined below.

$$SSH = Orbit - Altimeter Range - \sum_{i=1}^n Correction_i$$

with *AltiKa / Jason-2 Orbit = CNES orbit* (standard D) for GDR products, and

$$\begin{aligned} \sum_{i=1}^n Correction_i = & \textit{Dry troposphere correction} \\ & + \textit{Dynamical atmospheric correction} \\ & + \textit{Radiometer wet troposphere correction} \\ & + \textit{Ionospheric correction} \\ & + \textit{Sea state bias correction} \\ & + \textit{Ocean tide correction (including loading tide)} \\ & + \textit{Earth tide height} \\ & + \textit{Pole tide height} \end{aligned}$$

Hereafter a reminder of the standards used (from GDR products: GDR-T Patch2 for Saral/AltiKa and GDR-D for Jason-2):

| Parameter | Saral/AltiKa | Jason-2 |
|--|--|---------------------------------|
| Orbit | CNES POE-D (Doris/Laser) | CNES POE-D (Doris/Laser/GPS) |
| Dynamic atmospheric correction (Inverse barometer correction + Non-tidal High-frequency Dealiasing Correction) | Computed from ECMWF atmospheric pressures after removing S1 and S2 atmospheric tides (for inverse barometer) + Mog2D High Resolution ocean model | |
| .../... | | |

| Parameter | Saral/AltiKa | Jason-2 |
|--|---|---|
| Radiometer wet troposphere correction | MWR using P2 (dual-frequency radiometer) | AMR (tri-frequency radiometer) |
| Ionospheric correction | Based on Global Ionosphere TEC Maps from JPL | dual-frequency altimeter ionosphere correction |
| Sea State Bias | Hybrid method of SSB computation developed by R. Scharroo | MLE4 version derived from 1 year of MLE4 Jason-2 altimeter data with version 'd' geophysical models |
| Global ocean tide (load tide included) | GOT 4.8 ocean tide | |
| Earth tide | From Cartwright and Taylor tidal potential | |
| Pole tide | Wahr [1985] | |
| Mean Sea Surface | CNES_CLS_2011 | |

Table 8: Standards used for Saral and Jason-2

When not otherwise stated, the standards from table 8 are used.

5.2. Mean of SSH crossover differences

In this section, the analysis are done over the first 18 cycles of SARAL/AltiKa using GDR-T Patch2 products. For comparison, Jason-2 GDR data are shown over the same period. The map of SSH mean ascending/descending differences at crossovers should ideally be close to zero. Geographically correlated patterns on such maps indicate systematic differences between ascending and descending passes. This can indicate either problems in the orbit computation or in geophysical corrections. Figure 45 (left) shows the map of mean SSH differences at crossovers for SARAL/AltiKa. This map shows several geographically correlated patterns, with a longitude dependency (almost vertical stripes). Two negative patches are visible, one centered on South America, the other on southern Asia while two positive patches appear close to New Zealand and if the Gulf of Alaska. The amplitude of these differences is below $\tilde{2}$ cm. Slightly larger differences, but with smaller geographical extension, are observed in the North Atlantic Ocean north of Iceland and in the Arctic and Southern Oceans. Compared to a similar analysis performed on Jason-2 data (figure 45, right), SARAL/AltiKa differences exhibit a larger amplitude: Jason-2 map shows differences generally lower than $\tilde{1}$ cm.

Part of the observed differences might come from orbit errors, part might come from systematic errors in the geophysical corrections. Figure 46 illustrates the impact of changing a geophysical correction on the maps of SSH differences at crossovers. The map on the left panel is estimated using FES2012 tide model instead of GOT4.8 model: the two negative patches are reduced, but a positive pathc appears in the Pacific Ocean. The strongly positive patch in the Northern Atlantic Ocean is reduced, but a new one appears in the Barents Sea.

In addition to mapping the differences, we estimate, at each cycle the global average of SSH

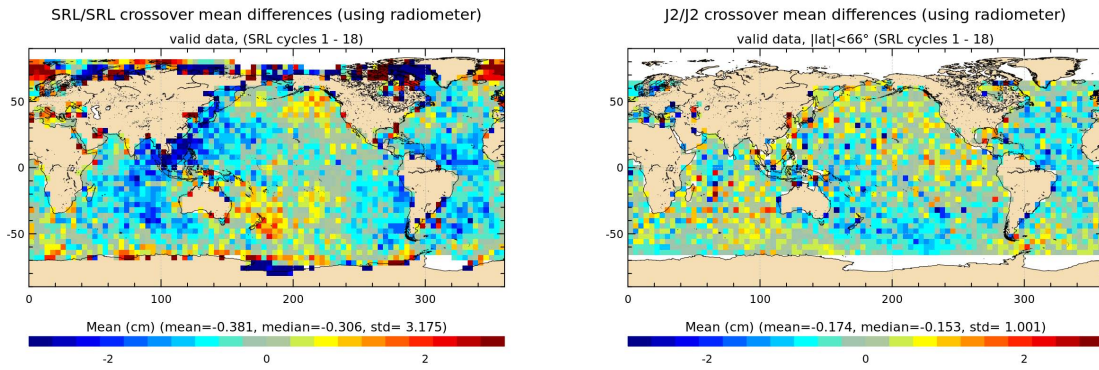


Figure 45: Map of mean of SSH crossovers differences for Saral/AltiKa (left) and Jason-2 for Saral cycles 1 to 18. Color scales are between ± 3 cm.

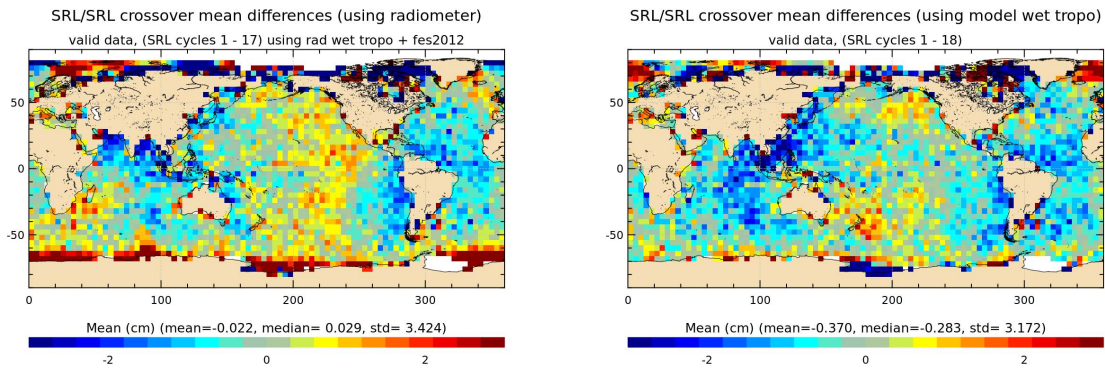


Figure 46: Map of mean of SSH crossovers differences for Saral/AltiKa for Saral cycles 1 to 18. Color scales are between ± 3 cm. Using FES 2012 ocean tide instead of GOT 4.8 (left) and using model wet troposphere (right).

differences at crossovers and monitor the time variability of this quantity to detect any issue on the mission. Over the first 18 cycles of the SARAL/AltiKa mission, the evolution of the cycle-average mean SSH difference at crossovers is plotted on figure 47 for SARAL/AltiKa and Jason-2. We present here two types of selection for crossovers (no selection at all and selection on bathymetry, latitude and oceanic variability) and two ways of averaging the SSH differences at crossovers (a simple ensemble mean and a latitude weighted based on the crossovers theoretical density). The weighted averaging method is described in appendix 10.3.. For SARAL/AltiKa, the mean difference is slightly negative $\approx -2/-3$ mm depending on the averaging method and the crossovers selection. The mean value is very stable over time except for a slight increase around cycles 12 and 13. Over the same period, Jason-2 appears a bit more centered with a mean SSH difference at crossovers about -1.5 mm depending on the selection and averaging method, but with a slightly larger variability over time.

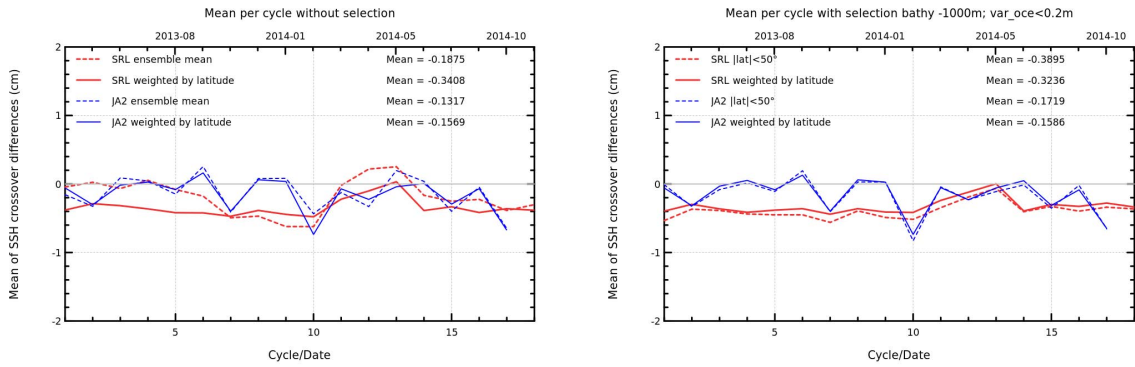


Figure 47: Cycle per cycle monitoring of ascending/descending SSH differences at mono-mission crossovers for Saral/AltiKa and Jason-2 for Saral cycles 1 to 18.

5.3. Mean of SSH crossover differences between Saral and other missions

Dual-mission crossover performances are computed between SARAL/AltiKa and Jason-2 in order to detect geographically correlated biases between missions as well as to check SARAL/AltiKa stability with respect to Jason-2. The temporal evolution of this difference is monitored in order to detect if there are drifts or jumps indicating a problem in one of the missions. The temporal evolution of the mean of SARAL/AltiKa/Jason-2 SSH differences at crossovers, based on Jason-2 cycles is shown on figure 48. On both panels a selection for latitudes lower than 50°, deep ocean and low oceanic variability areas is used. The left panel uses an ensemble mean estimation while the right panel is based on a latitude weighted average. The green line uses the radiometer wet tropospheric correction while the black line is based on the modeled correction. In all cases the temporal evolution of SSH differences at crossovers between SARAL/AltiKa and Jason-2 is very similar. The mean bias between the missions is estimated to -4.5 cm (Jason-2 being higher than SARAL/AltiKa) and is stable over the time period with a standard deviation of ≈ 0.2 cm. Over the available period, no SSH drift between the two missions is detectable. In general, switching from the radiometer to the model wet tropospheric correction has a little impact on the curves, except in September and October 2013 due to the saturation of the radiometer hot calibration counts.

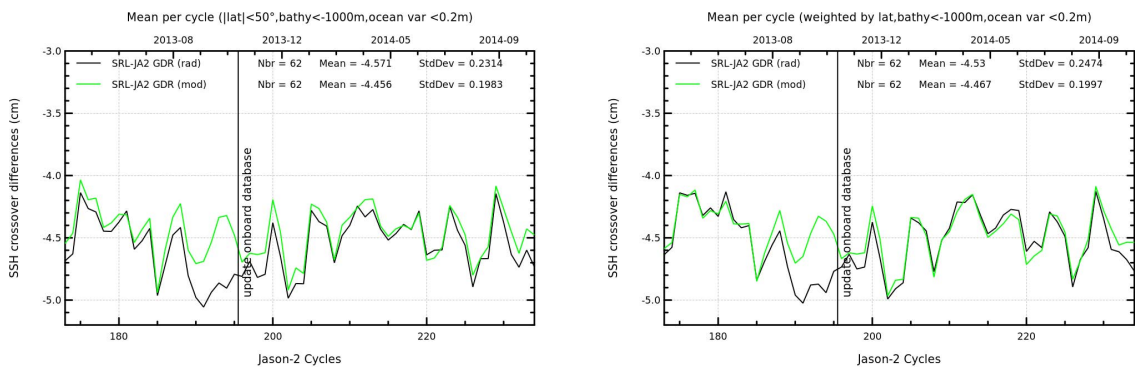


Figure 48: Monitoring of mean of Saral - Jason-2 differences at crossovers using radiometer wet troposphere correction (black line) or ECMWF model wet troposphere correction (green line) for GDR data with different selections. Statistics are computed on base of Jason-2 cycles.

Rather than looking at the temporal evolution, mapping the SSH differences between SARAL/AltiKa and Jason-2 over the first 18 cycles of SARAL/AltiKa provides information about any geographically correlated biases between the two missions. Such maps are shown on figure 49, where both maps are centered before plotting. Large scale differences are visible between the two missions with amplitudes around ± 2 cm. Using the radiometer on both missions (left of figure 49) shows a negative patch in the western tropical Pacific Ocean centered on Indonesia and a large positive patch in the Southern Ocean, which extends towards the north in Atlantic Ocean. As for mono-mission crossover differences, part of the observed pattern might come from orbit related issues and/or from geophysical corrections. Using the model wet tropospheric correction on both missions (right of figure 49) greatly reduces the Southern Ocean patch and also reduces the negative Indonesian patch (though to a lesser extent), as well as a positive patch at the southern tip of Greenland. However the positive patch in the southern Atlantic Ocean remains. Improvements are expected from an improved radiometer retrieval algorithm, as well as a new SSB model for SARAL/AltiKa as part of Patch 3.

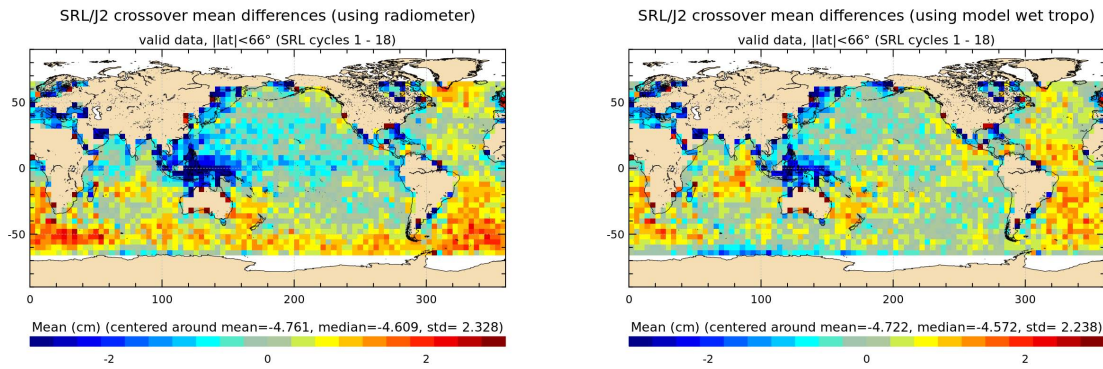


Figure 49: Map of mean of SSH crossovers differences between Saral/AltiKa and Jason-2 using either radiometer wet troposphere correction (left) or ECMWF model wet troposphere correction (right) for both missions. The maps are centered around the mean.

5.4. Standard deviation of SSH crossover differences

The standard deviation of SSH differences at crossovers is a key performance metric for satellite altimetry missions. In this section the standard deviation of SSH differences at crossovers is investigated for SARAL/AltiKa and compared to Jason-2.

The cycle per cycle standard deviation of SSH differences at crossovers is plotted on the left of figure 50 for different selections and averaging methods:

- black: no selection is applied, and the ensemble standard deviation is estimated without any weighting. In this case the standard deviation amounts to 6.7 cm and its temporal evolution is impacted by an annual signal due to the sea ice extension variations. The curve also shows an increase at cycle 17 which is impacted by the safe hold mode event.
- purple: as above no selection is applied on the crossovers, but the standard deviation is estimated after weighting the crossovers following the method described in section 10.3.. This process slightly reduced the standard deviation (6.2 cm) due to downweighting of crossovers at high latitudes and reduces the amplitude of the annual signal. Statistics for cycle 17 remain impacted by the safe hold mode event.
- red: shallow waters have been removed (bathymetry < -1000m) as well as latitudes greater than 50° and high ocean variability areas. This selection allows to validate the hypothesis of a steady ocean over 10 days which is underlying to crossovers analysis and therefore allows monitoring the SARAL/AltiKa system performance. In this case, the standard deviation of SSH differences drops to 5.3 cm and no annual cycle is observed. The statistic is also less impacted by the safe hold mode event.
- green: uses the same selection as above, combined to a latitude weighting of the crossovers before estimating the standard deviation (see section 10.3.). Using this method leads to a small increase of the standard deviation of SSH differences at crossovers (at 5.4 cm)

The right part of figure 50 displays the geographical distribution of the standard deviation of SSH differences at crossovers. This map shows the expected patterns with high standard deviation observed in high ocean variability areas and in the Arctic Ocean (where some geophysical corrections such as tides, are less accurate).

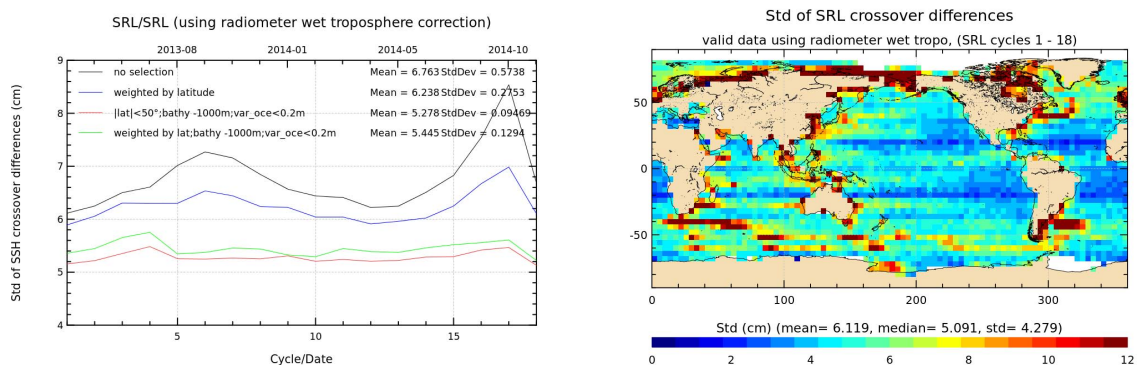


Figure 50: Cycle by cycle standard deviation of SSH crossover differences for Saral/AltiKa using several selections (left), map of standard deviation at crossover points (right), the radiometer wet troposphere correction is used.

As part of the routine Cal/Val activities, the performance of SARAL/AltiKa is compared to Jason-2 through the use of the standard deviation of SSH differences at crossovers. Figures 51 and 52 display comparisons between SARAL/AltiKa and Jason-2 performance at crossovers for different selections and weighing methods. In each case the performance using the radiometer and the model are displayed.

Figure 51 displays the ensemble standard deviation with no weighting applied. When using the radiometer, SARAL/AltiKa and Jason-2 performances are very close, especially when selecting only the deep ocean and removing high ocean variability areas. When using the model wet tropospheric correction, SARAL/AltiKa has a slightly lower standard deviation of SSH differences at crossovers than Jason-2. This indicates that using the radiometer correction rather than the modeled one brings a greater improvement on Jason-2 than on SARAL/AltiKa, but the future version of the product will have a new improved radiometer retrieval algorithm.

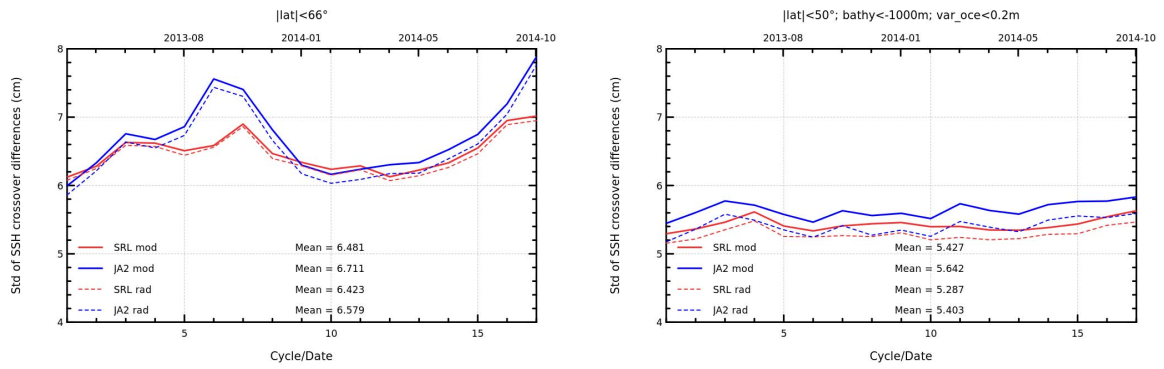


Figure 51: monitoring of the standard deviation of SSH differences at crossovers for SARAL/AltiKa and Jason-2 for Saral cycles 1 to 18 using radiometer (dotted lines) or model (plain lines) wet troposphere correction

To account for the uneven distribution of crossover points, we also estimate weighted statistics (figure 52) where the weights applied are a function of latitude based on the crossovers density. This allows to better compare the two missions that do not share the same ground track. Similar results are obtained with these weighted statistics: depending on the wet troposphere correction chosen, SARAL/AltiKa's performance is equivalent or even better than the Jason-2 one.

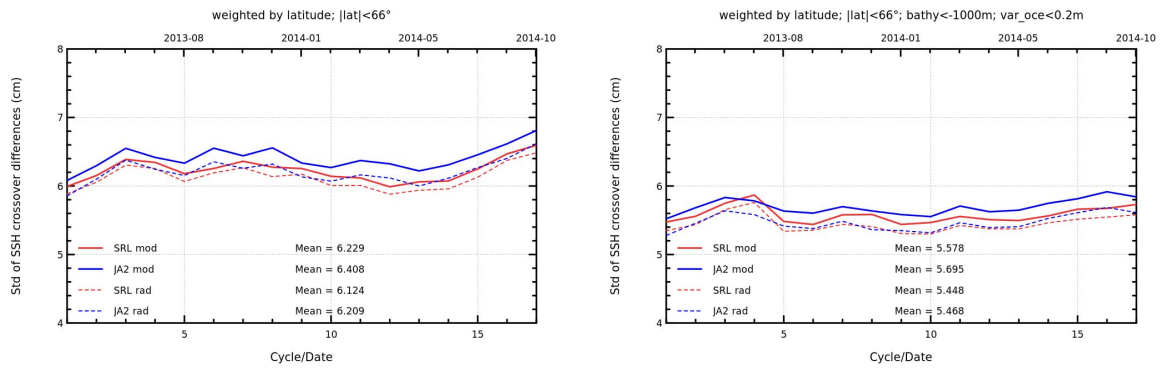


Figure 52: monitoring of the standard deviation of SSH differences at crossovers for SARAL/AltiKa and Jason-2 for Saral cycles 1 to 18 using radiometer (dotted lines) or model (plain lines) wet troposphere correction

5.5. Performances at crossover points of the different product types (Ogdr/Igdr/Gdr)

Saral/AltiKa data are also available as Ogdr and Igdr products, which are more rapidly available than Gdr products. The main differences between the different data products are listed in table 9.

| Auxiliary Data | Impacted Parameter | Ogdr | Igdr | Gdr |
|----------------|--|-----------------|-------------------------|-----------------------------|
| Orbit | Satellite altitude, Doppler correction, ... | DORIS Navigator | Preliminary (Doris MOE) | Precise (Doris + Laser POE) |
| Meteo Fields | Dry/wet tropospheric corrections, U/V wind vector, Surface pressure, Inverted barometer correction,... | Predicted | Restituted | Restituted |
| Pole Location | Pole tide height | Predicted | Predicted | Restituted |
| Mog2D | HF ocean dealiasing correction | Not available | Preliminary | Precise |
| GIM | Ionosphere correction | Predicted | Restituted | Restituted |

Table 9: Differences between the auxiliary data for the O/I/Gdr products (from [4])

Figure 53 displays the monitoring of the cycle per cycle mean and standard deviation of SSH differences at crossovers for the OGDR, IGDR and GDR products. Regarding the mean, all three products show a good stability, of course the temporal variability is greater for OGDR and IGDR than for GDR data. Regarding the standard deviation, as expected, OGDR data have the highest standard deviation at ≈ 7 cm, followed by IGDR data with 5.5 cm. As expected GDR products provide the best performance with a standard deviation of the differences at crossovers of 5.2 cm.

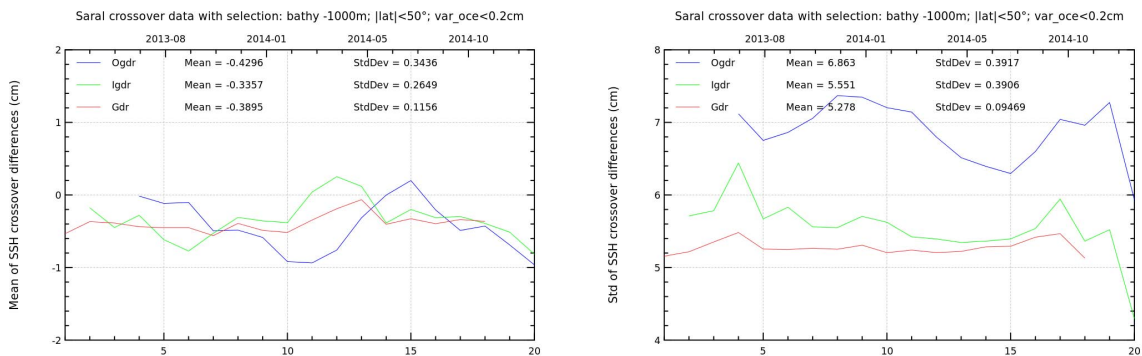


Figure 53: Cycle per cycle monitoring of mean and standard deviation of SSH crossover differences for SARAL/AltiKa using radiometer wet troposphere correction and geographical selection ($|latitude| < 50^\circ$, bathymetry < -1000 m and ocean variability < 20 cm rms).

5.6. Estimation of pseudo time-tag bias

The pseudo time tag bias is found by computing at crossovers the regression between SSH differences and orbital altitude rate (\dot{H}), also called satellite radial speed :

$$\Delta SSH = \alpha \dot{H}$$

This method allows us to estimate the time tag bias but it absorbs also other errors correlated with \dot{H} as for instance orbit errors. Therefore it is called "pseudo" time tag bias.

The Jason satellites had a pseudo time-tag bias close to -0.28 milliseconds with an approximately 60-days signal. The origin of this pseudo time tag bias of the Jason satellites was found by CNES in 2010 [5]. It has a mean of about -0.25 milliseconds and is dependent on the altitude of the satellite. For Jason-2 GDR-D data, the datation was directly modified in order to correct it properly, whereas for Jason-1 GDR-C product it is taken into account thanks to a correction (pseudo_datation_bias_corr_ku). Therefore the average of the pseudo datation bias is now close to zero for the Jason satellites, nevertheless the periodic signal remains and is not yet explained.

Figure 54 shows the monitoring of the pseudo datation bias for SARAL/AltiKa and Jason-2 on a cyclic basis (respectively 35 and almost 10 days).

On average SARAL/AltiKa has a slightly larger pseudo time-tag bias than Jason-2, around -0.04 ms, but which appears to be more stable over time.

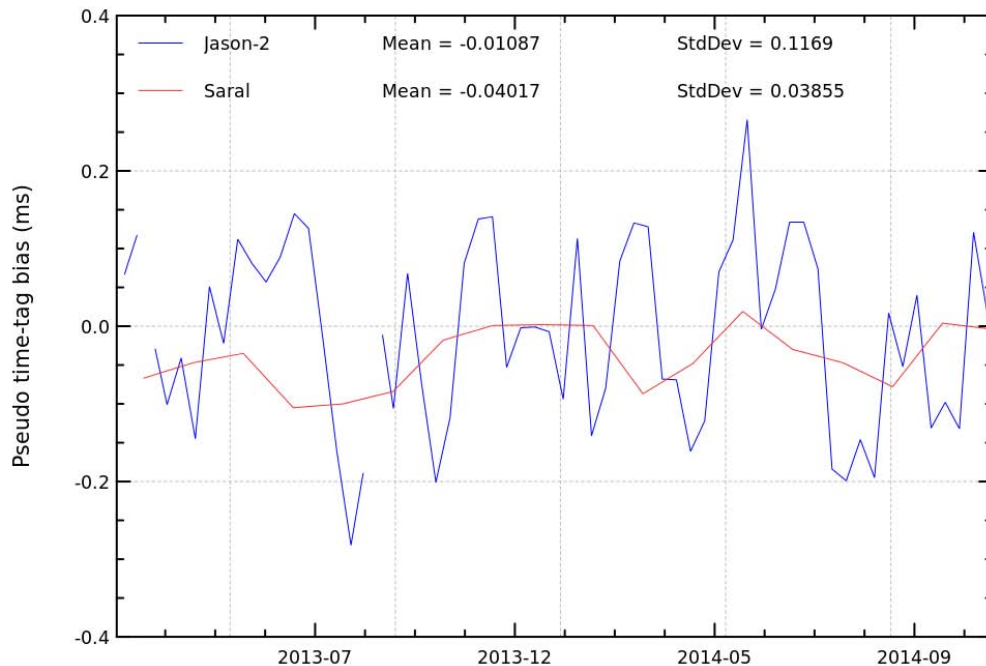


Figure 54: Cyclic monitoring of pseudo time tag bias for SARAL/AltiKa and Jason-2

6. Sea Level Anomalies (SLA) Along-track analysis

6.1. Overview

The Sea Level Anomalies (SLA) are computed along track from the SSH minus the mean sea surface with the SSH calculated as defined in previous section 5.1. :

$$SLA = SSH - MSS(CNES/CLS2011)$$

Figure 55 shows the average SLA difference between SARAL/AltiKa and Jason-2 over the first 17 cycles of SARAL/AltiKa, using the radiometer or modeled wet troposphere correction. Both maps show geographically correlated differences of the order of ≈ 2 cm. The patterns are very similar to the ones observed at SARAL/AltiKa/Jason-2 crossovers with a positive patch in the Atlantic Ocean and a negative one around Indonesia. However there is a very good agreement between SARAL/AltiKa and Jason-2 over the first two years of SARAL/AltiKa regarding SLA patterns.

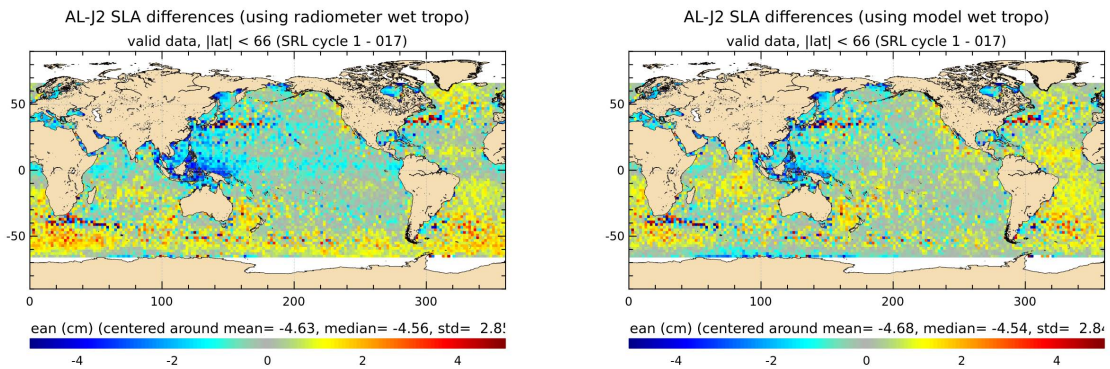


Figure 55: Map of SLA differences between SARAL/AltiKa and Jason-2 using the radiometer (left) and modeled (right) wet troposphere correction for the 17 first cycles of SARAL/AltiKa.

6.2. Along-track performances for Saral/AltiKa (GDR-T Patch1) and Jason-2

SLA analysis is a complementary indicator to estimate the altimetry system performances. It allows us to study the evolution of SLA mean (detection of jump, abnormal trend or geographical correlated biases), and also the evolution of the SLA variance highlighting the long-term stability of the altimetry system performances. Hereafter daily monitoring of mean (top left of figure 55) and standard deviation (top right of figure 55) of SARAL/AltiKa and Jason-2 SLA are shown.

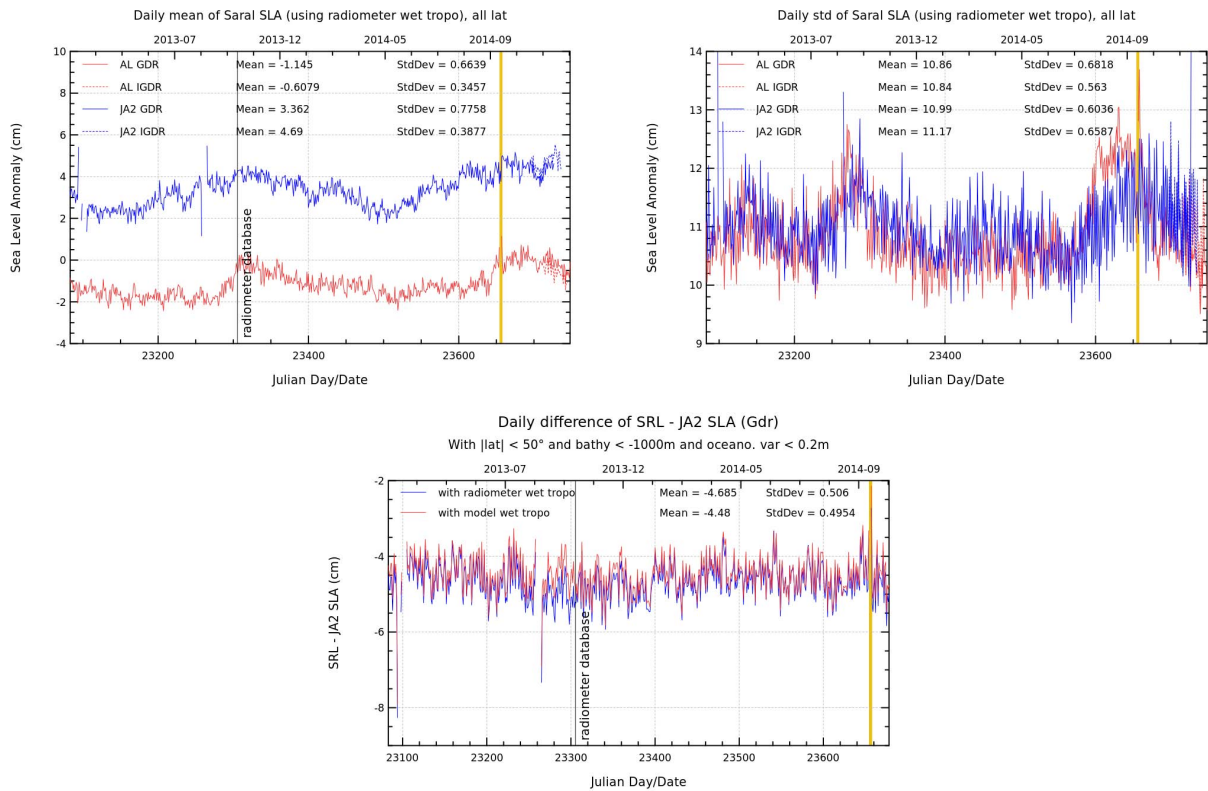


Figure 56: Daily monitoring of mean (top left) and standard deviation (top right) of SLA (using radiometer wet troposphere correction) of GDR data (plain lines) and IGDR data (dotted lines). The statistics are done for valid data with all available latitudes. The gold band indicates the safe hold mode on Saral/AltiKa. Bottom: Difference of daily Saral/AltiKa minus Jason-2 SLA using either radiometer or model wet troposphere correction. The statistics are done for valid data with $|\text{latitudes}| < 50^\circ$, bathymetry < -1000 m and low ocean variability.

Saral/AltiKa and Jason-2 daily mean of SLA show similar signals and evolution. There is an offset between SARAL/AltiKa and Jason-2 SLA of around -4.5 cm when using the radiometer wet troposphere correction, and -4.7 cm using the model wet troposphere correction. This bias between missions appears to be very stable over time, with no drift detected over the available period. The safe hold mode on SARAL/AltiKa might have had an impact on this bias, this question is addressed in section 7.3.. The daily standard deviations of SARAL/AltiKa and Jason-2 SLA are very similar (top right of figure 55), except for about one month before the SARAL/AltiKa’s safe hold mode, when platform pointing accuracy was degraded.

6.3. Along-track performances of the different product types (Ogdr/Igdr/Gdr)

SARAL/AltiKa products are available for three data types (with different latency and precision): Ogdr, Igdr and Gdr. There are also some differences in the product content (see table 9). Hereafter the daily mean and standard deviation of SLA of the different data types is monitored (see figure 57). Note that only the Gdr data are an homogeneous data set (using Patch2 version for all cycles). For Ogdr and Igdr data Patch1 version was only used from July onwards (for precise dates see table 1). This explains the jumps visible in the Ogdr and Igdr SLA series. Another jump affects the IGdr and OGdr curves which occur when we switch from Cal/Val to DUACS database. These jumps correspond to the change in the MSS reference period: while Cal/Val uses a MSS referenced over a 7 years period (like in the products), DUACS uses a 20 years reference period. At the beginning of the period, Ogdr SLA exhibits furthermore some additional short-term (about 14 days period) variability. These were indentified in the 2013 SARAL annual report, after the application of Patch 2, the amplitude of these signals is greatly reduced, thanks to the new version of TRIODE software used to estimate the Ogdr orbit. The temporal evolution of the mean of Ogdr, Igdr and Gdr SLA are very close, observed biases come from the different MSS reference periods used. The standard deviation of SLA shows low values for all products (between 11 and 12 cm): standard deviation of Gdr product is the lowest and the one of Ogdr products is the highest. But even the performance of Ogdr products is already very good (thanks to the good quality of the Doris/Diode navigator orbit).

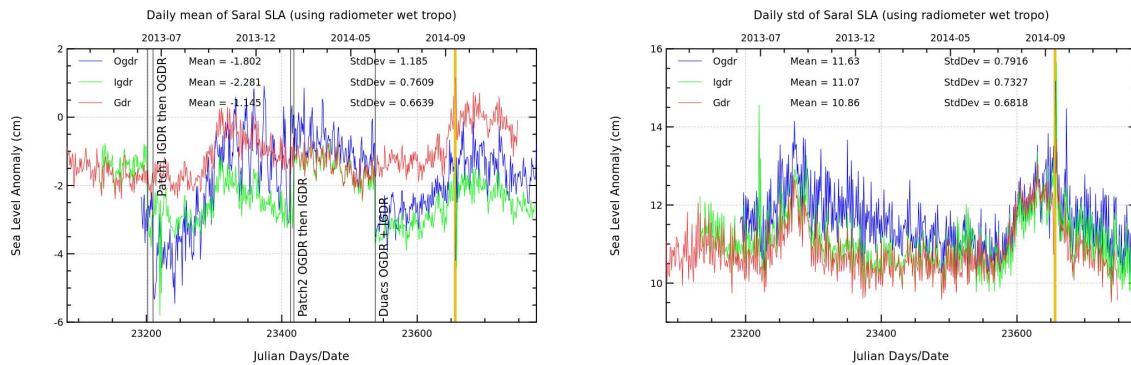


Figure 57: Daily monitoring of mean and standard deviation of valid Saral/AltiKa SLA (with radiometer wet troposphere correction) for Ogdr, Igdr and Gdr products. No particular selection is used (latitude is not limited).

6.4. SARAL/AltiKa as part of the GMSL record

SARAL/AltiKa data can easily be merged to the global Global Mean Sea Level (GMSL) record. The period is of course short to draw quantitative conclusions, but the results are shown here as an illustration of SARAL/AltiKa's very good performance level.

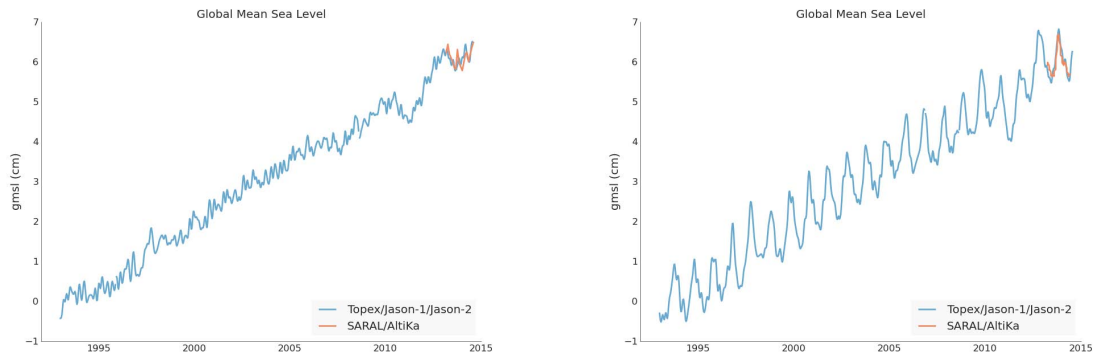


Figure 58: SARAL/AltiKa global mean record compared to the reference global mean sea level from TOPEX/Poseidon, Jason-1 and Jason-2, with and without the seasonal signal

7. Particular Investigations

7.1. Mispointing

At the beginning of the mission, SARAL/AltiKa's pointing was very accurate. As a result of an increase in reaction wheel friction, SARAL/AltiKa has been impacted by mispointing events from cycle 16 onward. The number of mispointing events rised and the reaction wheel eventually stopped, leading to the reconfiguration of the spacecraft to three wheel mode. Following this re-configuration, ISRO performed a software upload, which failed (partial upload during the station overfly) leading to the spacecraft going into safe hold mode from cycle 17, pass 324 to pass 414 (from October 6th to 9th, 2014). Figure 59 illustrates the rise of SARAL/AltiKa mispointing from cycle 7 (a typical early mission situation) to cycle 17 where the safe hold mode event occurred. Cycle 18 presents a typical post-SHM situation (three wheel pointing) where several areas of high mispointing remain, related to the command law of the spacecraft (zero-crossings of the RW speed):

- near the equator, with a ionosphere-like shaped pattern
- a band in the southern hemisphere going from Africa to America across the Indian and Pacific oceans
- in the high latitudes of the northern Atlantic Ocean

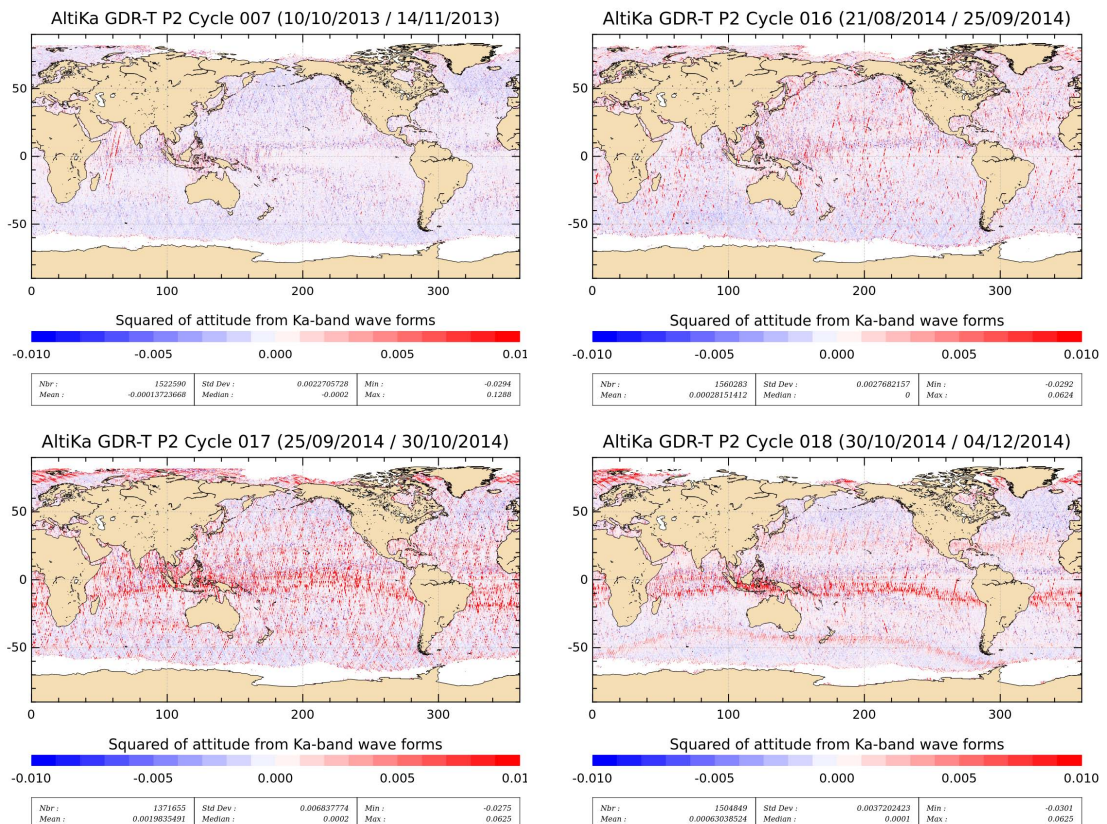


Figure 59: maps of SARAL/AltiKa mispointing for cycles 7, 16, 17 and 18

In order to get an overview of how the mispointing increased we used a track section detection algorithm to monitor the number of high mispointing events. In this case we look for high mispointing events defined as at least 10 consecutive 1Hz measurements where the mispointing exceed $0.015deg^2$. Left panel of figure 60 monitors the number of mispointed sections (red) as well as the average length of the sections (blue) and the total duration of mispointing events (average length times number of events, in green). For the first part of the mission, there were no mispointing events, except during maneuvers. The number of mispointing events rises rapidly a few days before the SHM tops at ≈ 300 events. After the SHM, the situation seems to be stable around 10-15 events per day with an average length of ~ 30 seconds. This represents a large increase with respect to the beginning of the mission.

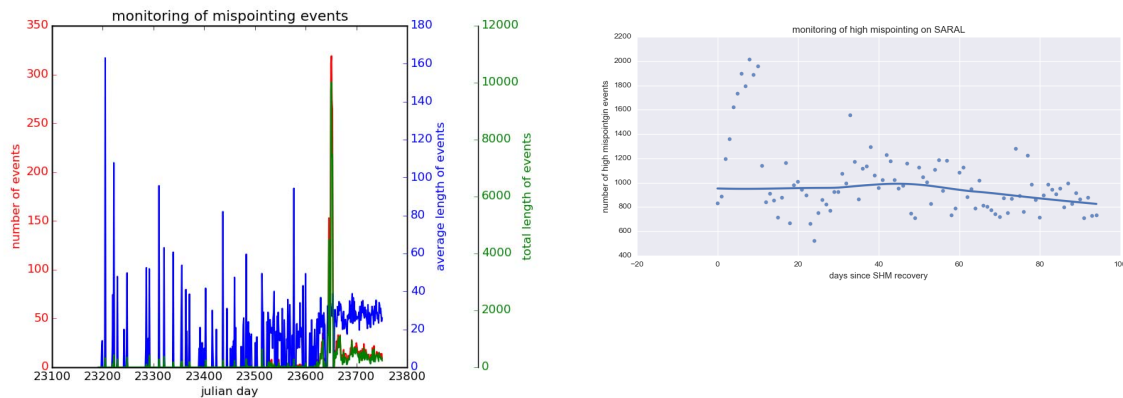


Figure 60: number of mispointed track sections (left) and number of mispointing events after the SHM recovery (right)

We also monitor the number of mispointed measurements (where the mispointing exceed $0.01deg^2$) per day since the SHM recovery. During the first 12 days, an important rise is observed, but the period is impacted by several maneuvers. After that the number of mispointed measurements seems to be stable or even slowly declining. The "high" mispointing events we monitor here remain below the specified pointing accuracy of $0.0225deg^2$.

7.2. Correction of the hot calibration count saturation

As mentioned in section 4.7.1., the current (GDR Patch 2) wet troposphere correction is impacted by the saturation of hot calibration counts. A solution to compensate for the observed drift was proposed and implemented ([1]). The impact of this correction on the radiometer wet troposphere correction is illustrated on figure 61 which displays daily averages of the radiometer minus model corrections. The green curve corresponds to the Jason-2 mission and is used as a reference. The red line corresponds to the current product status and show a $\approx 5mm$ drift upwards which is corrected abruptly when the onboard radiometer database was updated. The blue line shows the status of the wet tropo difference with the correction applied. Clearly, with the correction applied wet tropo difference for SARAL/AltiKa follows much more closely Jason-2.

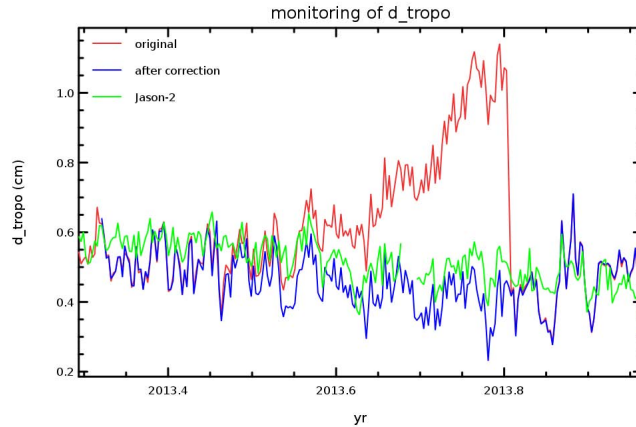


Figure 61: *Daily averages of the wet troposphere differences (radiometer - model) for SARAL/AltiKa patch 2 data (red), SARAL/AltiKa after the correction and Jason-2 (green)*

7.3. Checking for any impact of the safe hold mode on SARAL/AltiKa SLA

SARAL/AltiKa experienced a safe hold in 2014 from October 6th to 9th. When such events happen it is important to check if everything is working properly on the spacecraft. We particularly checked if no SLA bias was observed after the SHM. The SLA results presented here use the radiometer wet tropospheric correction with the empirical correction for the saturation of hot calibration counts presented at section 7.2..

Figure 62 presents the monitoring of SLA for Jason-2 and SARAL/AltiKa, and their differences, since the beginning of the SARAL/AltiKa mission. The left panel depicts the daily averages of SLA from Jason-2 and SARAL/AltiKa, the difference between the two curves is shown in black, referenced to the scale on the left (all curves are centered). This curve shows no large bias between SARAL/AltiKa and Jason-2 SLA after the SHM. But there is an annual signal in the daily SLA differences between SARAL/AltiKa and Jason-2 and therefore a very precise evaluation of the SHM impact is made difficult.

To reduce the effect of this annual signal, we plot the same curves per year, overlaying years 2013 and 2014 (right panel of figure 62). The safe-hold mode periods (on Jason-2 and SARAL/AltiKa) are represented as the gray bars. No impact of the SHM mode on SARAL/AltiKa is visible on these curves.

If we try a more quantitative approach, the mean of SARAL/AltiKa minus Jason-2 SLA differences before the SHM amounts to -4.3cm . From October 9th, this mean difference amounts to -4.5cm . The typical standard deviation of the SLA differences between SARAL/AltiKa and Jason-2 is $\approx 5\text{mm}$, which gives an estimate of the uncertainty on the mean over this period of $\approx 5/\text{sqrt}(100) = 0.5\text{mm}$ and we therefore can't say that the mean differences after the SHM differs from the mean difference before the SHM.

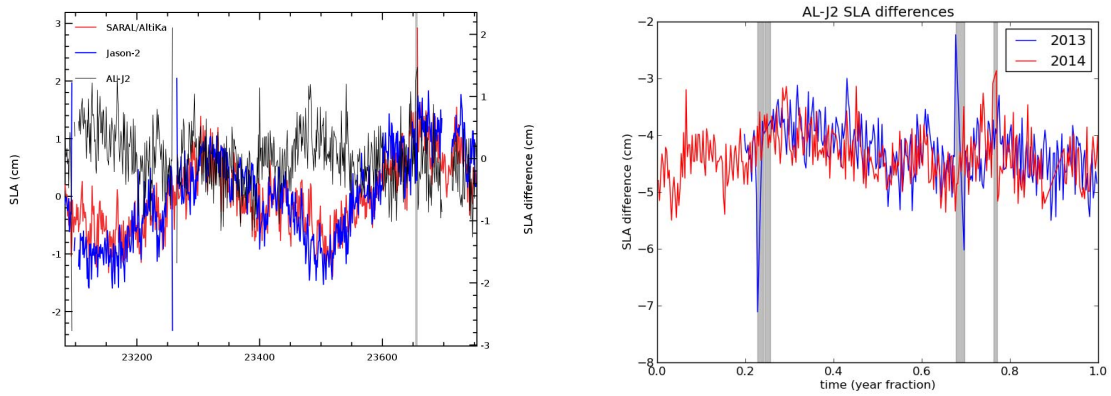


Figure 62: daily monitoring of global SLA for Jason-2 and SARAL/Altika, the difference is shown in black (left) and the daily differences of SLA between Jason-2 and SARAL/Altika for years 2013 and 2014 (right)

8. Conclusion

Saral/AltiKa was launched on February, 25th 2013. Since March, 13th, Saral / AltiKa is on its operational orbit. It's the first altimeter satellite using the Ka-band frequency, instead of Ku-band. Despite this new frequency, the OGDR/IGDR products were opened to users end of June/beginning of July 2013. The GDR products (GDR-T version Patch1) were available to the PI from 2nd of August 2013 onwards. Following the Saral/AltiKa NRT Verification workshop held end of August 2013 in Toulouse, the GDRs were released to all users from 12th September 2013.

A second version of the products was released to users (GDR-T Patch 2) about a year after launch (early February 2014, cycle 10) for real-time products and from cycle 8 onwards for GDR products. The first 7 cycles of the GDR product were reprocessed in 2014 in order to provide a consistent dataset.

In fall 2014, SARAL/AltiKa has experienced an increase in the friction of one reaction wheel, leading to an increase of the number of measurements impacted by high platform mispointing. This resulted in the wheel eventually stopping and the spacecraft going into safe-hold mode for three days from October 6th.

Though direct point to point comparison to other satellites are not possible (due to different ground tracks) we now have a variety of results, including comparisons with Jason-2 that demonstrate the excellent quality of the SARAL/AltiKa mission.

SARAL/AltiKa provides an excellent coverage of the ocean, with more than 99% of measurements available over ocean. The data quality is excellent, with only 2.4% of edited measurements, a value lower than the Jason-2 one by about 1%.

Regarding SLA statistics, no long term drift with respect Jason-2 is detectable, however, two years is still a short period. SARAL/AltiKa and Jason-2 observe very similar SLA features, both considering the temporal evolution of global averages and the geographical patterns. Regarding global daily averages of SLA, the standard deviation of the differences between SARAL/AltiKa and Jason-2 is only 5 mm, despite the fact that the two missions are not flying over the same ground track. For statistics at crossovers, the SARAL/AltiKa mission shows a performance similar to the Jason-2 one with a standard deviation of 5.3 cm. To account for the uneven distribution of crossovers over the ocean due to different orbits between missions, we introduced a new weighed statistics to compare these two missions which also demonstrate a similar performance of the two missions.

Saral/AltiKa is a key mission side by side with Jason-2 and Cryosat in multi-mission analysis systems such as Duacs.

9. References

References

- [1] M.-L. Frery *et al.*, 2014, Correction du canal 37GHz du radiomètre AltiKa, CLS/DOS/NT-14-115
- [2] L. Aouf and J.-M. Lefèvre: The impact of Saral/Altika wave data on the wave forecasting system of Météo-France : update. Oral presentation at SARAL/AltiKa 1st Verification Workshop, 27th to 29th August 2013, Toulouse, France. Available at http://www.avisooceanobs.com/fileadmin/documents/ScienceTeams/Saral2013/24_wave_lotfi.pdf
- [3] Brown G.S., "The average impulse response of a rough surface and its application", *IEEE Transactions on Antenna and Propagation*, Vol. AP 25, N1, pp. 67-74, Jan. 1977.
- [4] SARAL/AltiKa Products handbook, July 2013 *SALP-MU-M-OP-15984-CN* edition 2.3. Available at: http://www.avisooceanobs.com/fileadmin/documents/data/tools/SARAL_Altika_products_handbook.pdf
- [5] Boy, François and Jean-Damien Desjonqueres. 2010. Note technique datation de l'instant de réflexion des échos altimètres pour POSEIDON2 et POSEIDON3 *Reference: TP3-JPOS3-NT-1616-CNES*
- [6] Desjonquères, J. D. , Carayon, G. , Steunou, N. and Lambin, J. (2010) Poseidon-3 Radar Altimeter: New Modes and In-Flight Performances, *Marine Geodesy*, **33:1**, 53 - 79. Available at http://pdfserve.informaworld.com/542982__925503482.pdf
- [7] Y. Faugere, A. Delepouille, F.Briol, I. Pujol and DUACS Team, N. Picot, E. Bronner. Altika in DUACS: Status after 2 months (and perspectives). Oral presentation at SARAL/AltiKa 1st Verification Workshop, 27th to 29th August 2013, Toulouse, France. Available at http://www.avisooceanobs.com/fileadmin/documents/ScienceTeams/Saral2013/34_Altika_in_Duacs_Faugere.pdf
- [8] D. Griffin and M. Cahill: Use of AltiKa NRT sea level anomaly in the Australian multi-mission analysis. Oral presentation at SARAL/AltiKa 1st Verification Workshop, 27th to 29th August 2013, Toulouse, France. Available at http://www.avisooceanobs.com/fileadmin/documents/ScienceTeams/Saral2013/33_multi_mission_gridding_GRIFFIN.pdf
- [9] Lillibridge, J., Scharroo, R., Abdalla, S., and Vandemark, D. (2013) One-and Two-Dimensional Wind Speed Models for Ka-band Altimetry. *Journal of Atmospheric and Oceanic Technology*. doi: <http://dx.doi.org/10.1175/JTECH-D-13-00167.1>
- [10] N. Picot, A. Guillot, P. Senegenès, J. Noubel, N. Steunou, S. Philipps, P. Prandi, G. Valladeau, M. Ablain, S. Desai, B. Haines, S. Fleury. DATA QUALITY ASSESSMENT OF THE SARAL/ALTIKA KA-BAND MISSION. Oral presentation at OSTST, 8th-11th October 2013, Boulder, USA. Available at http://www.avisooceanobs.com/fileadmin/documents/OSTST/2013/oral/Picot_SARAL_Data_Quality_Assessment.pdf.
- [11] S. Philipps, V. Pignot: Saral/AltiKa reprocessing GDR-T Patch2. 2014. SALP-RP-MA-EA-22345-CLS. CLS.DOS/NT/14-031.

- [12] Scharroo, R., and J. L. Lillibridge. Non-parametric sea-state bias models and their relevance to sea level change studies, in *Proceedings of the 2004 Envisat & ERS Symposium*, Eur. Space Agency Spec. Publ., ESA SP-572, edited by H. Lacoste and L. Ouwehand, 2005.
- [13] N. Stenou, P. Sengenès, J. Noubel, N. Picot, J.D. Desjonquères, J.C. Poisson, P. Thibaut, F. Robert and N. Tavenea. ALTIKA INSTRUMENT : IN-FLIGHT STABILITY AND PERFORMANCES. Oral presentation at OSTST 2013, Boulder, USA. Available at http://www.avisioceanobs.com/fileadmin/documents/OSTST/2013/oral/Steunou_OSTST2013_AltiKa_Instrument.pdf
- [14] SARAL System Requirements *SRL-SYS-SP-010-CNES*
- [15] Thibaut, P. O.Z. Zanifé, J.P. Dumont, J. Dorandeu, N. Picot, and P. Vincent, 2002. Data editing: The MQE criterion. *Paper presented at the Jason-1 and TOPEX/Poseidon Science Working Team Meeting, New-Orleans (USA), 21-23 October.*

10. Annex

10.1. Content of Patch1

Hereafter the content of Patch1 is recalled. All GDR data were produced with this patch, whereas IGDR data were only produced with this patch from cycle 4 pass 395 onwards.

Altimeter calibration file : The altimeter calibration stability has been analysed. Based on the actual data, we have implemented an averaging of the calibrations over a 7 days window for the low pass filter (identical to Jason-2) and 3 days for the internal path delay and total power (not used on Jason-2). This will slightly reduce the daily noise observed in the altimeter calibration data.

Altimeter characterization file : We have updated the altimeter characterization file using the flight calibration of the gain values (4 calibrations performed). The impact is very small (of the order of 0.01 dB).

Retracking look-up tables : We have updated the ocean retracking look-up tables using the flight calibration data (PTR). The impact is very small on the range and sigma0 values but of the order of 15 cms on SWH for low sea states.

MQE : We have analyzed the altimeter flight data and based on the observed MQE values over ocean a threshold of $2.3E-3$ (Jason-2 value is $8E-3$) is used for the 1Hz data computation.

Neural network : A first linear relation has been computed between the measured BT and the simulated one. This linear relation is applied on the 23.8 GHz only – the same analysis will be conducted on the 37 GHz and sigma0. This generates a bias on the radiometer wet tropospheric correction which is now much more consistent with the model one.

Atmospheric attenuation : The value outputted by the neural algorithm is now recorded in the level2 products (it was set to 0 at the beginning of the mission). Rad_water_vapor and rad_liquid_water: The values have been corrected to comply with the actual unit in the level2 products (kg/m^2). But the rad_liquid_water remains not reliable as an anomaly has been noticed in the neural network.

SSHA : The radiometer wet tropospheric correction is now used to compute this value (the model value was used at the beginning of the mission).

Controls parameters : The threshold values have been updated with the flight data. This is a first tuning – additional work is necessary.

10.2. Content of Patch2

Hereafter the content of Patch2 is recalled. It will probably be activated mid-January 2014. GDRs will be produced using Patch2 from cycle 8 onwards. Cycles 1 to 7 will be reprocessed with the Patch2.

Wind look-up table : The table provided by NOAA is used. This table is only based on the measured σ_0 , taking into account the atmospheric attenuation (σ_0 at the surface). (Reference: Lillibridge et al. [9])

SSB look-up table : The table provided by R. Scharroo is used (same method as in [12]). We use only the significant wave height to compute the SSB.

Radiometer neural algorithm : Taking into account several months of AltiKa measurements, the neural network coefficients have been updated. Note that this modifies the radiometer related parameters (radiometer wet troposphere correction, atmospheric attenuation, radiometer liquid water content and radiometer water vapor content).

Ice-2 retracking algorithm : The algorithm has been updated taking into account the AltiKa Ka band specificities (ice2 algorithm was based on ENVISAT Ku band experience).

FES2012 tide model : This new tide model is included, improving the SSH accuracy in coastal zones. (Reference : <http://www.avisio.oceanobs.com/en/data/products/auxiliary-products/global-tidefes2004-fes99/description-fes2012.html>)

Matching pursuit algorithm : The algorithm based on J. Tournadre proposal has been tuned to comply to AltiKa Ka band specificities.

MQE parameter scale factor : The scale factor of the MQE has been modified.

Update of the altimeter characterization file : The altimeter characterization file has been modified in order to account for 63 values of altimeter gain control loop (AGC). This has impacts over sea ice and land hydrology, in some cases the AGC was set to default value in current P1 products.

Doris on ground processing (Triode) : The Doris navigator ground processing has been upgraded to reduce the periodic signal observed on the altitude differences with MOE/POE.

10.3. Weighted averaging method for SSH crossover points

SSH differences at crossovers is a key mission performance metric. To compare missions which are not on the same ground track, two methods of measurements are currently used:

- Ensemble statistics of all crossovers
- Binning on grid before estimating statistics.

Figure 63 shows these two statistic methods to compute the standard deviation of SSH crossover differences on SARAL/AltiKa and Jason-2 for each SARAL/AltiKa cycle. It appears clearly that they give different results.

Binning on a grid is equivalent to applying a low pass filter on the data and therefore leads to much lower estimates of the standard deviation of SSH differences at crossovers.

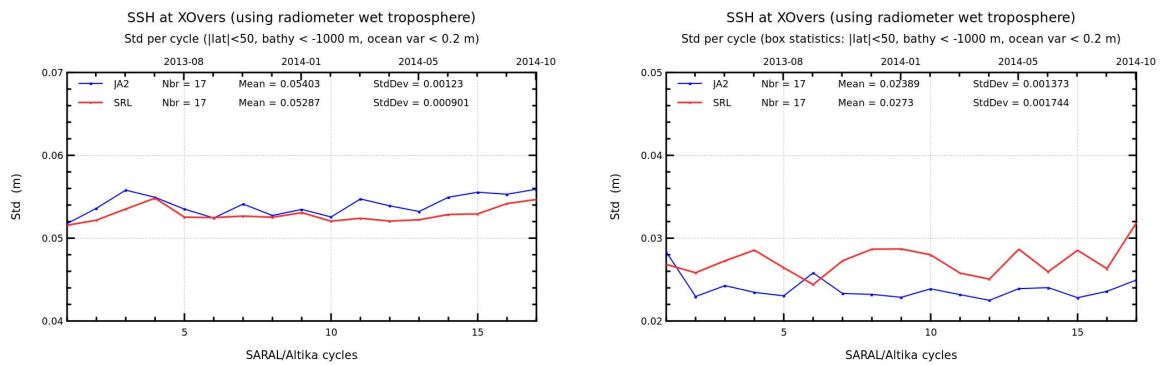


Figure 63: Cycle by cycle standard deviation of SSH crossover differences for Saral/AltiKa and Jason-2 using selection on bathymetry, ocean variability and latitude computed with ensemble statistics (left) or box statistics $4^\circ \times 4^\circ$ (right).

Moreover, crossover points are unevenly distributed due to high densities at high latitudes and low densities at low latitudes and the distribution of crossover points differs from one mission to another (see figure 64).

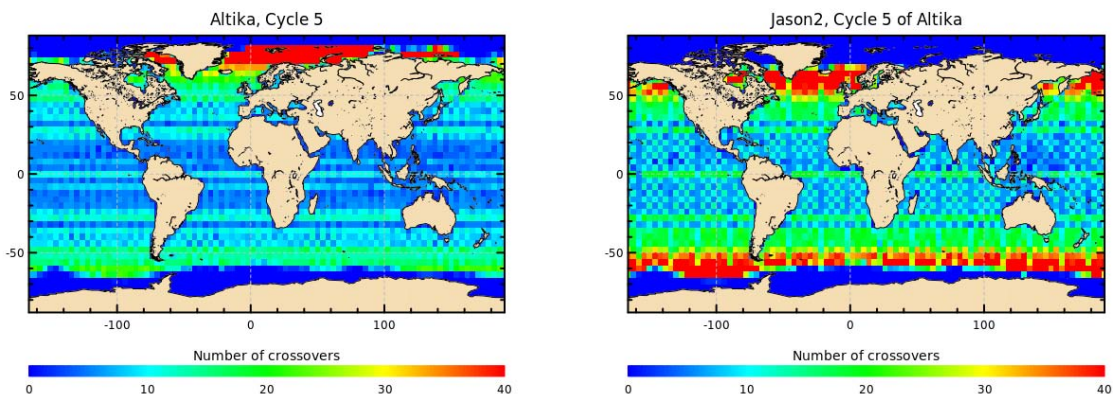


Figure 64: Distribution of number of crossovers on Saral/AltiKa cycle 5

To solve these irregularities and to homogenize the results, a new statistic method based on a weighting of crossovers depending on latitudes has been developed. It relies on the density of

crossovers estimated from the theoretical ground tracks and expressed as a function of latitude (see figure 65).

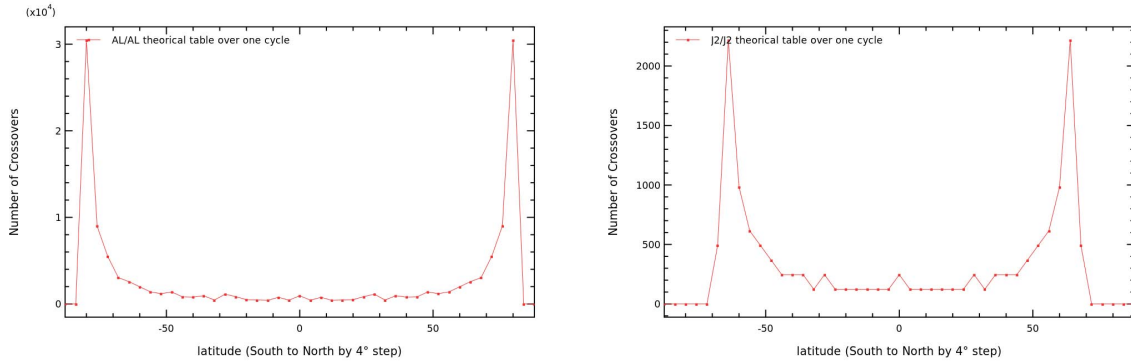


Figure 65: *Density of crossovers by latitude*

Considering the ensemble mean and standard deviation of crossovers:

$$\bar{X} = \frac{1}{\sum_{i=1}^n w_i} \sum_{i=1}^n w_i X_i \quad S = \sqrt{\frac{1}{\sum_{i=1}^n w_i} \sum_{i=1}^n w_i (X_i - \bar{X})^2}$$

w_i is the weighted parameter depending on the inverse of the crossover density. To compute the ensemble non weighted statistics as usual, w_i will be set to 1.

Figure 66 compares the non weighted method with the weighted method for the standard deviation of SSH differences at crossovers. Using the non weighted method, an annual signal due to high latitude ice coverage remains. This annual signal is removed using the weighted by latitude method because high latitudes points are no longer dominant.

Regarding mission performance (standard deviation of SSH differences at crossovers) weighted statistics generally give lower (better performance) results than non weighted statistics, as they downweigh high latitudes where larger errors are expected. This is especially true for SARAL/AltiKa which covers latitudes up to 82°. Of course results are not strongly impacted when using a usual selection on bathymetry, ocean variability and latitudes below 50° because the weighing function is very flat in this latitude band.

This method allows to efficiently compare the performance of missions with different ground tracks, without the need for latitude dependent selections. Weighed statistics are now routinely estimated durant cyclic Cal/Val activities, in addition to previously used methods.

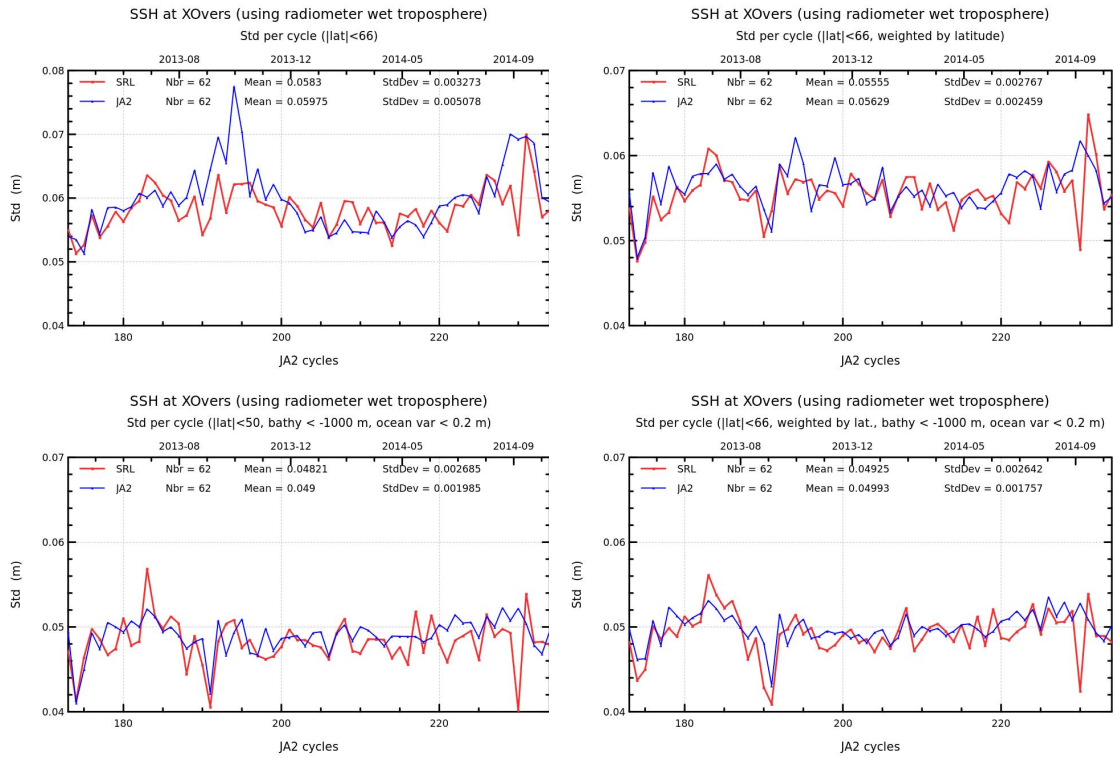
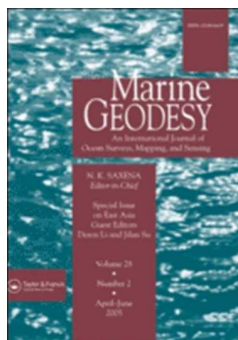


Figure 66: Monitoring of standard deviation SSH crossovers differences for SARAL/AltiKa and Jason-2 based on Jason-2 cycles using non weighted ensemble statistics method (left) and weighted by latitude method (right) with latitude < 66° (top) or with selection on bathymetry, ocean variability and latitude (bottom)

10.4. SARAL/AltiKa global statistical assessment and cross-calibration with Jason-2

In 2014, we submitted a publication to Marine Geodesy to participate in their special issue on SARAL/AltiKa. The preprint of this publication is reproduced here.

Marine Geodesy



SARAL/AltiKa global statistical assessment and cross-calibration with Jason-2

| | |
|------------------|--|
| Journal: | <i>Marine Geodesy</i> |
| Manuscript ID: | UMGD-2014-0069.R2 |
| Manuscript Type: | SARAL special issue |
| Keywords: | Altimetry < Satellite Altimetry, Sea Level, Calibration/Validation, SARAL/AltiKa |
| | |

SCHOLARONE™
Manuscripts

1 SARAL/AltiKa global statistical 2 assessment and cross-calibration with 3 Jason-2

4 5 **Abstract**

6 The CNES/ISRO mission SARAL/AltiKa was successfully launched on 25th of February 2013. It reached
7 its nominal orbit on 13th of March 2013. AltiKa is the first altimeter using the Ka-band frequency.
8 This paper presents the results of the calibration and validation activities performed on the first year
9 of the SARAL/AltiKa mission. The main objective of the paper is to assess the SARAL/AltiKa data
10 quality and to estimate the altimeter system performance using GDR products. To achieve this goal,
11 we present mono-mission metrics and compare them to Jason-2 over the same period. Even if these
12 missions do not have the same ground track, precise comparisons are still possible. They allow
13 assessing parameter discrepancies and SSH consistency between both missions in order to detect
14 geographically correlated biases, jumps or drifts. These results show that SARAL/AltiKa data quality is
15 excellent: ocean data coverage is greater than 99.5%, standard deviation at cross-overs is 5.4 cm.
16 The mission therefore fully fulfills the requirements of high precision altimetry and can ~~even~~ be used
17 (in conjunction with Jason-2) to monitor the global mean sea level, ensuring the continuity of the
18 record over [ERS/Envisat](#) historical ground track. Possible improvements and open issues are also
19 identified, foreseeing an even better mission performance in the near future.

20 **Introduction**

21 The French/Indian mission SARAL/AltiKa (hereafter SRL) was launched on February 25th, 2013. An
22 overview of the SRL mission is given by (Verron et al., 2014). Among other particularities SRL embarks
23 AltiKa which is the first Ka-band altimeter (Vincent et al., 2006; Steunou et al., 2014a), has a variable
24 pulse repetition frequency and a reduced footprint. AltiKa is associated with a dual frequency
25 radiometer (Stenou et al., 2014b). Science products were rapidly disseminated to users (O/IGDR
26 products end of June 2013, GDR products September 2013). This allowed an almost gap-less
27 replacement of the Jason-1 mission (last data on 21/06/2013) by SRL data in multi-mission systems

1
2
3
4
5
6
7 28 such as the Data Unification and Altimeter Combination System (see the SSALTO/DUACS User
8 29 Handbook).

9
10 30 Calibration and Validation activities are an important part of any satellite altimetry mission. They
11 31 provide quick feedback to the project teams in case any suspicious event is detected and essential
12 32 metrics regarding mission performance to the users of the data. A precise calibration between
13 33 mission, as well as the careful monitoring of the mission performance over time is also crucial to
14 34 ensure the continuity of the historical satellite altimeter record and allow for climatic studies (*e. g.*
15 35 Mitchum, 1998). Since the launch of [SARAL/AltiKa/SRL](#), different teams used a variety of methods to
16 36 assess the mission performance (*e. g.* Babu, 2014; Dettmering et al., 2014).

17
18
19
20 37 In order to ensure efficient monitoring of altimeter and radiometer parameters and system
21 38 performances, the Calibration/Validation activities are based on three axes: 1) intrinsic mono-mission
22 39 monitoring, 2) cross-calibration with other altimeter systems and 3) comparison with external data
23 40 either at dedicated calibration sites (Bonfond et al., 2014) or considering global averages
24 41 (Valladeau et al., 2012). This paper addresses the first two of these topics. First the data used are
25 42 described, along with their availability and validity. Then key altimeter parameters and corrections
26 43 are analyzed. Eventually the global mission performance is assessed using Sea Surface Height (SSH)
27 44 differences at crossovers and global mean Sea Level Anomaly (SLA) estimation.

28 45 **Data used and processing**

29 46 In this study the SRL Geophysical Data Record (GDR) data in version “T patch2” are used for cycles 1
30 47 to 14, which corresponds to about one and a half year (14 March 2013 to 17 July 2014). This is a
31 48 homogeneous dataset since GDR from cycle 8 onwards were produced using patch2 and previous
32 49 GDR cycles (1 to 7) were reprocessed in spring 2014. Details of the reprocessing are described in
33 50 (Philipps, 2014b). In this study, usual editing procedures based on thresholds (Bronner et al., 2013),
34 51 crossover analyses, statistical monitoring and visualization tools are used. When compared to Jason-
35 52 2, attention is paid to limit comparisons to the same geographical coverage (+/- 66°). GDR-D data
36 53 were used for Jason-2. The SSH calculation is defined below for SRL and Jason-2:

$$37 54 \quad SSH = Orbit - Altimeter Range - \sum Corrections$$

38 55 where the altimeter range is corrected for instrumental effects. The corrections used for
39 56 [SARAL/AltiKa/SRL](#) and Jason-2 are described in Table 1. More information on the corrections can be
40 57 found in Bronner et al. (2013) for SRL and Dumont et al. (2011) and Ablain et al. (2010) for Jason-2.

58 Data coverage and edited measurements

59 The end-user data availability results from the combination of the frequency of unavailable data and
60 the ratio of edited data which depends on the quality of measurements. In this paper we focus on
61 open ocean applications and the editing strategy is therefore tuned to match this goal, for other
62 applications like coastal studies another editing procedure might be more relevant.

63 Missing Measurements

64 Missing measurements are detected by comparison to SRL's theoretical ground track. A similar
65 process is applied on Jason-2 data to provide a reference. Various events can affect the data
66 coverage and lead to missing measurements; these events are either planned like special calibrations
67 or unexpected like missing telemetry, reception station problems or safe hold modes. The
68 monitoring of the daily percentage of missing measurements is displayed on [Error! Reference source
69 not found.](#) [Figure 1](#) and shows the excellent data coverage of SRL. Over all surfaces, SRL has less
70 missing measurements than Jason-2 except when Jason-2 uses the Digital Elevation Model (DEM)
71 mode during cycle 209 (from March 5th to 15th, 2014). At the beginning of the mission, different
72 acquisition and tracking modes were experimented on SRL (Vincent et al., 2006; Stenou et al.,
73 2014a). Different tracking modes may lead to a change in the percentage of missing measurements,
74 in particular the DEM mode was used during a 7 days sub-cycle of cycle 1 from April 4th to April 10th,
75 2013, during this period the data coverage was about 99 % over all surfaces. The Earliest Detectable
76 Part (EDP) tracker was also experimented at the beginning of the SRL mission for 7 days during cycle
77 1 and 14 days during cycle 3. The use of this tracking mode rather than the median tracker slightly
78 improves the number of missing measurements over all surfaces, but to a much lesser extent than
79 the DEM mode. Most of the missing measurements are located over mountains; in such regions
80 Jason-2 has more missing measurements than SRL likely due to the smaller footprint of SRL. Note
81 that SRL routine calibrations are performed over deserts in Australia, Mongolia, South Africa and the
82 Sahara leading to low data coverage in these areas.

83 If limited to ocean only, SRL has slightly less available data than Jason-2 (when safe hold events are
84 excluded for the latter), yet its data coverage exceeds 99.5 %, which meets the mission requirements
85 (Vincent et al., 2006). Over ocean, the impact of the tracking mode on the percentage of available
86 data is not detectable.

87 In Ka-band, a higher sensitivity to rain events is expected than in Ku-band which may lead to missing
88 measurements (e.g. Vincent et al., 2006; Tournadre et al., 2014) [Error! Reference source not
89 found.](#) [Figure 1](#) (right panel) displays the missing measurements over ocean from SRL over the month

1
2
3
4
5
6
7 90 of May 2013, overlaid on monthly mean precipitation rates from the Global Precipitation Climatology
8 91 Project (Adler et al, 2003). The spatial distribution of missing data is clearly correlated with high rain
9 92 rates, over the same period this is not the case for Jason-2 (not shown), and illustrates the impact of
10 93 rain events on the Ka-band altimeter data availability. However the margins taken on the altimeter
11 94 link budget (Steunou et al., 2014a) limit the effect of high rain rates on data availability and in some
12 95 regions like the western tropical Pacific Ocean SRL has less missing measurements than Jason 2.

15 96 Edited Measurements

16 97 Not all available measurements are valid for the sea level estimation. The purpose of the editing
17 98 procedure is to remove all invalid measurements in order to keep only high quality altimeter data. Of
18 99 course the editing results from a tradeoff between the quality of valid data and their number. The
19 100 editing strategy used for this study is dedicated to the deep open ocean and might not be suitable for
20 101 other applications like coastal studies. The thresholds applied to select valid measurements can be
21 102 found in the SRL Product Handbook (Bronner et al., 2013). It should be noted that in this analysis the
22 103 Caspian Sea is fully edited since the ocean tide is set to the default value in this area in the products.

23 104 Monitoring the percentage of edited measurements shows the excellent performance of SRL, as
24 105 shown on [Error! Reference source not found.Figure 2](#). Over all surfaces (ocean and ice), less data are
25 106 edited for SRL than Jason-2. This is directly linked to the different orbits of the two missions: for polar
26 107 latitudes north/south of 66° a majority of measurements are performed over ice surfaces. After
27 108 removing ice covered areas using the product sea-ice flag, about 2.5 % of SRL data are edited, less
28 109 than Jason-2 ([Error! Reference source not found.Figure 2](#), right). As a comparison, about 3.5 % of
29 110 Jason-2 data over ocean are edited by thresholds (Ablain et al., 2010). Before launch, concerns were
30 111 raised about the sensitivity of the Ka-band to rain events, leading to missing and invalid
31 112 measurements. Such impact is not observed on the global mean percentage of edited data. However,
32 113 a regional impact might exist and we also compare the spatial distribution of these edited data,
33 114 either to Jason-2 over the same time span or to Envisat. No time coincident comparison is possible
34 115 with Envisat, yet it provides useful information as the two missions are flying over the same ground
35 116 track [Error! Reference source not found.Figure 3](#) maps the differences between percentages of
36 117 edited measurements between SRL and Jason-2 (left), and between SRL and Envisat (right), negative
37 118 values meaning that less data are edited on SRL. [Error! Reference source not found.Figure 3](#) shows
38 119 that SRL edits less data than Jason-2 in the western tropical Pacific, despite high tropospheric water
39 120 content in this area. The comparison with Envisat shows a different pattern: SRL seems to edit more
40 121 data than Envisat almost everywhere and especially in the tropical band where the highest rain rates

1
2
3
4
5
6
7 122 are found. This comparison to Envisat illustrates the impact of the use of the Ka-band rather than Ku-
8 123 band on SRL on the ratio of edited measurements.

10 124 **Analysis of altimeter and radiometer parameters**

12 125 As part of the routine calibration and validation activities performed on SRL, many of the GDR fields
13 126 are checked and monitored in order to detect any unusual event. Some of these parameters are
14 127 presented in this section. It should be noted that global statistics are estimated from valid data only,
15 128 and when compared to Jason-2, a geographical selection is applied to consider only latitudes lower
16 129 than 66°.

18 130 SRL is a single frequency altimeter and therefore no dual frequency ionospheric correction is
19 131 available. Moreover the ionospheric impact on the Ka-band is about 7 times smaller than on the Ku-
20 132 band (Vincent et al., 2006) and the GIM model is used in the product. The assessment of this
21 133 correction is not presented in this paper.

23 134 **Apparent Squared Mispointing from Waveforms**

24 135 The off-nadir angle is one the parameter estimated from the retracking of the altimeter waveforms.
25 136 Far Cal/Val purposes, we compute and monitor the daily averages of the mispointing. [Error!](#)
26 137 [Reference source not found.](#) Figure 4 displays the temporal evolution of the mean and standard
27 138 deviation of this parameter. At the beginning of the mission, SRL mispointing was positive around
28 139 0.003 deg². On April 22nd 2013 a cross maneuver was performed and determined that a -0.045 deg
29 140 correction was needed on the pitch. This correction was performed on April 25th and a second cross
30 141 maneuver on April 30th confirmed that the correction was successfully applied. The mispointing from
31 142 SRL is now close to zero and extremely stable both temporally and geographically, which ensures
32 143 reliable estimations of altimeter parameters (Amarouche et al., 2004). Extrapolating from this Jason-
33 144 2 study, and given the SRL antenna aperture, we consider squared mispointings lower than 0.15 deg²
34 145 to be valid. Compared to Jason-2, SRL mispointing shows a much greater stability which results from
35 146 the much narrower antenna beam pattern on SRL (Vincent et al., 2006).

36 147 **Backscatter Coefficient (Sigma0)**

37 148 With a new frequency, interactions between the radar wave and the ocean surface may be different,
38 149 with a direct impact on backscatter coefficient (Steunou et al., 2014a). Indeed differences in the
39 150 mean backscatter coefficient are observed with about 11.1 dB for SRL and 13.5 dB for a Jason-2 over
40 151 the same period. In addition to these 2.4 dB mean differences, the data distribution appears to be
41 152 different. [Error! Reference source not found.](#) Figure 5 displays the histogram of backscattering
42 153 coefficients estimated over the first 2 cycles of SRL and clearly shows different distributions for the

1
2
3
4
5
6
7 154 two missions. The SRL histogram is more widely spread and shows a slight bump around 9 dB which
8 155 is not visible on the Jason-2 data distribution. It should be noted that backscatter coefficients are
9 156 affected by the hot calibration counts saturation (see the wet troposphere correction section and
10 157 Picard et al., 2014) through atmospheric attenuation. To limit the impact of this event, the
11 158 corresponding period has not been considered to estimate the histogram of [Error! Reference source](#)
12 159 [not found.Figure 5](#).

13
14
15
16 160 In the Patch 2 version of the products, the wind speed is estimated using the algorithm of Lillibridge
17 161 et al. (2013) ~~and is heavily dependent on backscatter, where in their paper~~ they also provide
18 162 comparisons with Ku-band wind speed, ~~which are not addressed in this work~~.

163 Significant Wave Height (SWH) and Sea State Bias (SSB)

164 ~~Plotting the spatial distribution~~ Mapping SRL SWH values ([Error! Reference source not found.Figure](#)
165 ~~6, right panel~~) of SRL SWH shows ~~a classical mapan~~ expected spatial distribution, consistent with
166 ~~other missions observations~~, with high SWH regions located in the Northern Atlantic Ocean and the
167 Antarctic Circumpolar Current, and lower SWH in the tropical band, around Indonesia and in the
168 Mediterranean Sea.

169 ~~Left panel of Figure 6 c~~Comparing the daily means of SWH for SRL and Jason-2 (~~not shown~~) allows
170 ~~to estimate the temporal agreement between both missions:- w~~hen limited to latitudes lower than
171 66°, the two missions show ~~a~~ very consistent ~~temporal behavior~~ variability, the correlation coefficient
172 between the two time series is larger than 0.98. ~~We evaluate the SWH bias between SRL and Jason-2~~
173 ~~Since the two missions do not fly over the same ground track, comparing daily averages is not the~~
174 ~~most precise way to evaluate the SWH bias between the two missions, as the ocean sample is not the~~
175 ~~same. A better way to evaluate the bias is tby estimating e~~ estimate the cosine latitude weighted
176 average of gridded data ~~SWH data to account for the difference spatial sampling of the two missions~~
177 ~~(due to its different inclination Jason-2 has a higher data density around 50° than SRL which biases~~
178 ~~the Jason-2 non-weighted mean towards high SWH)~~. Applying this method on SRL's first year reveals
179 no significant SWH bias between SRL and Jason-2. ~~This seems contradictory to Figure 6 where Jason-~~
180 ~~2 appears to be higher than SRL, but results from the different spatial sampling between the two~~
181 ~~missions: Jason 2 has a higher data density around 50° than SRL which biases the Jason 2 daily non-~~
182 ~~weighted mean towards high SWH.~~

183 Since SRL Patch2, the SSB distributed in the products is an hybrid SSB by Scharroo et al. (2013). This
184 new model is an improvement over the previous SSB used in the previous version of SRL products
185 which was simply -3.5% of SWH. [Error! Reference source not found.Figure 7](#) displays the change in

Field Code Changed

Field Code Changed

1
2
3
4
5
6
7 186 the variance of SSH differences at crossovers obtained when comparing the hybrid and one
8 187 parameter SSB solutions, negative values indicating a decrease in variance and therefore better
9 188 mission performance. The hybrid model provides a large improvement in regions of high SWH like
10 189 the North Atlantic Ocean and the Antarctic Circumpolar Current. On average the variance reduction
11 190 amounts to 1.8 cm². Comparing the histograms for Ku (Jason-2) and Ka (SRL) bands SSB estimated
12 191 over the same period and geographical area reveals that the SSB is on average lower on SRL than on
13 192 Jason-2. The estimation of a non parametric SSB for SRL is planned for Patch 3, following a method
14 193 similar to Tran et al. (2012) and will likely provide further improvements of SRL performance.

18 194 **Wet Troposphere Correction**

19 195 SRL uses a dual frequency radiometer (Stenou et al., 2014b) to retrieve the wet tropospheric
20 196 correction, water vapor and liquid water contents and atmospheric attenuation. More details of the
21 197 radiometer processing on SRL can be found in Picard et al. (2014). For validation activities, the wet
22 198 tropospheric correction derived from the ECMWF model is used as a reference to check the stability
23 199 of the radiometer derived correction. Left panel of [Error! Reference source not found. Figure 8](#)
24 200 displays the temporal evolution of the daily differences between the radiometer and the model for
25 201 SRL and Jason-2. There is a clear drift on SRL related to the saturation of the hot calibration counts
26 202 causing a drift of the 37 GHz brightness temperatures (Picard et al., 2014). The onboard
27 203 parameterization database was corrected on October 22nd, 2013 and the daily mean differences then
28 204 come back to a level similar to the Jason-2 one. An empirical correction of this drift is planned (Picard
29 205 et al. 2014).

30 206 The temporal variability of the wet tropospheric differences between the radiometer and the model
31 207 remains higher for SRL than for Jason-2: the daily standard deviation of the differences is around 1.6
32 208 cm for SRL and only 1.2 cm for Jason-2 (not shown). [Error! Reference source not found. Figure 8](#) also
33 209 displays ~~a map~~ [the geographical distribution](#) of the radiometer minus model wet tropospheric
34 210 correction differences for SRL data. This map was estimated from October 22nd until the end of SRL
35 211 cycle 12 in order to remove the measurements impacted by the radiometer drift. The map shows
36 212 large geographically correlated patterns which suggest that there is still room for improvement of
37 213 the radiometer retrieval algorithms on SRL, even if the current algorithms provide a much better
38 214 performance than the model as shown by the crossovers analysis below (see also Picard et al. 2014).
39 215 The same analysis performed on Jason-2 (not shown) shows a similar pattern for the radiometer
40 216 minus model differences but with reduced amplitude (about two times).

217 Sea level performances

218 In the previous sections of this paper we analyzed SRL data availability and the main parameters of
219 the mission. In this section, we investigate the accuracy the SSH estimated from SRL data. Different
220 types of analysis are performed to reach this goal: SSH differences at crossovers, along-track SLA
221 statistics and Global Mean Sea Level evolution.

222 SSH Crossover differences

223 SSH differences at crossovers is the main metric to assess the overall performance of satellite
224 altimetry missions. When applied on a single mission, they provide information about the SSH
225 consistency between ascending and descending tracks. When crossovers are estimated from two
226 different missions, they provide a relative SSH bias estimation and allow to detect drifts between
227 missions. SSH differences at crossovers are routinely calculated as part of the validation activities,
228 selecting time differences shorter than 10 days, and performing an additional geographical selection
229 to remove high latitudes (larger than 50°), shallow waters (depth lower than 1000m) and high
230 oceanic variability areas.

231 Standard Deviation of SSH Crossover Differences

232 The standard deviation of mono-mission SSH differences at crossovers is the main mission
233 performance indicator. When comparing SRL to Jason-2, two missions that ~~fly-overcover~~ different
234 ground tracks, the geographical distribution of crossovers is not the same for both missions and may
235 bias the statistics. In order to overcome this issue, we estimate global metrics using latitude
236 weighted statistics where the weighing depends on the crossovers theoretical density. **Error!**
237 **Reference source not found.** Figure 9 compares the standard deviation of SSH differences at
238 crossovers of Jason-2 and SRL. Using either the radiometer or the model, SRL shows a slightly lower
239 standard deviation at crossovers: 5.4 cm versus 5.6 cm (using the radiometer) indicating a slightly
240 better mission performance than Jason-2. For both missions, using the radiometer wet tropospheric
241 correction rather than the one derived from the model brings a reduction of the standard deviation
242 of SSH differences at crossovers. This means that on both missions, the radiometer performs better
243 than the model.

244 Mean of SSH Crossover Differences

245 **Error! Reference source not found.** Figure 10 displays the cycle-by-cycle monitoring of the mean SSH
246 differences at crossovers. The left panel estimates monomission differences and provides
247 information about systematic inconsistencies between ascending and descending arcs. For SRL, this
248 difference is slightly negative at -4 mm, larger than for Jason-2 (about -1 mm). However SRL shows a
249 lower variability from one cycle to another than Jason-2, but the latter is impacted by safe hold

1
2
3
4
5
6
7 250 | modes during the period that can have an impact on this metric. Using the model derived wet
8 251 | tropospheric correction rather than the radiometer one does not change significantly the pattern
9 252 | observed on both missions. The right panel displays the result of a multimission analysis where SSH
10 253 | differences are estimated at crossovers between SRL and Jason-2. This provides an efficient way to
11 254 | detect drifts between two missions. The first part of the period (approximately until cycle 8) shows a
12 255 | drift when the radiometer wet tropospheric correction is used, due to the drift of the radiometer
13 256 | measurements. No drift is observed when the model wet tropospheric correction is used, and the
14 257 | two curves come close again after the correction of the onboard radiometer database. This plot also
15 258 | exhibits a bias between the two missions, which is discussed in the Sea Level Anomaly section of this
16 259 | paper.

20
21 260 | [Error! Reference source not found, Figure 11](#) provides information about the geographical
22 261 | distribution of the global biases observed on [Error! Reference source not found, Figure 10](#). For SRL
23 262 | mono-mission crossovers the map is rather homogeneous with differences generally lower than 1
24 263 | cm. However, there is one negative patch around Indonesia, and a strongly positive patch in the
25 264 | Northern Atlantic Ocean. The comparison to Jason-2 at crossovers ([Error! Reference source not
26 265 | found, Figure 11](#), right) shows again a patch around Indonesia, but with an opposite sign, which
27 266 | seems to extend all along the equator and is likely related to the radiometer wet tropospheric
28 267 | correction (the patch is reduced when using the model, not shown). A negative patch is also
29 268 | observed in the Southern Ocean south of Africa, a region of high SWH. Differences remain low
30 269 | elsewhere.

36 270 | **Pseudo Time Tag Bias Estimation**

37 271 | By regressing the mono-mission SSH differences at crossovers against the orbital altitude rate, we
38 272 | can estimate a pseudo time-tag bias. This kind of linear model may merge real time-tag errors and
39 273 | other errors correlated with the orbital altitude rate, thus the “pseudo”. This coefficient is routinely
40 274 | estimated for each cycle. [Error! Reference source not found, Figure 12](#) shows the temporal evolution
41 275 | of this pseudo time-tag bias for SRL and Jason-2: the mean value is slightly negative at -0.05 ms,
42 276 | which has a negligible impact on the SSH estimation (about 1 mm). This monitoring also shows that
43 277 | this parameter is less variable on SRL than on Jason-2. Jason-2 is still impacted by a 60-day signal on
44 278 | the pseudo time-tag bias of unknown origin (Jason-2/OSTM 2012 annual report available at:
45 279 | http://www.aviso.altimetry.fr/fileadmin/documents/calval/validation_report/J2/annual_report_j2_2012.pdf) which does not appear on SRL. However a periodic behavior could be suspected considering
46 280 | [Error! Reference source not found, Figure 12](#), but can't be confirmed at the moment given the short
47 281 | period available.

283 Analysis of Sea Level Anomalies

284 Analysis of SLA is another mission performance indicator. In this section, we present comparisons
285 between SRL and Jason-2 global SLA. SLA is estimated by subtracting the CNES/CLS 11 mean sea
286 surface (Schaeffer et al., 2012) from valid SSH measurements and we perform a geographical
287 selection to remove latitudes ~~greater-larger~~ than 66° on SRL. Since the two missions are not on the
288 same ground track, no point-wise comparison is possible such as during the verification period
289 between Jason-1 and Jason-2 (Ablain et al, 2012). ~~However we have a tempore now have an~~
290 overlap ~~period~~ between Jason-2 and SRL longer than one year and useful comparisons can be drawn
291 ~~from the differences~~ between these two missions.

292 Mean and Standard Deviation of Along-track SLA

293 ~~Error! Reference source not found.~~ [Figure 13](#) displays the evolution of the daily mean and standard
294 deviation of global SLA for SRL and Jason-2. The monitoring shows no statistically significant drift of
295 global SLA differences over the period. The two time series display similar temporal evolution,
296 despite excursions of the Jason-2 mean SLA due to safe hold events resulting in a reduced
297 geographical coverage. In order to account for the different orbits, the mean SSH bias between SRL
298 and Jason-2 is estimated from the cosine latitude weighted average of gridded SLA over the whole
299 period. This leads to an estimated SSH bias of -4.8 cm using the radiometer wet tropospheric
300 correction and -4.5 cm when using the model correction, with a standard deviation of 20mm in both
301 cases. These values are consistent with other techniques used to estimate this bias: Bonnefond et
302 al. (2014) find a -54 mm absolute bias, associated with a 20 mm standard deviation, while the Jason-
303 2 absolute bias is evaluated to -4 mm

304 A slight drift is observed on the time series of the differences as a result of the saturation of the
305 radiometer hot calibration counts. ~~After the update of the radiometer database, there is no longer a~~
306 ~~saturation of the hot calibration counts, and no drift is observed at the end of the time series of the~~
307 ~~differences but with no impact after the update of the onboard radiometer database.~~ The standard
308 deviation of the global daily SLA is lower for SRL than for Jason-2 with 10.6 cm versus 11 cm. This low
309 figure for SRL suggests again a high quality of the data.

310 The spatial distribution of the differences is also of interest as it might indicate geographically
311 correlated patterns with no signature on the global mean. ~~Error! Reference source not found.~~ [Figure](#)
312 [14](#) displays the map of SLA differences between SRL and Jason-2 estimated using the radiometer and
313 the model wet tropospheric correction. When using the correction derived from the radiometer, the
314 differences show a small East/West pattern with negative values in the Pacific Ocean and positive
315 values in the Atlantic Ocean as well as a stronger negative anomaly in the Western Tropical Pacific

1
2
3
4
5
6
7 316 Ocean. When using the modeled correction, the negative anomaly in the Pacific Ocean is reduced,
8 317 yet a small positive anomaly remains in the Atlantic Ocean. These differences might originate from a
9 318 combination of different errors like orbit solutions or remaining errors in SRL's SSB solution.

11 319 Although Global Mean Sea Level (GMSL) monitoring was not in the primary goals of the mission, SRL
12 320 can be used to perform GMSL analyses. [Error! Reference source not found.](#) Figure 15 displays the
13 321 global mean sea level estimated from SRL data, overlaid over the reference mean sea level time
14 322 series (Ablain et al., 2009), available from the AVISO website
15 323 (ftp://ftp.avis.oceanobs.com/pub/oceano/AVISO/indicators/msl/MSL_Serie_MERGED_Global_IB_R
16 324 [WT_GIA_Adjust.nc](ftp://ftp.avis.oceanobs.com/pub/oceano/AVISO/indicators/msl/MSL_Serie_MERGED_Global_IB_R)). The two time series observe the same variability at the mm level. This illustrates
17 325 the great quality of SRL and its potential as a part of the climate monitoring system. However, with
18 326 just over one year of data collected so far, the time span is too short to perform a reliable trend
19 327 analysis.

25 328 Conclusion

27 329 Calibration and validation activities represent an essential part of satellite altimetry processing: they
28 330 allow a quick feedback to operational teams and experts and perform the necessary data quality
29 331 assessment before the GDR products are delivered to users. The Cal/Val activities performed on
30 332 [SARAL/AltiKaSRL](#) during the commissioning phase of the mission allowed to establish the excellent
31 333 performance of the mission. We demonstrate in this paper that, over ocean, [SSARAL/AltiKaRL](#)
32 334 provides an excellent data coverage with more than 99.5% of available measurements over ocean,
33 335 and that the quality of the measurements is also excellent (5.4 cm standard deviation of SSH
34 336 differences at crossovers), slightly better than the Jason-2 one. As a result [SARAL/AltiKaSRL](#) fully
35 337 fulfills its mission requirements and provides crucial information on the Envisat historical ground
36 338 track not only for oceanic applications ([Faugère et al., 2014](#)) but also for other scientific studies (e.g.
37 339 Rémy et al., 2014).

43 340 Despite this already excellent mission performance, improvements are already foreseen in the near
44 341 future concerning the radiometer retrieval algorithms, the [sea state biasSSB](#), new standards (POE
45 342 [GDR-E](#)) for the orbit estimation or a tuned rain flag. The mission will also benefit from the
46 343 improvement of geophysical corrections, new tidal models or a new MSS for example.

49 344 The long term monitoring of the mission parameters and sea surface height will continue, as part of
50 345 data validation activities to detect any jump or drift on the [SARAL/AltiKaSRL](#) record. As shown in the
51 346 present study, and as demonstrated in previous ones (e. g. Ablain et al., 2012), precise comparisons
52 347 are possible with Jason-2, even if the two mission do not have the same ground track. These

1
2
3
4
5
6
7 348 comparisons show that despite a relative SSH bias estimated to -48 mm, the two missions show an
8 349 excellent agreement regarding spatial and temporal SSH variability. The longer the period available
9 350 to perform these comparisons will become, the more accurately one will detect an anomaly on one
10 351 mission. In-situ measurements (tide gauges or Argo profiles) provide an important and independent
11 352 external data source to detect SSH humps or drifts, that will become relevant as soon as the
12 353 [SARAL/AltiKaSRL](#) time series is long enough (Valladeau et al., 2012).

15 354 **Acknowledgements**

16 355 This work is supported by the Centre National d'Etudes Spatiales (CNES) in the frame of the SALP
17 356 project. We friendly acknowledge all the CNES SARAL/AltiKa project members, as well as their ISRO
18 357 colleagues for fruitful discussions. We also thank two anonymous reviewers for their helpful
19 358 comments.

20 359 **Keywords:** saral, altika, altimetry, calibration/validation, sea level, mean sea level

23 360 **References**

- 24 361 Ablain M., A. Cazenave, K. DoMinh, S. Guinehut, W. Llovel, A. Lombard and G. Valladeau, 2009: A
25 362 new assessment of global mean sea level from altimeters highlights a reduction of global slope from
26 363 2005 to 2008 in agreement with in-situ measurements, *Ocean Sciences*, 5, 193-201
- 27 364 Ablain, M., S. Philipps, N. Picot, E. Bronner, 2012: Jason-2 Global Statistical Assessment and Cross-
28 365 Calibration with Jason-1. *Marine Geodesy*, Vol. 33, Iss. sup1.
- 29 366 Adler, R.F., G.J. Huffman, A. Chang, R. Ferraro, P. Xie, J. Janowiak, B. Rudolf, U. Schneider, S. Curtis, D.
30 367 Bolvin, A. Gruber, J. Susskind, P. Arkin, 2003: The Version 2 Global Precipitation Climatology Project
31 368 (GPCP) Monthly Precipitation Analysis (1979-Present). *J. Hydrometeor.*, 4,1147-1167.
- 32 369 Amarouche, L., Thibaut, P., Zanife, O.Z., Dumont, J.P, Vincent, P., Steunou, N. : "Improving the Jason-
33 370 1 Ground Retracking to better Account for Attitude effects", *Marine Geodesy*, Special Issue on Jason-
34 371 1 Calibration/Validation, vol 27, Part II : 171-197, 2004
- 35 372 Babu, K. N. Absolute calibration of SARAL-AltiKa in Kavaratti during its initial Calibration-Validation
36 373 phase. Presented at SARAL International Science and Applications Meeting, 22-24 April, Ahmedabad,
37 374 available from [http://www.aviso.altimetry.fr/fileadmin/documents/ScienceTeams/Saral2014/22-04-
38 375 2014/Session-3/KNBabuAltiKaApril2014.pdf](http://www.aviso.altimetry.fr/fileadmin/documents/ScienceTeams/Saral2014/22-04-2014/Session-3/KNBabuAltiKaApril2014.pdf)

1
2
3
4
5
6
7
8
9
10
11
12
13
14
15
16
17
18
19
20
21
22
23
24
25
26
27
28
29
30
31
32
33
34
35
36
37
38
39
40
41
42
43
44
45
46
47
48
49
50
51
52
53
54
55
56
57
58
59
60

376 Bonnefond P., P. Exertier, O. Laurain, A. Guillot, N. Picot, M. Cancet, F. Lyard: SARAL/AltiKa absolute
377 calibration from the multi-mission Corsica facilities, 2014, this issue

378 Bosch, W.; Dettmering, D.; Schwatke, C. Multi-Mission Cross-Calibration of Satellite Altimeters:
379 Constructing a Long-Term Data Record for Global and Regional Sea Level Change Studies. Remote
380 Sens. 2014, 6, 2255-2281.

381 Bronner E., A. Guillot and N. Picot, SARAL/AltiKa Products Handbook, 2013. SALP-MU-M-OP-15984-
382 CN (CNES). Issue 2 rev4. Available at
383 http://www.aviso.altimetry.fr/fileadmin/documents/data/tools/SARAL_Altika_products_handbook.p
384 [df](#)

Field Code Changed

Formatted: English (U.S.)

385 S. Brown, C. Ruf, S. Keihm, and A. Kitiyakara, "Jason Microwave Radiometer Performance and On-
386 Orbit Calibration," /Mar. Geod./, vol. 27, no. 1–2, pp.199–220, 2004.

387 Carrère, L. and F. Lyard, 2003: Modeling the barotropic response of the global ocean to atmospheric
388 wind and pressure forcing – comparison with observations, Geophys. Res. Lett., 30(6), 1275.

Formatted: English (U.S.)

389 Cartwright, D. E., A. C. Edden, 1973, "Corrected tables of tidal harmonics," Geophys. J. R. Astr. Soc.,
390 33, 253-264.

391 Couhert A., L. Cerri, J.-F. Legeais, M. Ablain, N. P. Zelensky, B. J. Haines, F. G. Lemoine, W. I. Bertiger,
392 S. D. Desai, M. Otten, Towards the 1 mm/y stability of the radial orbit error at regional scales,
393 Advances in Space Research, Available online 10 July 2014, ISSN 0273-1177,
394 <http://dx.doi.org/10.1016/j.asr.2014.06.041>.

395 [Dettmering, D., Schwatke, C., Bosch, W.: Global calibration of SARAL/AltiKa using multi-mission sea](#)
396 [surface height crossovers, this issue](#)

397 Dumont et al., 2011: OSTM/Jason-2 products handbook, 2011. SALP-MU-M-OP-15815-CN (CNES),
398 EUM/OPS-JAS/MAN/08/0041 (EUMETSAT), OSTM-29-1237 (JPL), Polar Series/OSTM J400
399 (NOAA/NESDIS). Issue 1 rev8. Available at:
400 http://www.aviso.altimetry.fr/fileadmin/documents/data/tools/hdbk_j2.pdf

Field Code Changed

401 [Iijima, B.A., I.L. Harris, C.M. Ho, U.J. Lindqwister, A.J. Mannucci, X. Pi, M.J. Reyes, L.C. Sparks, B.D.](#)
402 [Wilson, Automated daily process for global ionospheric total electron content maps and satellite](#)
403 [ocean altimeter ionospheric calibration based on Global Positioning System data, Journal of](#)
404 [Atmospheric and Solar-Terrestrial Physics, Volume 61, Issue 16, 1 November 1999, Pages 1205-1218,](#)
405 [ISSN 1364-6826, http://dx.doi.org/10.1016/S1364-6826\(99\)00067-X](#)

Formatted: English (U.S.)

- 1
2
3
4
5
6
7 406 Lillibridge, J., Scharroo, R., Abdalla, S., and Vandemark, D. (2013) One-and Two-Dimensional Wind
8 407 Speed Models for Ka-band Altimetry. Journal of Atmospheric and Oceanic Technology. doi:
9 408 <http://dx.doi.org/10.1175/JTECH-D-13-00167.1>
- 11 409 ~~Gary T. Mitchum, G. T.~~-1998: Monitoring the Stability of Satellite Altimeters with Tide Gauges. J.
12 410 Atmos. Oceanic Technol., 15, 721–730. doi: <http://dx.doi.org/10.1175/1520->
13 411 [0426\(1998\)015<0721:MTSOSA>2.0.CO;2](http://dx.doi.org/10.1175/1520-0426(1998)015<0721:MTSOSA>2.0.CO;2)
- 16 412 Philipps, S. and V. Pignot, 2014: Saral/ AltiKa reprocessing GDR-T Patch2. CLS.DOS/NT/14-031. SALP-
17 413 RP-MA-EA-22345-CLS. Issue 1 rev 1. Available at
19 414 http://www.aviso.altimetry.fr/fileadmin/documents/calval/validation_report/SaralPatch2Reprocessi
20 415 [ngReport.pdf](http://www.aviso.altimetry.fr/fileadmin/documents/calval/validation_report/SaralPatch2ReprocessingReport.pdf)
- 22 416 Picard B., M.L. Frery, E. Obligis, L. Eymard, N. Steunou and N. Picot: First Year of the Microwave
23 417 Radiometer aboard SARAL/AltiKa: In-Flight Calibration, Processing, and Validation of the Geophysical
24 418 Products. Marine Geodesy. 2014, this issue
- 27 419 Ray, R., 1999: A Global Ocean Tide model from Topex/Poseidon Altimetry, GOT99.2. Rapport n°
28 420 NASA/TM-1999-209478, Goddard Space Flight Center Ed., NASA, Greenbelt, MD, USA. pp. 58.
- 31 421 Remy, F., T. Flament, A. Michel and D. Blumstein: Envisat and SARAL/AltiKa observations of the
32 422 Antarctic ice sheet: a comparison between the Ku-band and the Ka-band, 2014, this issue
- 34 423 Schaeffer P., Y. Faugère, J. F. Legeais, A. Ollivier, T. Guinle and N. Picot, 2012, The CNES_CLS11 Global
35 424 Mean Sea Surface Computed from 16 Years of Satellite Altimeter Data, *Marine Geodesy*, 35(S1):3-19
- 37 425 Scharroo R., J. Lillibridge, S. Abdalla and D. Vandemark, 2013: Early look at SARAL/AltiKa data, oral
38 426 presentation at OSTST 2013, available at
40 427 http://www.aviso.altimetry.fr/fileadmin/documents/OSTST/2013/oral/Scharroo_Early_look_at_SAR
41 428 [AL.pdf](http://www.aviso.altimetry.fr/fileadmin/documents/OSTST/2013/oral/Scharroo_Early_look_at_SAR_AL.pdf)
- 43 429 SSALTO/DUACS User Handbook : (M)SLA and (M)ADT Near-Real Time and Delayed Time Products,
44 430 2014, CLS-DOS-NT-06-034, Issue 4 rev 1. Available at:
46 431 http://www.aviso.altimetry.fr/fileadmin/documents/data/tools/hdbk_duacs.pdf
- 48 432 Steunou N., J.D. Desjonquères, N. Picot, P. Sengenes, J. Noubel, J.C. Poisson: AltiKa altimeter:
49 433 instrument description and in flight performance, 2014a, this issue
- 51 434 Steunou N., N. Picot, P. Sengenes, J. Noubel, M.L. Frery: AltiKa radiometer: instrument description
52 435 and in flight performance, 2014b, this issue

Field Code Changed

1
2
3
4
5
6
7
8
9
10
11
12
13
14
15
16
17
18
19
20
21
22
23
24
25
26
27
28
29
30
31
32
33
34
35
36
37
38
39
40
41
42
43
44
45
46
47
48
49
50
51
52
53
54
55
56
57
58
59
60

436 Tournadre J., J.C. Poisson, N. Steunou, B. Picard: Validation of AltiKa Matching Pursuit rain flag, 2014,
437 this issue

438 Tran N., S. Labroue, S. Philipps, E. Bronner and N. Picot, 2010, Overview and update of the sea-state
439 bias corrections for the Jason-2, Jason-1 and TOPEX missions, *Marine Geodesy* 33(S1):348-362

440 Valladeau G., J. F. Legeais, M. Ablain, S. Guinehut and N. Picot, 2012: Comparing Altimetry with Tide
441 Gauges and Profiling Floats for Data Quality Assessment and Mean Sea Level Studies, *Marine*
442 *Geodesy*, 35(S1):42-60

443 Verron J., P. Sengenès, J. Lambin, J. Noubel, N. Steunou, A. Guillot, N. Picot, S. Coutin-Faye, R.
444 Gairola, D.V.A. Raghava Murthy, J. Richman, D. Griffin, A. Pascual, F. Rémy, P. K. Gupta: The
445 SARAL/AltiKa altimetry satellite mission, 2014, this issue

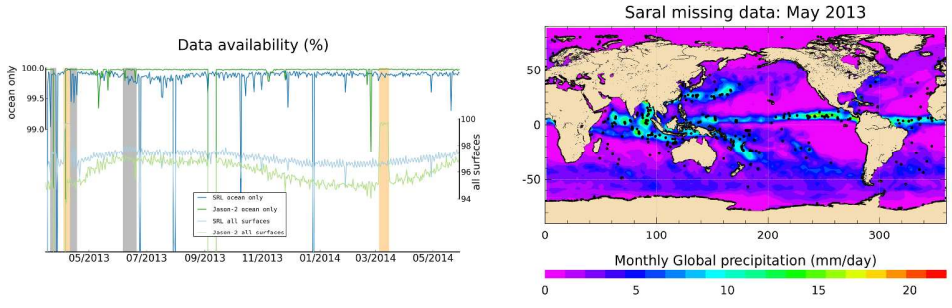
446 Vincent, P., N. Steunou, E. Caubetq, L. Phalippou, L. Rey, E. Thouvenot and J. Verron, 2006, "AltiKa: a
447 Ka-band Altimetry Payload and System for Operational Altimetry during the GMES Period." *Sensors* 6,
448 no. 3: 208-234.

449 Wahr, J. W., 1985, "Deformation of the Earth induced by polar motion," *J. Geophys. Res. (Solid*
450 *Earth)*, 90, 9363-9368.

| Correction | SARAL/AltiKA | Jason-2 |
|---|---|------------------------------------|
| Orbits | CNES POE GDR -D standards (Couhert et al., 2014) | |
| Dry Troposphere correction | ECMWF model | |
| Wet troposphere correction | radiometer(Brown et al., 2004) | radiometer (Picard et al., 2014) |
| Dynamical atmospheric correction | high resolution Mag2D model (Carrere and Lyard, 2003) | |
| Ionospheric correction | GIM model(Iijima et al., 1999) | filtered dual frequency correction |
| Sea state bias | hybrid SSB (Scharroo et al., non-parametric (Tran et al., 2013) 2010) | |
| Ocean tide | GOT4.8 model (Ray, 1999) | |
| Solid earth tide | elastic response to tidal potential (Cartwright and Edden, 1973) | |
| Pole tide | (Wahr, 1985) | |

Formatted: English (U.S.)
 Formatted: English (U.S.)
 Formatted: Font color: Text 1, English (U.S.)

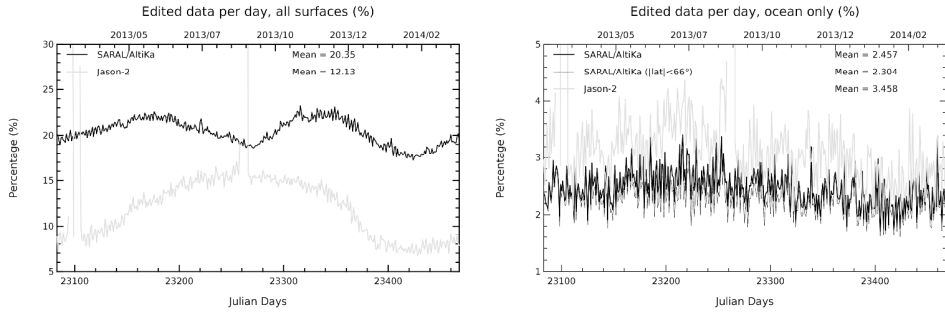
1
2
3
4
5
6
7
8
9
10
11
12
13
14
15
16
17
18
19
20
21
22
23
24
25
26
27
28
29
30
31
32
33
34
35
36
37
38
39
40
41
42
43
44
45
46
47
48
49
50
51
52
53
54
55
56
57
58
59
60



(left) temporal evolution of the daily percentage of missing data over all surfaces and ocean only for SRL and Jason-2, the grey bands indicate the EDP tracker periods (SRL only) while DEM mode periods are highlighted in beige (SRL and Jason-2), and (right) map of the missing SRL data (black dots) for the month of May 2013 overlaid on monthly precipitation rate.
346x115mm (300 x 300 DPI)

Peer Review Only

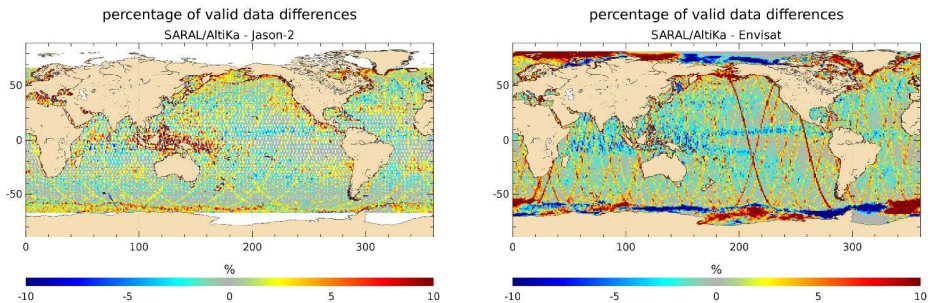
1
2
3
4
5
6
7
8
9
10
11
12
13
14
15
16
17
18
19
20
21
22
23
24
25
26
27
28
29
30
31
32
33
34
35
36
37
38
39
40
41
42
43
44
45
46
47
48
49
50
51
52
53
54
55
56
57
58
59
60



temporal evolution of the daily percentage of edited data for SRL and Jason-2 over ocean and ice surfaces (left) and over ocean only (right)
346x115mm (300 x 300 DPI)

Peer Review Only

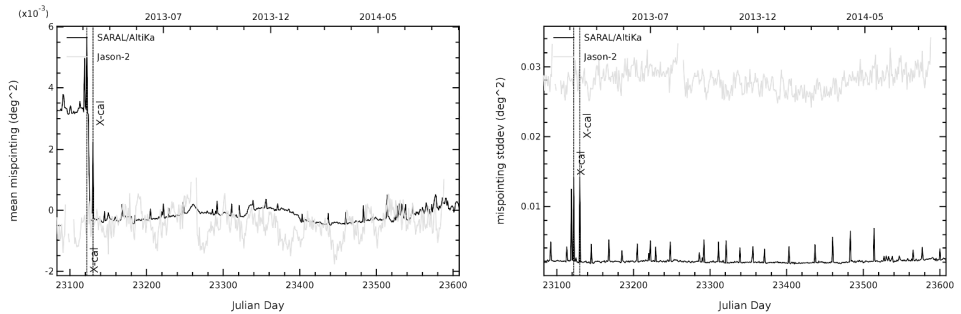
1
2
3
4
5
6
7
8
9
10
11
12
13
14
15
16
17
18
19
20
21
22
23
24
25
26
27
28
29
30
31
32
33
34
35
36
37
38
39
40
41
42
43
44
45
46
47
48
49
50
51
52
53
54
55
56
57
58
59
60



map of differences of the percentage of edited data between Jason-2 and SRL (left) and between Envisat and SRL (right) over one year of data. Envisat data is taken 4 years before.
346x115mm (300 x 300 DPI)

Peer Review Only

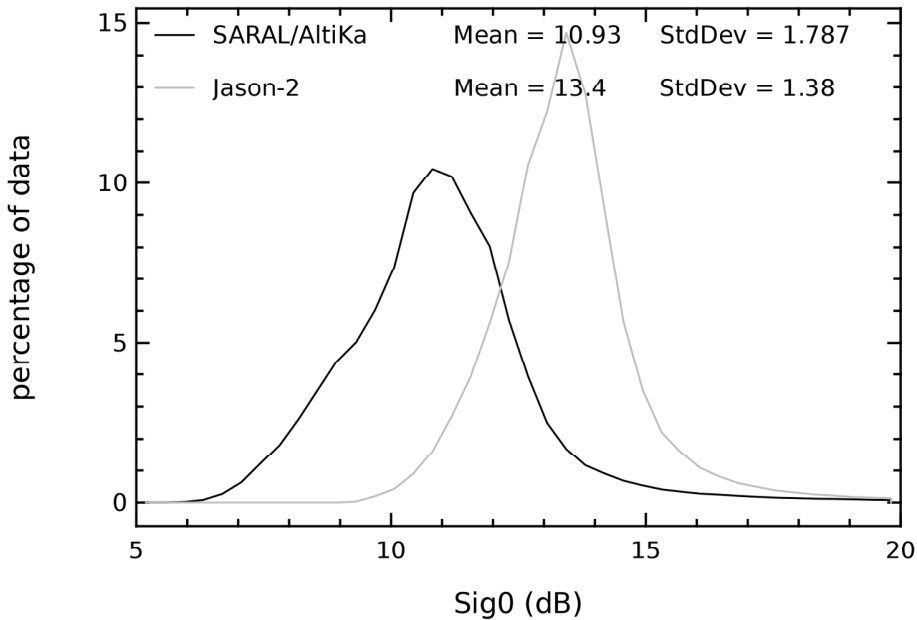
1
2
3
4
5
6
7
8
9
10
11
12
13
14
15
16
17
18
19
20
21
22
23
24
25
26
27
28
29
30
31
32
33
34
35
36
37
38
39
40
41
42
43
44
45
46
47
48
49
50
51
52
53
54
55
56
57
58
59
60



temporal evolution of the daily mean (left) and standard deviation (right) of the apparent squared mispointing from waveforms for SRL and Jason-2
346x115mm (300 x 300 DPI)

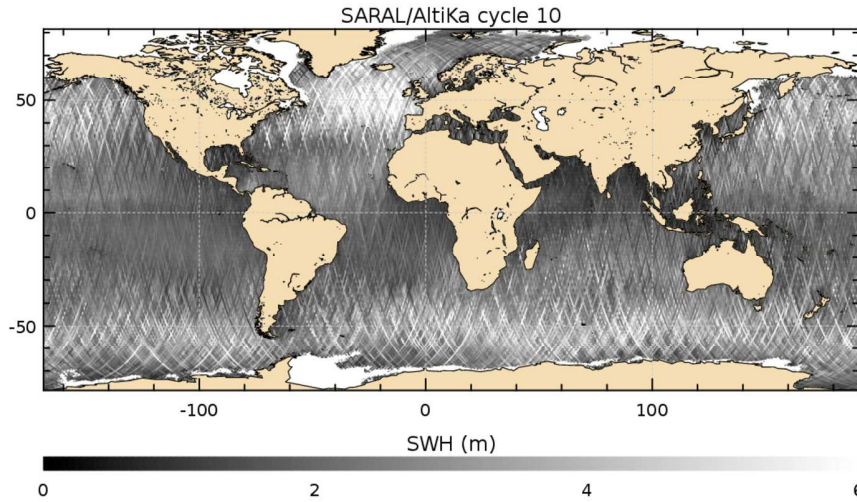
Peer Review Only

1
2
3
4
5
6
7
8
9
10
11
12
13
14
15
16
17
18
19
20
21
22
23
24
25
26
27
28
29
30
31
32
33
34
35
36
37
38
39
40
41
42
43
44
45
46
47
48
49
50
51
52
53
54
55
56
57
58
59
60



histogram of backscatter coefficient values for SRL (black) and Jason-2 (grey) in dB
722x479mm (72 x 72 DPI)

Review Only

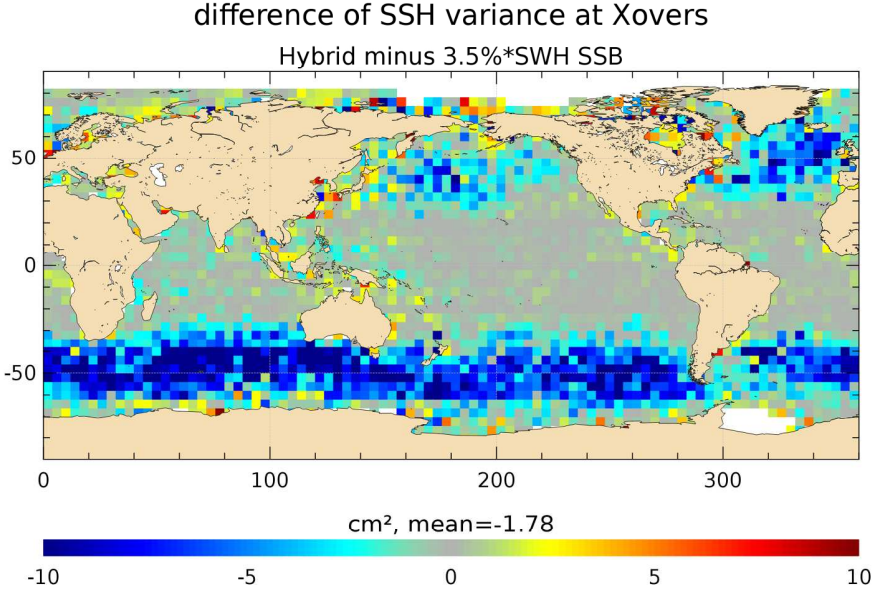


map of SRL SWH measurements over SRL's cycle 10 (Jan 23rd to Feb 27th, 2014)
959x529mm (72 x 72 DPI)

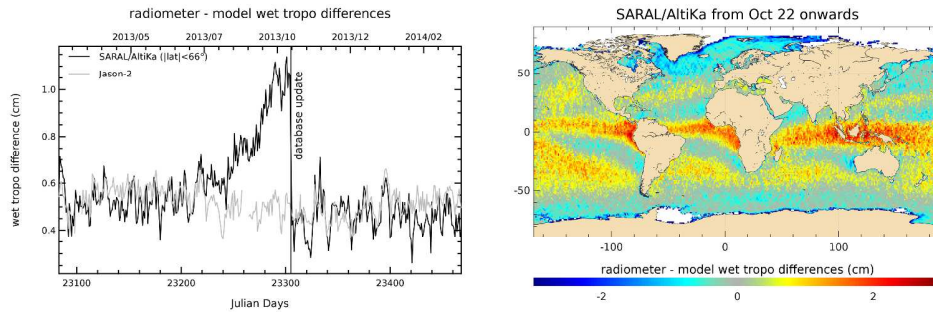
Review Only

1
2
3
4
5
6
7
8
9
10
11
12
13
14
15
16
17
18
19
20
21
22
23
24
25
26
27
28
29
30
31
32
33
34
35
36
37
38
39
40
41
42
43
44
45
46
47
48
49
50
51
52
53
54
55
56
57
58
59
60

1
2
3
4
5
6
7
8
9
10
11
12
13
14
15
16
17
18
19
20
21
22
23
24
25
26
27
28
29
30
31
32
33
34
35
36
37
38
39
40
41
42
43
44
45
46
47
48
49
50
51
52
53
54
55
56
57
58
59
60



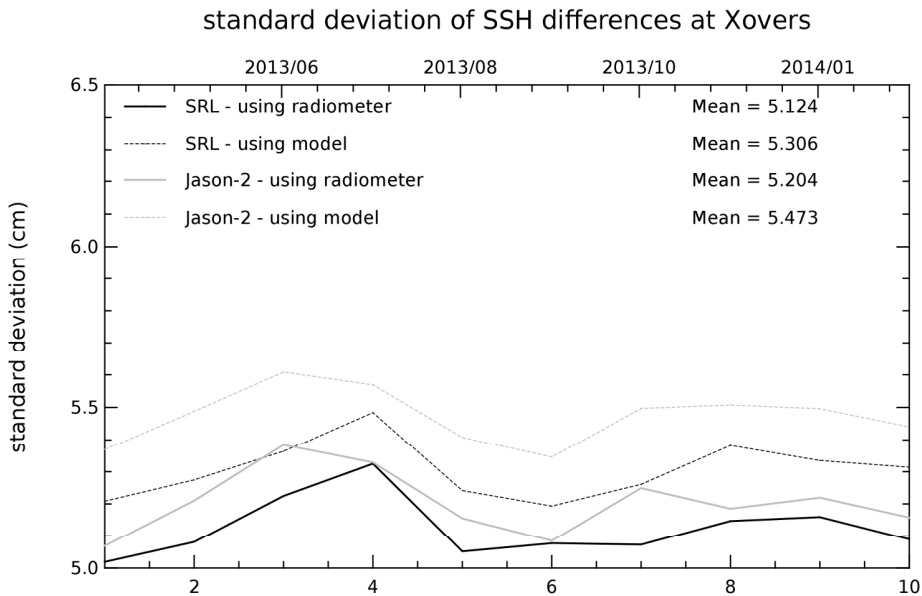
map of the variance change of SSH differences at crossovers between the hybrid (Patch 2) and one parameter (Patch 1) SSB models on SRL
722x479mm (72 x 72 DPI)



temporal evolution of the daily mean differences between the radiometer and model wet tropospheric corrections for SRL and Jason-2 (left) and map of the mean differences between the radiometer and model wet tropospheric correction for SRL from October 22nd, 2013 to May 8th, 2014 (end of cycle 12) (right).
346x115mm (300 x 300 DPI)

Peer Review Only

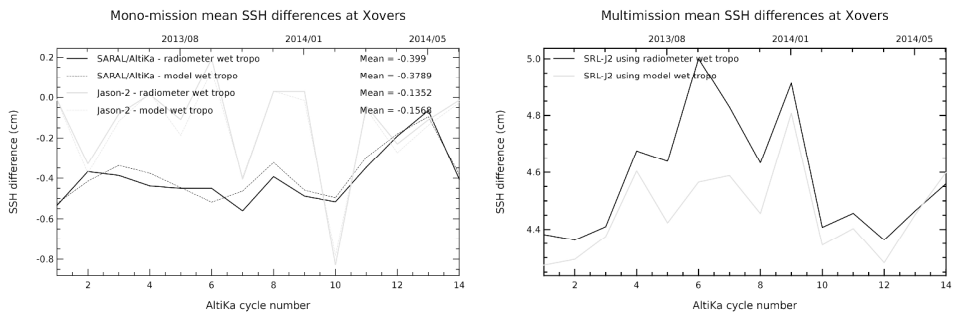
1
2
3
4
5
6
7
8
9
10
11
12
13
14
15
16
17
18
19
20
21
22
23
24
25
26
27
28
29
30
31
32
33
34
35
36
37
38
39
40
41
42
43
44
45
46
47
48
49
50
51
52
53
54
55
56
57
58
59
60



cycle by cycle standard deviation of the SSH differences at crossovers for SRL and Jason-2, the statistics are estimated over areas with latitudes lower than 50°, depths greater than 1000m and low ocean variability
722x479mm (72 x 72 DPI)

Review Only

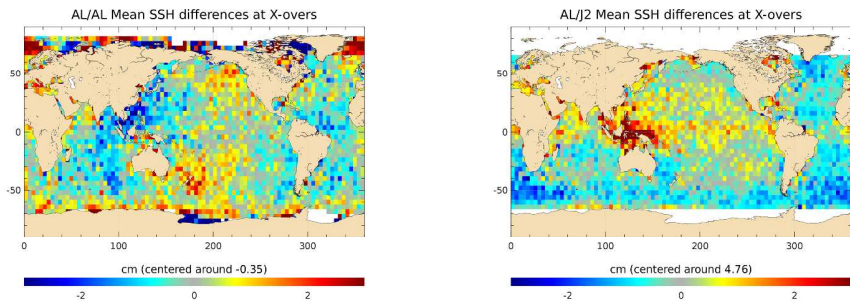
1
2
3
4
5
6
7
8
9
10
11
12
13
14
15
16
17
18
19
20
21
22
23
24
25
26
27
28
29
30
31
32
33
34
35
36
37
38
39
40
41
42
43
44
45
46
47
48
49
50
51
52
53
54
55
56
57
58
59
60



cycle by cycle mean of SSH differences for monomission (SRL and Jason-2, left) and multimission (SRL minus Jason-2, right) analyses. Only regions with latitudes lower than 50°, depths greater and 1000m and low ocean variability are considered here.
346x115mm (300 x 300 DPI)

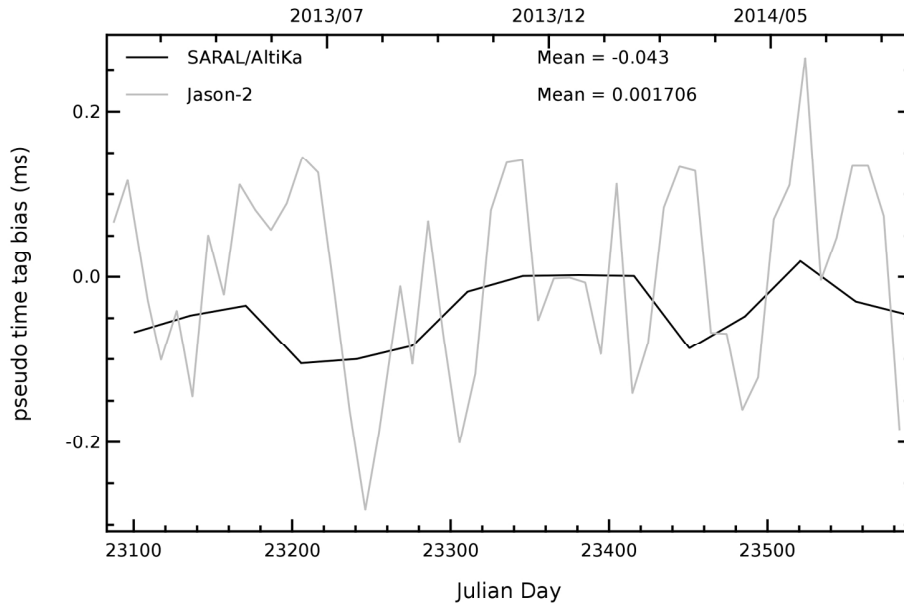
Peer Review Only

1
2
3
4
5
6
7
8
9
10
11
12
13
14
15
16
17
18
19
20
21
22
23
24
25
26
27
28
29
30
31
32
33
34
35
36
37
38
39
40
41
42
43
44
45
46
47
48
49
50
51
52
53
54
55
56
57
58
59
60



map of the mean SSH differences at crossovers for mono-mission (SRL analysis, left) and multi-mission (SRL minus Jason-2, right), in cm estimated over the first 12 cycles of SRL.
346x115mm (300 x 300 DPI)

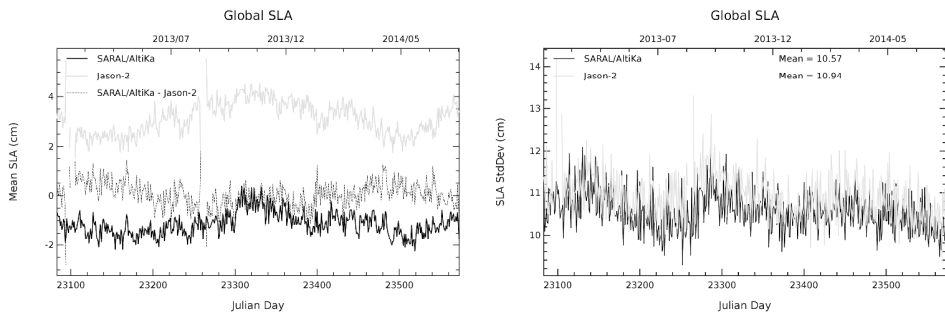
Peer Review Only



temporal evolution of the pseudo time tag bias in milliseconds for Jason-2 (grey) and SRL (black)
722x479mm (72 x 72 DPI)

Review Only

1
2
3
4
5
6
7
8
9
10
11
12
13
14
15
16
17
18
19
20
21
22
23
24
25
26
27
28
29
30
31
32
33
34
35
36
37
38
39
40
41
42
43
44
45
46
47
48
49
50
51
52
53
54
55
56
57
58
59
60

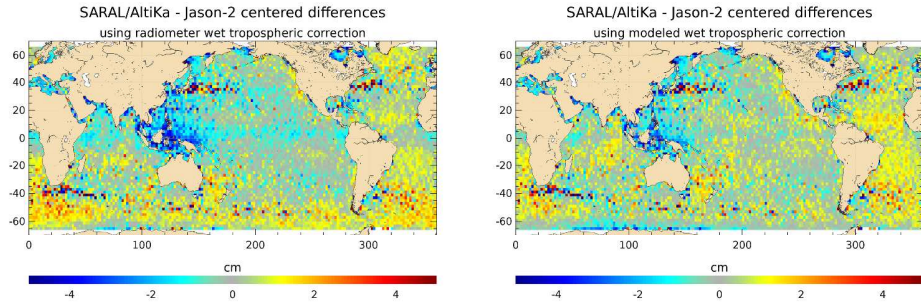


daily mean (left) and standard deviation (right) of global sea level anomaly for SRL and Jason-2. The daily mean of the differences has been centered.

346x115mm (300 x 300 DPI)

Peer Review Only

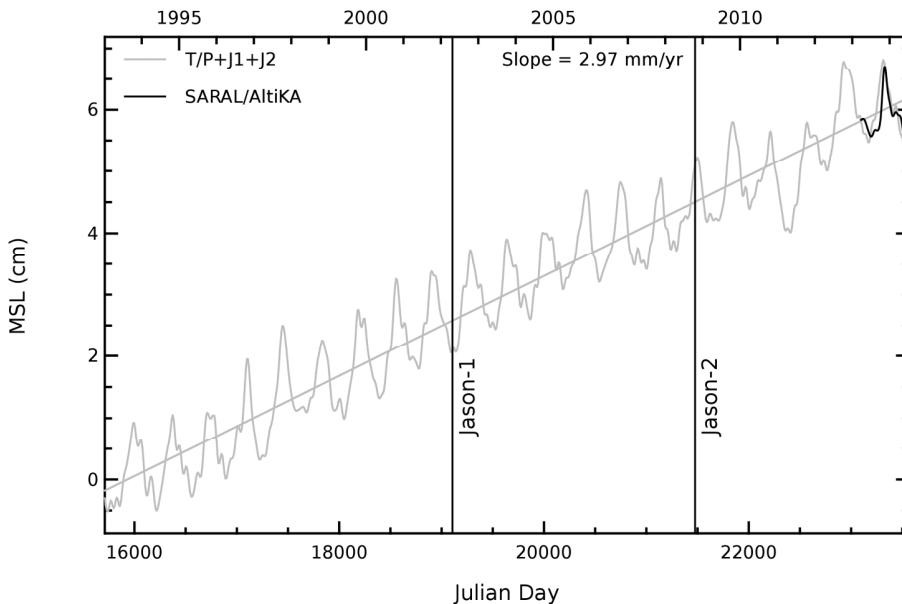
1
2
3
4
5
6
7
8
9
10
11
12
13
14
15
16
17
18
19
20
21
22
23
24
25
26
27
28
29
30
31
32
33
34
35
36
37
38
39
40
41
42
43
44
45
46
47
48
49
50
51
52
53
54
55
56
57
58
59
60



maps of SLA differences between SARAL and Jason-2 using the radiometer (left) and model (right) wet tropospheric differences
346x115mm (300 x 300 DPI)

Peer Review Only

1
2
3
4
5
6
7
8
9
10
11
12
13
14
15
16
17
18
19
20
21
22
23
24
25
26
27
28
29
30
31
32
33
34
35
36
37
38
39
40
41
42
43
44
45
46
47
48
49
50
51
52
53
54
55
56
57
58
59
60



the global mean sea level record from Topex/Poseidon, Jason-1 and Jason-2 with SRL's record overlaid
722x479mm (72 x 72 DPI)

Review Only